

UIC CLASS VI GEOLOGIC STORAGE OF CO₂ PERMIT APPLICATION

South Midland CCS Hub
South Midland Facility
Upton County, Texas

Section 1: Site Characterization & Narrative

[40 CFR §146.82, §146.83]

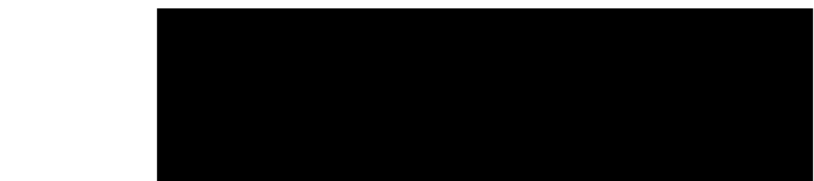
Prepared for:

EPA Region 6
Underground Injection Control Section
1201 Elm Street, Suite 500 | Dallas, Texas 75270



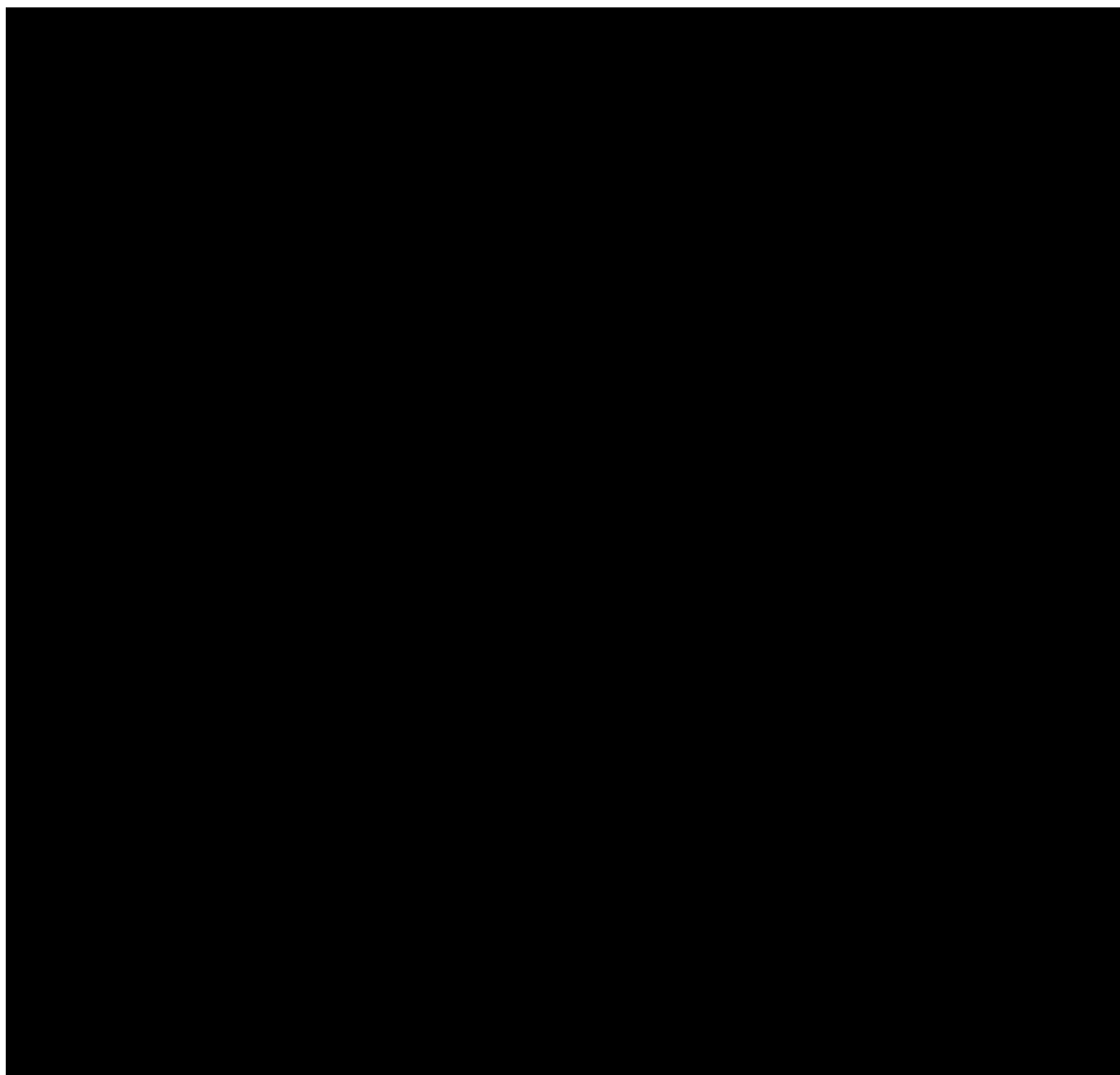
Prepared and submitted by:

Milestone Carbon Midland CCS Hub, LLC
840 Gessner Rd, Suite 600
Houston, Texas 77024

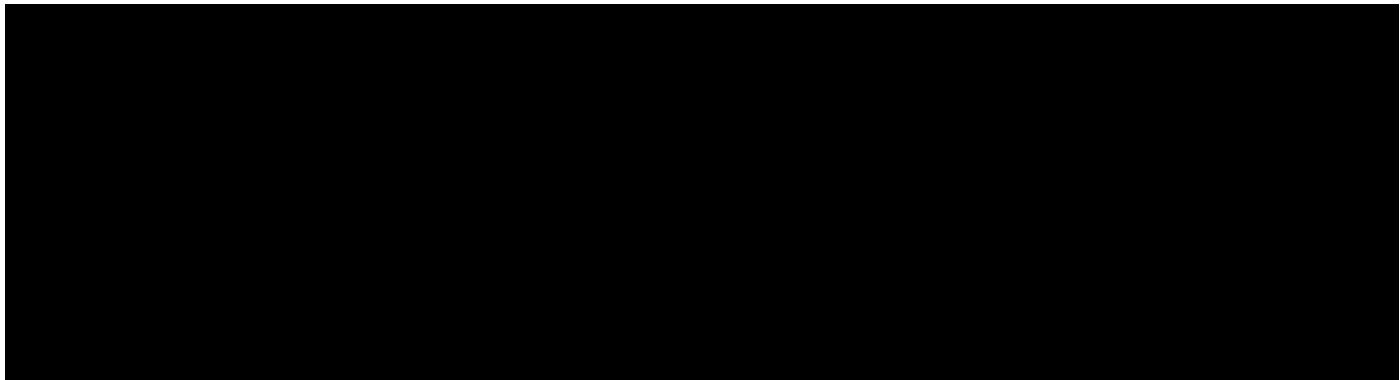


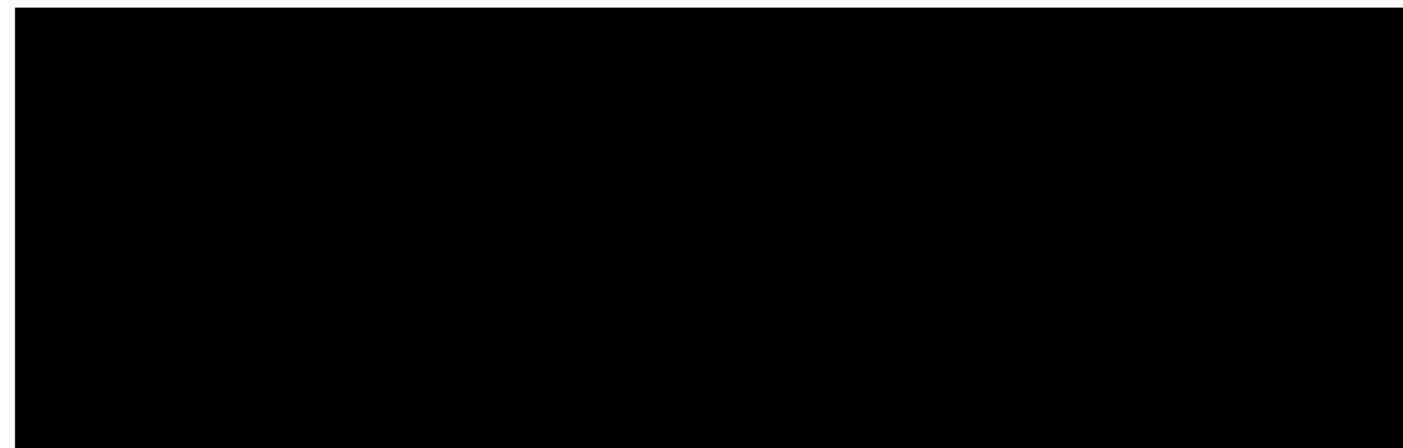
Updated 18 October 2024

Table of Contents



List of Tables





List of Figures

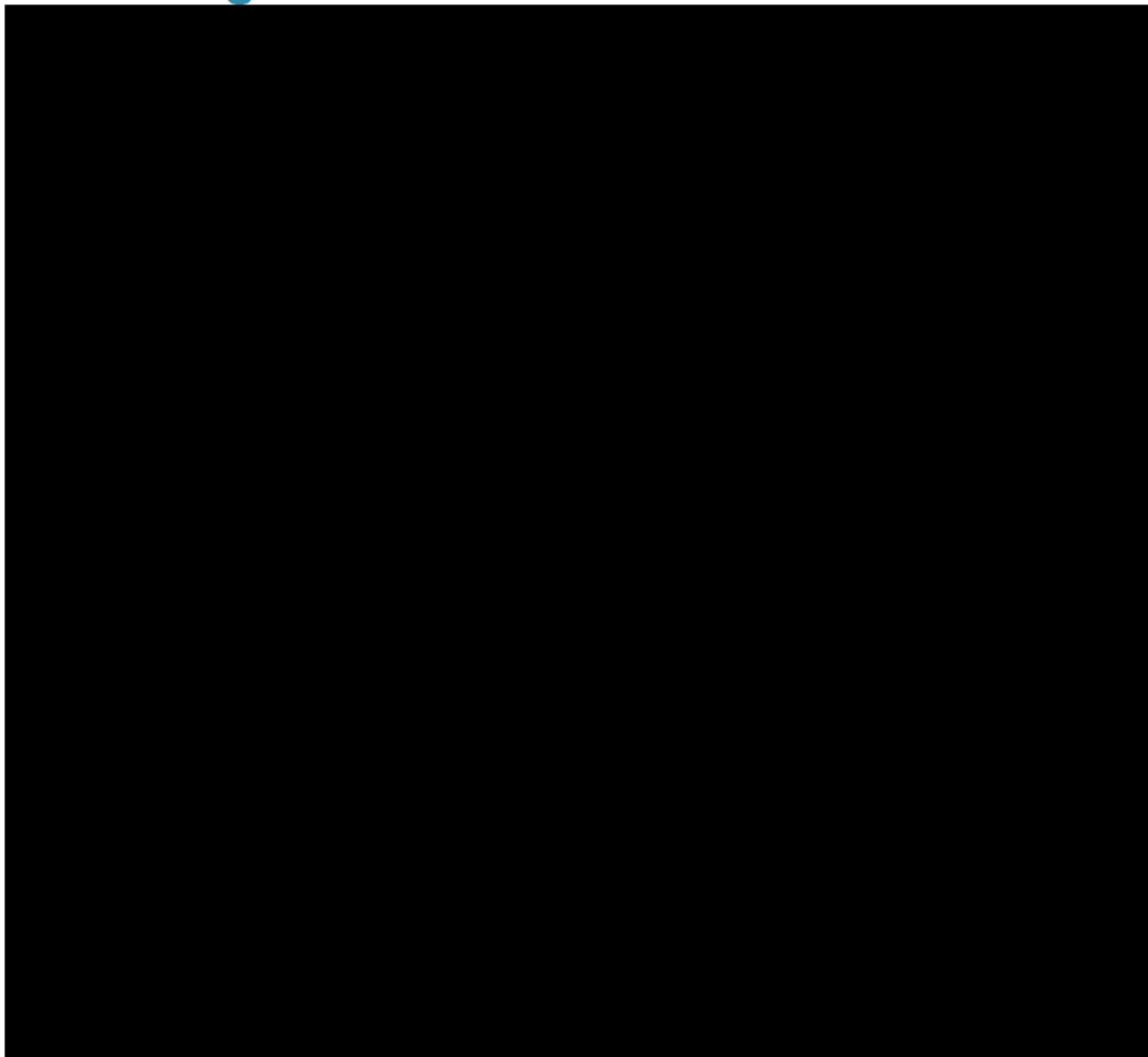
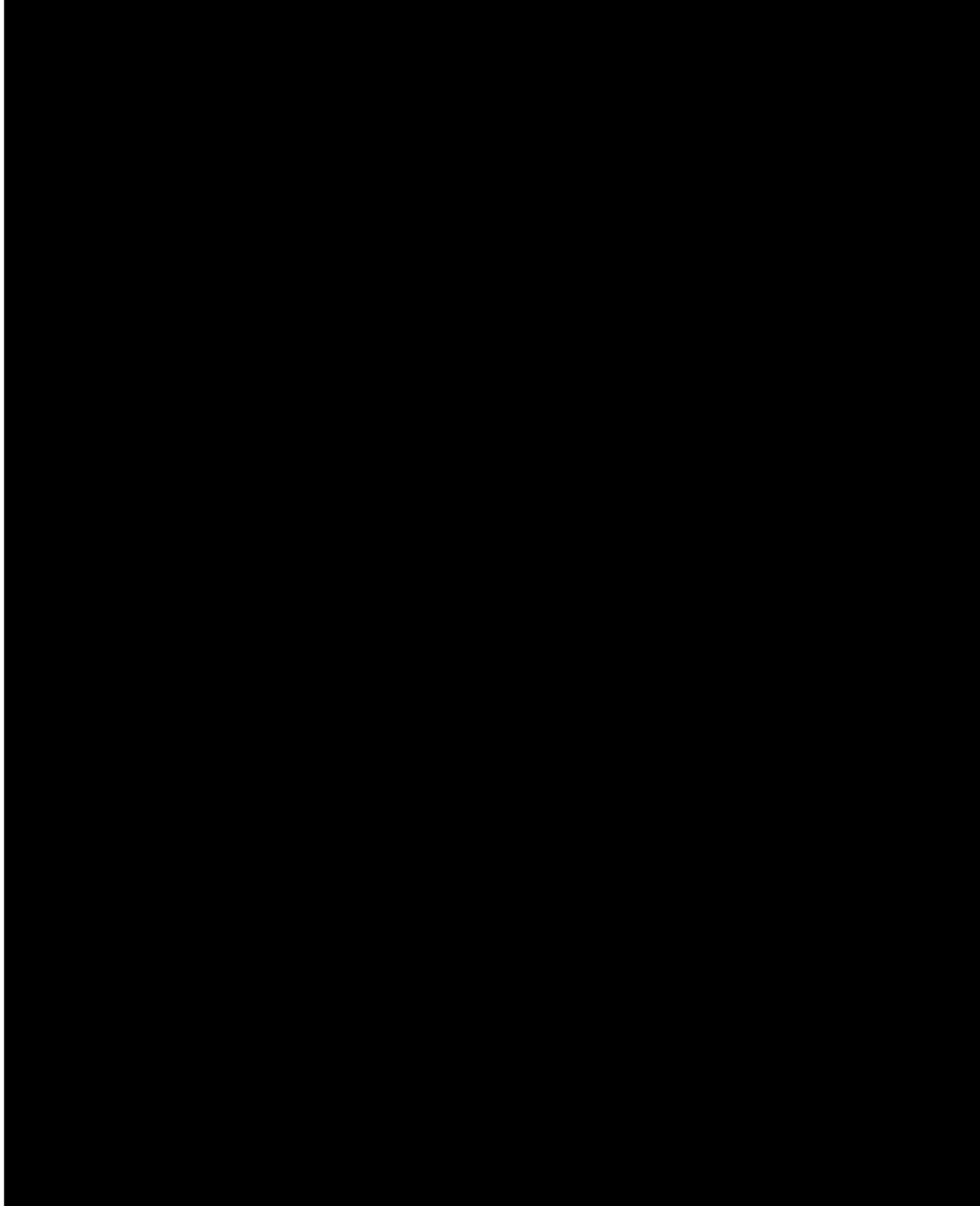


Figure 1-44: Ellenburger Thickness Map 64



List of Equations

1.0 SITE CHARACTERIZATION [40 CFR 146.82 (a);] [40 CFR 144.31(e)(1-6)]

1.1 Facility Information [40 CFR 146.82 (a)(1)]

Facility Name: South Midland Facility
Midland CCS #2 Well

Facility Contact:

Well Location:

Facility Address:

Owner and Operator Information: Milestone Carbon Midland CCS Hub, LLC
840 Gessner Rd, Suite 600. Houston, TX 77024
Front Desk Phone: 832-739-6700
Privately Held Delaware Limited Liability Corporation

SIC Codes: 4953 – Refuse Systems
8999 – Environmental Consulting

Key Terms. For the purposes of this permit application, the following terms and their relationship to the proposed Class VI well application are as follows:

- Milestone Carbon Midland CCS Hub, LLC (Milestone) – The Operator of the “Facility,” the “Well,” and “Operational Area,” hereafter referred to simply as “Milestone”
- South Midland Facility – The “Facility”
- Facility – South Midland Facility which includes all injection and monitoring wells
- Midland CCS #2 – The Injection “Well”

qualifier used

- Injection Well – Midland CCS #2

Milestone Carbon Midland CCS Hub, LLC Class VI Permit Application
South Midland Facility, Upton County, Texas
Section 1: Site Characterization & Narrative | page 7 of 149

1.2 Project Introduction [40 CFR 146.82 (a)(1)]

Milestone Carbon Midland CCS Hub, LLC (Milestone) is submitting this application to request authorization of the construction and operation of a Class VI Underground Injection Control (UIC) well in Upton County, Texas. The proposed Midland CCS #2 carbon capture and sequestration (CCS) Class VI well (the Well) will be sited within the Milestone South Midland CCS Facility and is designed to inject carbon dioxide from nearby oil and gas processing sources, power plants and cement plants, into deep underground brine aquifer formations to safely and permanently sequester it.

Milestone has extensive experience with slurry injection and landfill operations associated with energy waste in Upton County, Texas. Accordingly, Milestone understands both the technical and regulatory obligations associated with responsibly managing project operations in this area. This Application demonstrates how Milestone will meet all applicable regulatory and monitoring requirements associated with the proposed Class VI Well in order to protect underground sources of drinking water (USDW) during pre-construction, pre-injection, operation, and post-injection periods.

Objectives and Benefits of the Well include:

1. **Climate Change Mitigation**: Natural gas combustion accounts for 22% of the world's greenhouse gas (GHG) emissions. Sequestering the carbon dioxide (CO₂) related to these emissions will help mitigate GHG effects on climate change. The Permian Basin, as one of the largest oil and gas producing provinces in the United States, emits approximately 60 million metric tonnes (MMta) of CO₂ annually (IEA, 2020 Report).
2. **Energy Security**: The Facility will help to ensure energy security by enabling the continued use of fossil fuels while reducing GHG. The Texas electricity market has one of the narrowest supply vs demand ranges in the USA. Therefore, disruptions in energy can have catastrophic effects on property and life in the state (Electric Reliability Council of Texas (ERCOT) Website, 2023).
3. **Economic Development**: The Facility will support economic development by creating new jobs in the area related to construction, including injection well, monitoring well, pipeline, and capture facility construction. Additional oil and gas service industry jobs related to monitoring such as seismic acquisition and well logging will be created/retained.
4. **Technological Advancement**: The Facility will help to advance the carbon sequestration industry by demonstrating the effectiveness of long-term brine aquifer CO₂ sequestration while minimizing risk to USDWs in the area. Novel techniques and process efficiencies are likely to be discovered during injection and monitoring operations.

Milestone proposes to [REDACTED]

[REDACTED] here is a total of 16.1 MMta of emissions within a radius of 30 miles (Emissions Source: Enverus, 2024). A summary of operational parameters is presented in **Table 1-1**.

Milestone will be the owner and operator of the Well and Facility [REDACTED]

An aquifer exemption will not be required. The Railroad Commission of Texas (RRC) Groundwater Advisory Unit (GAU) provides Groundwater Protection Determinations for surface casing,

underground injection and other underground activities. The GAU has determined the base of USDW is estimated to occur at a depth [REDACTED] the area of the Well (GAU Determination letter, permit **Section 13, Appendix I**). The top of the injection unit, [REDACTED] than the lowest known USDW. Additional information on local aquifers, salinity, and water chemistry is detailed subsequently in **Sections 1.4, 1.9 and 1.11**.

The project is not located on, or near, federal Indian lands or Indian reservations. The nearest Indian reservation is the Mescalero Apache reservation, located in New Mexico. The reservation is located over 220 mi northwest (NW) from the calculated area of review (AoR).

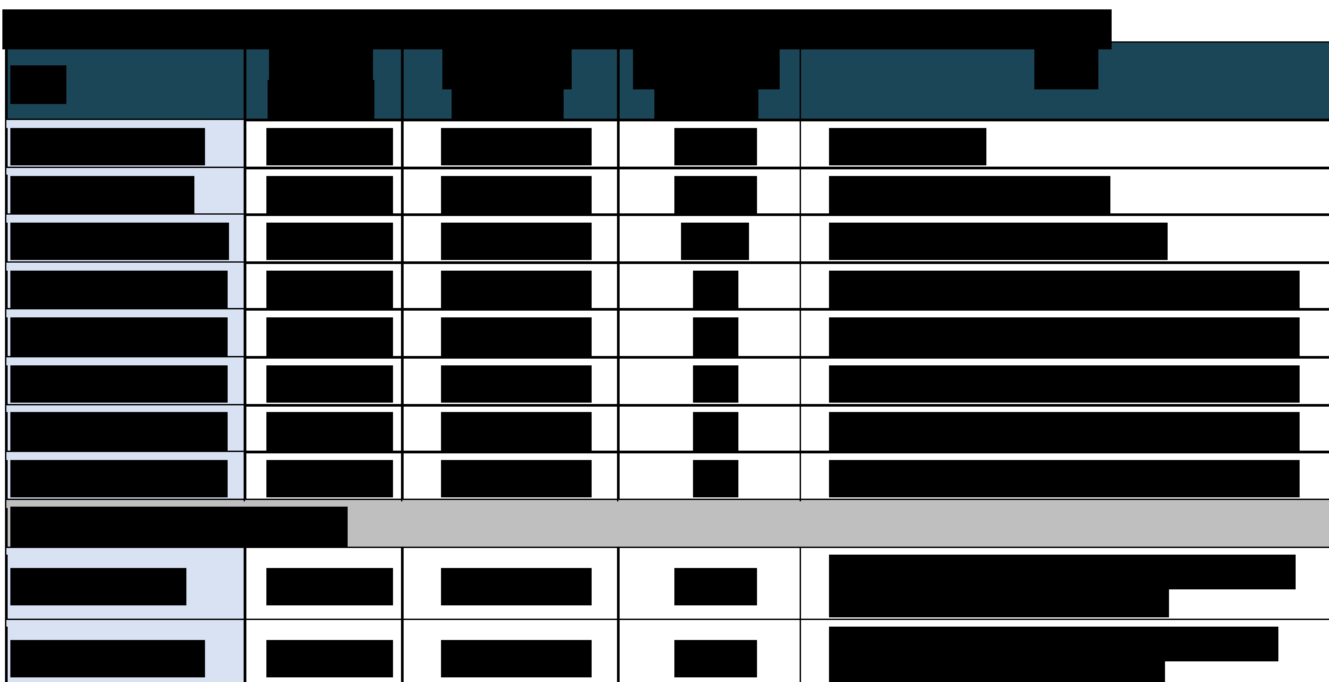
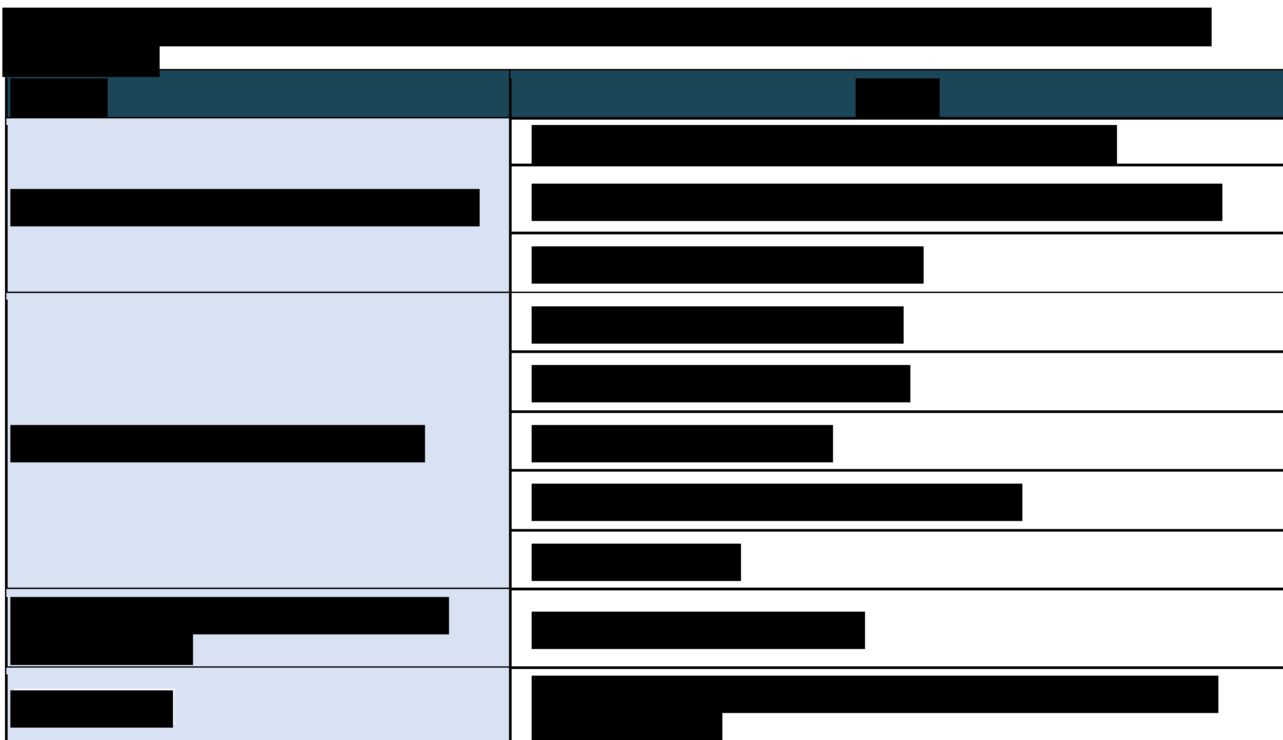
Milestone holds no known prior Resource Conservation and Recovery Act (RCRA), Federal UIC, National Pollution Discharge Elimination System (NPDES) or Prevention of Significant Deterioration (PSD) permits.

A list of applicable federal, state and local contacts within the AoR is presented in **Table 1-2** [40 CFR 146.82(a)(20)]. A list of non-UIC federal, state and local permits is presented in **Table 1-3** [40 Code of Federal Regulation (CFR) 146.82 (a) (1)].

the *Journal of the American Statistical Association* (1980, 75, 311-322) and the *Journal of the Royal Statistical Society, Series B* (1981, 43, 1-37). The latter paper is the most comprehensive treatment of the topic, and it is the source of the following summary.

A horizontal bar chart with 12 categories on the y-axis. The x-axis represents the number of samples, ranging from 0 to 1500. The bars are black, and the background is light blue. The distribution is highly skewed, with most categories having fewer than 500 samples, and a few categories having between 500 and 1000 samples. The categories are: 1, 2, 3, 4, 5, 6, 7, 8, 9, 10, 11, 12.

Category	Approx. Number of Samples
1	100
2	200
3	300
4	400
5	500
6	600
7	700
8	800
9	900
10	1000
11	1100
12	1200



1

1.3 Overview Maps of AoR [40 CFR 146.82(a)(2)]

Table 1-4 contains the coordinates for all injection and monitoring wells. **Figures 1-1 to 1-6** illustrate the proposed Well location, along with all pertinent items as required in 40 CFR 146.82(a)(2). The information is separated into various maps for ease of reference and discussion. An omnibus map encompassing every element in this section is located in **Section 1.3.5, Figure 1-7**.

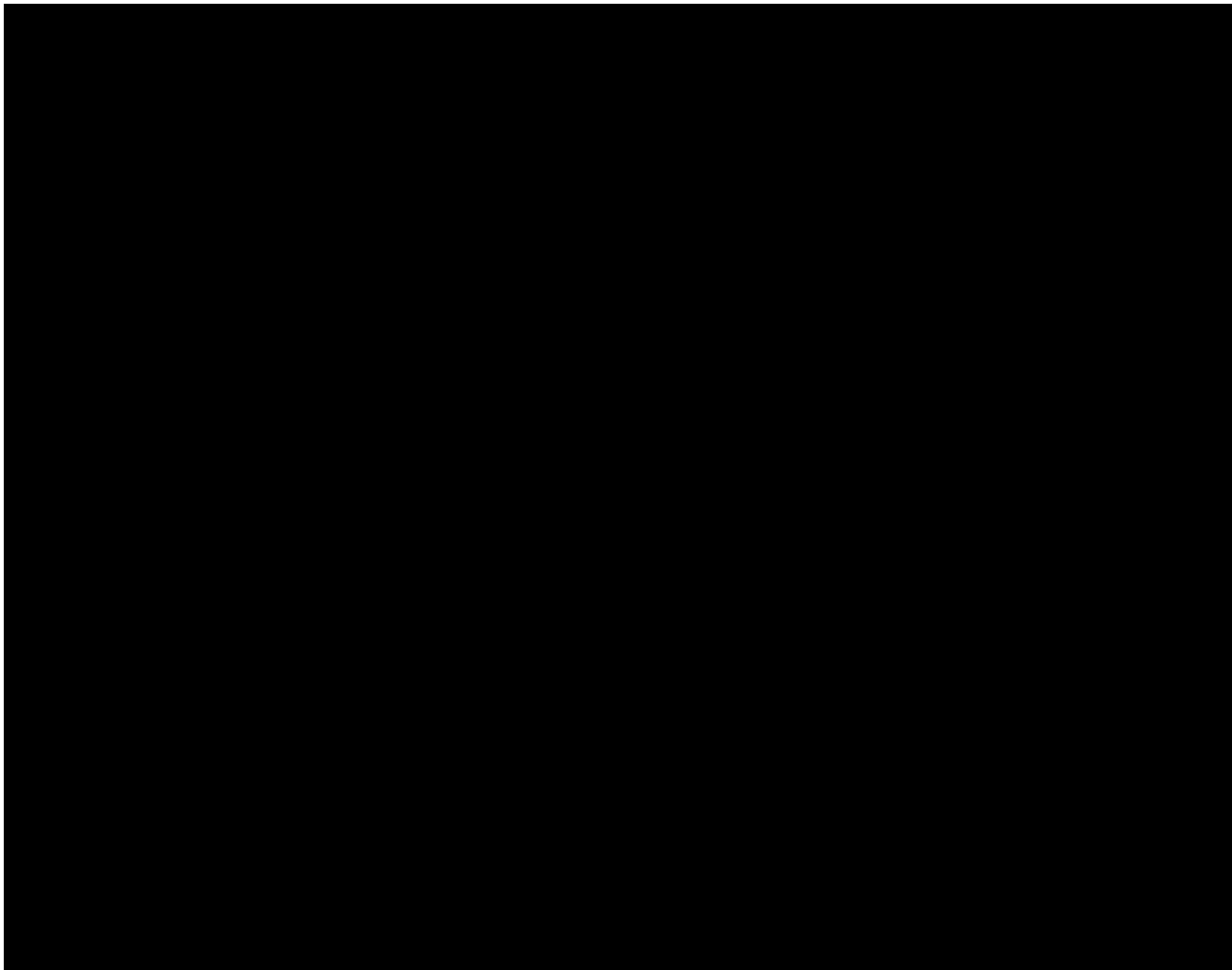
1.3.1 Major Roads Nearby Injection Site

The Facility will be situated in the northern part of Upton County, Texas. The property on which the well is located, leased by Milestone,

(Figure 1-1).

The Well is situated in the unincorporated community of

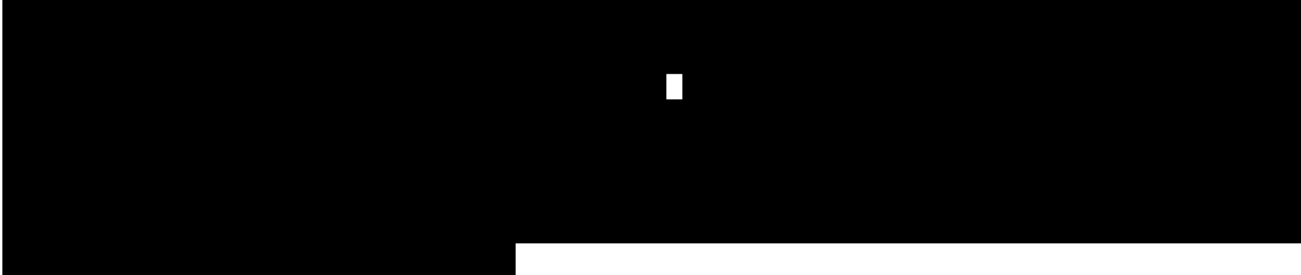
. There are a large number of unnamed lease roads in the vicinity associated with oil and gas activity (Figure 1-2).



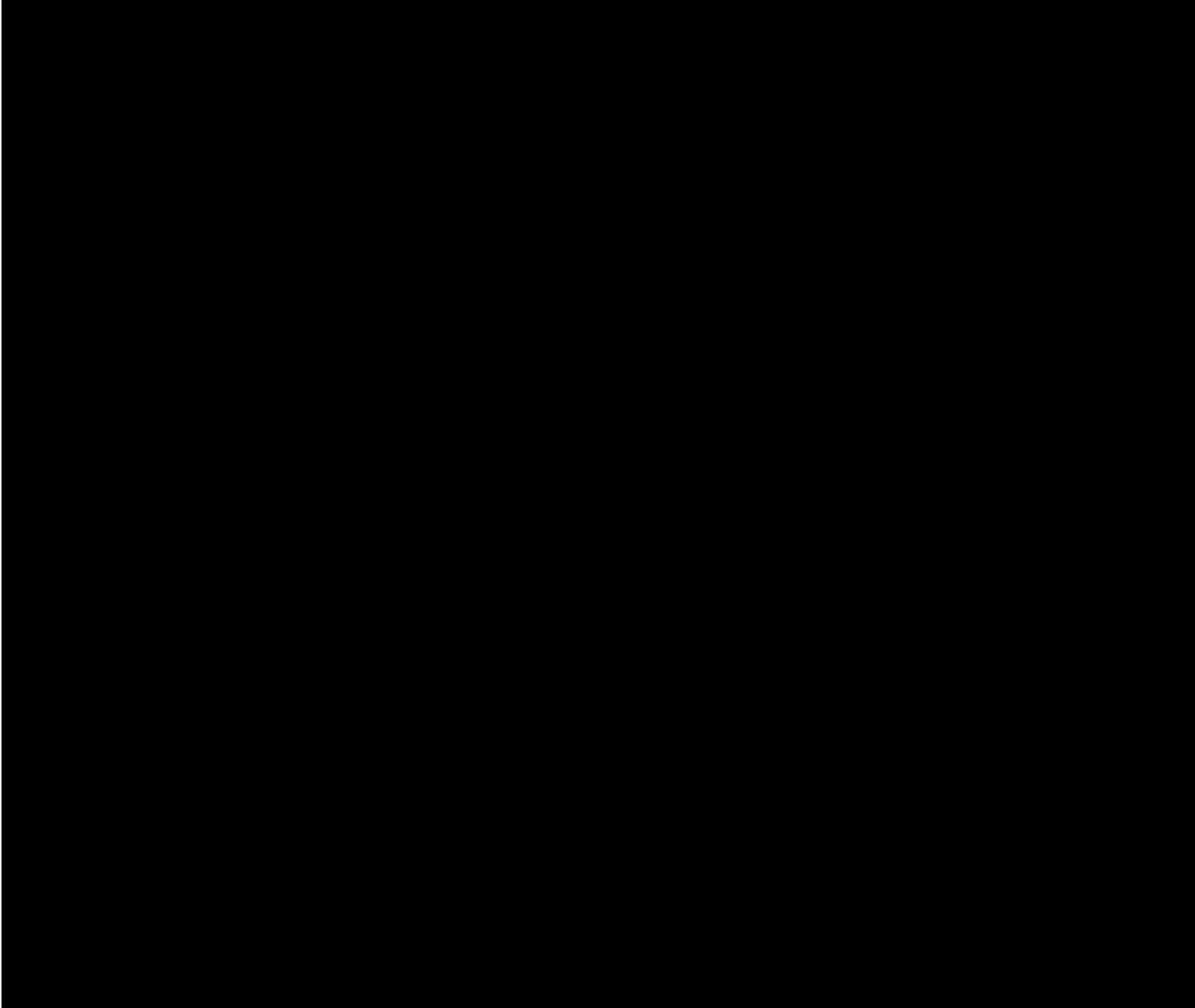
Figure

1.3.2 *Mines, Superfund Sites, Quarries, Other Hazardous Sites*

No EPA sites of any kind occur within the AoR.



See Figure 1-3 for



1.3.3 Map of Rivers, Springs, Wells, Other Water Features

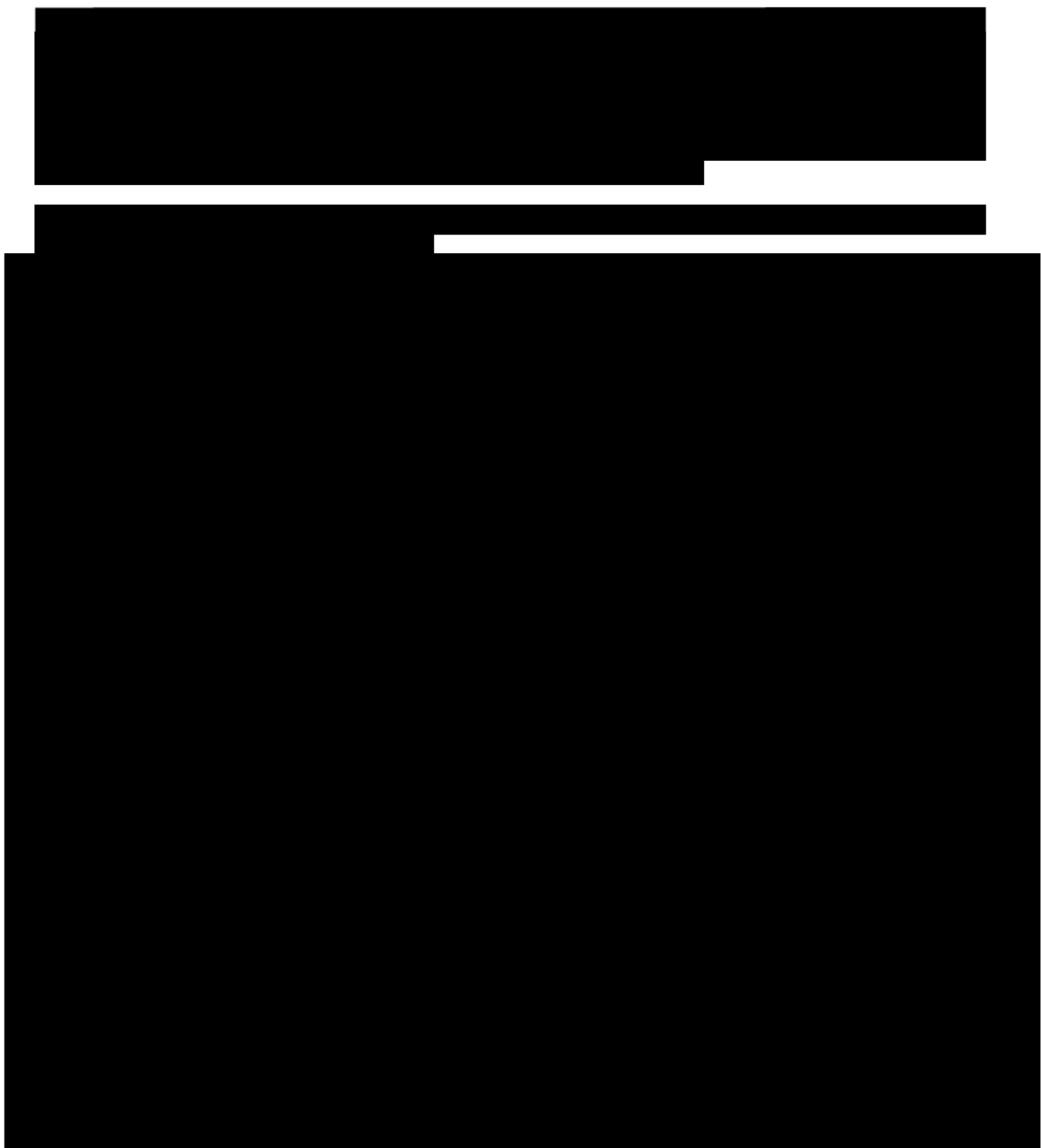
Climate in Upton County is a *hot semi-arid* based on the Koppen climate classification (Beck, et al. 2018). There are limited natural water sources in the vicinity of the AoR.



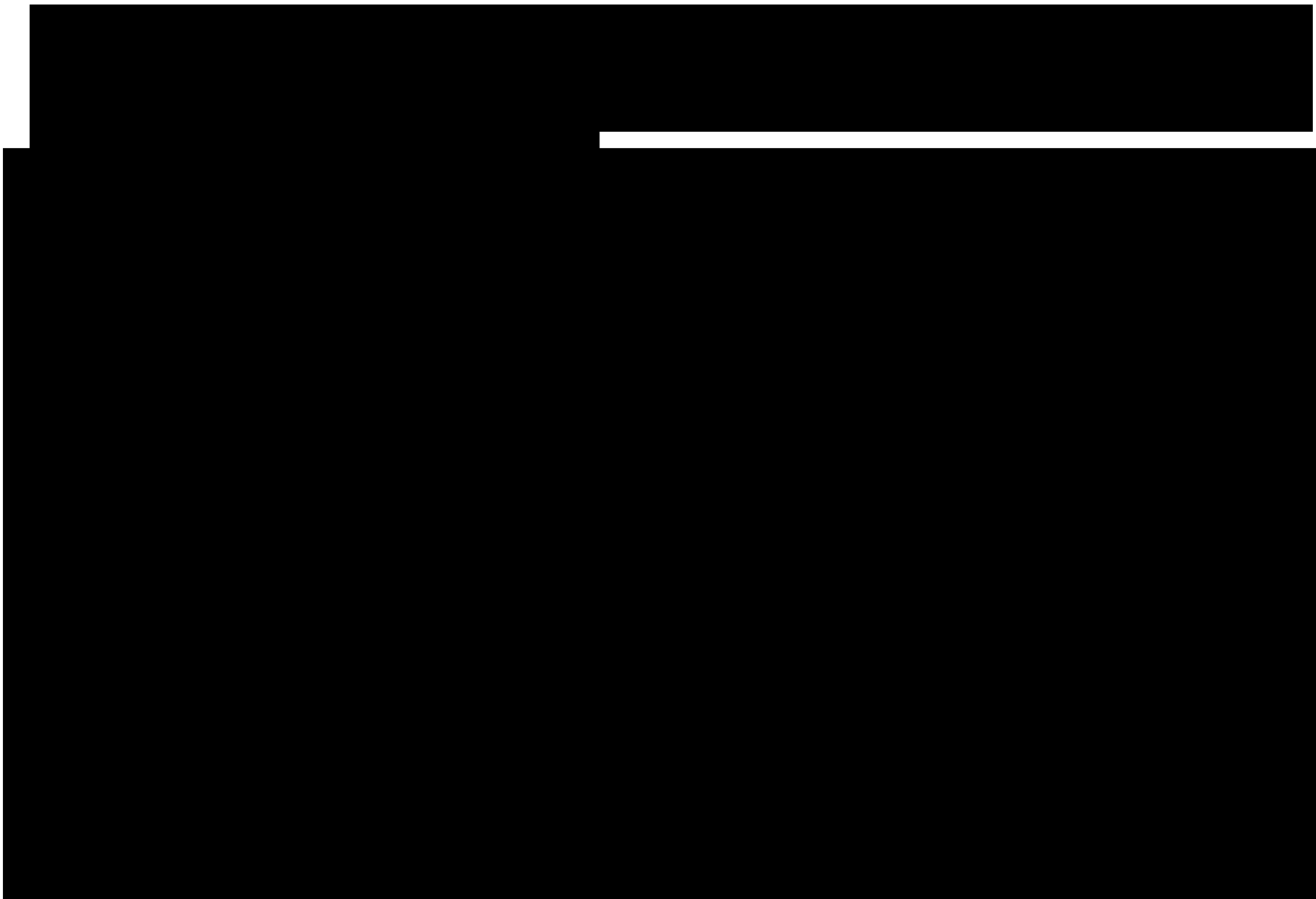
Sample records are included in as an appendix attachment, *TWDB Individual Water Well Files*. The wells are labelled with an assigned index number. A table of water wells with locations, index number, and available TWDB information is presented in **Table 1-27, Section 1.14**



1.3.4 Map of Oil and Gas and Injection Wells in the Area of Review (AoR)

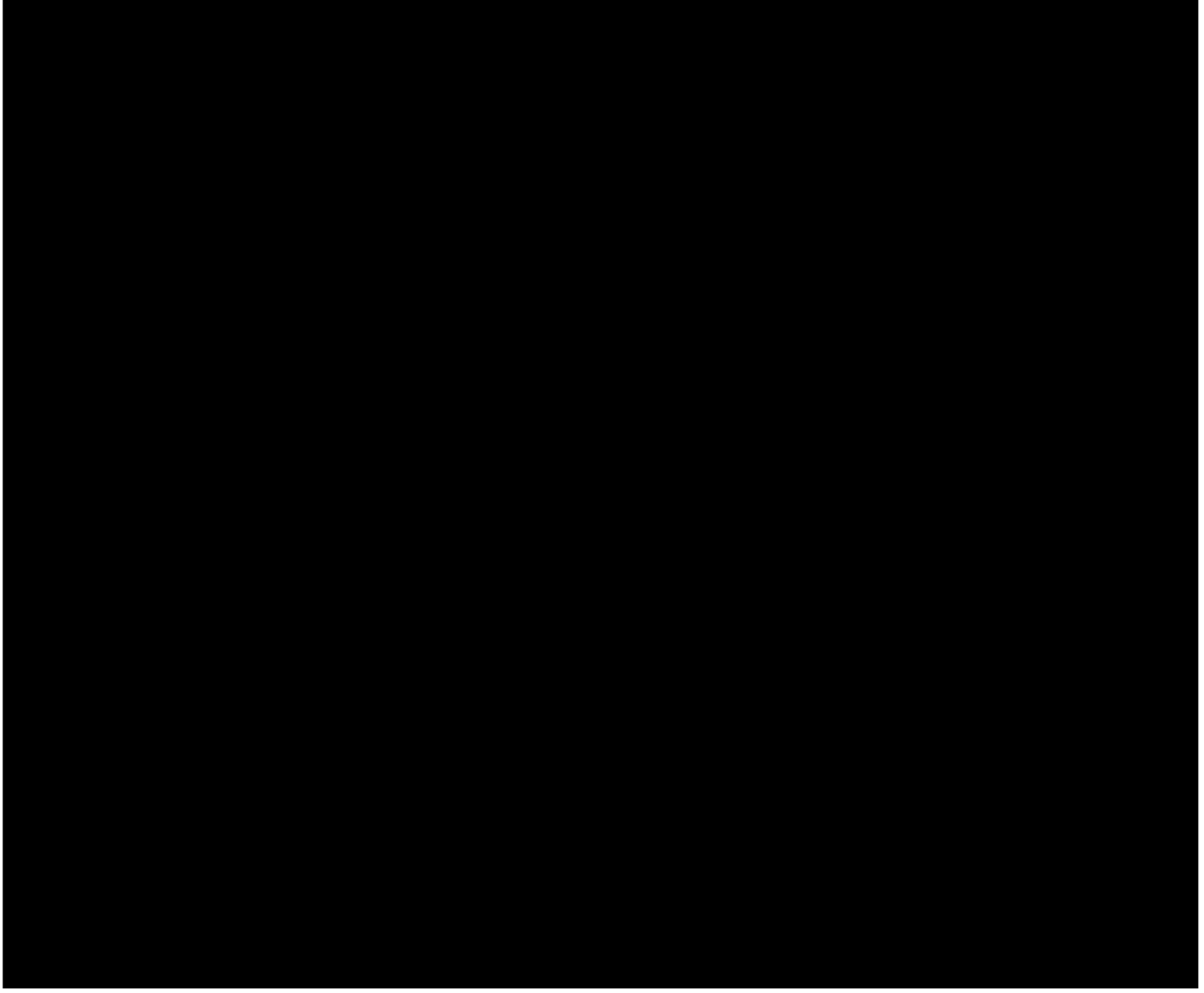


1.3.5 *Structures Near AoR*



1.3.6 *Omnibus Map [40 CFR 146.82(a)(2)]*

The information contained in **Sections 1.3.1 through 1.3.5** is contained in the map in **Figure 1-7**. Deep penetrations are labeled at the surface location by the well index number is presented in **Table 1-28**. Water wells are labeled with index number is presented in **Table 1-27**.



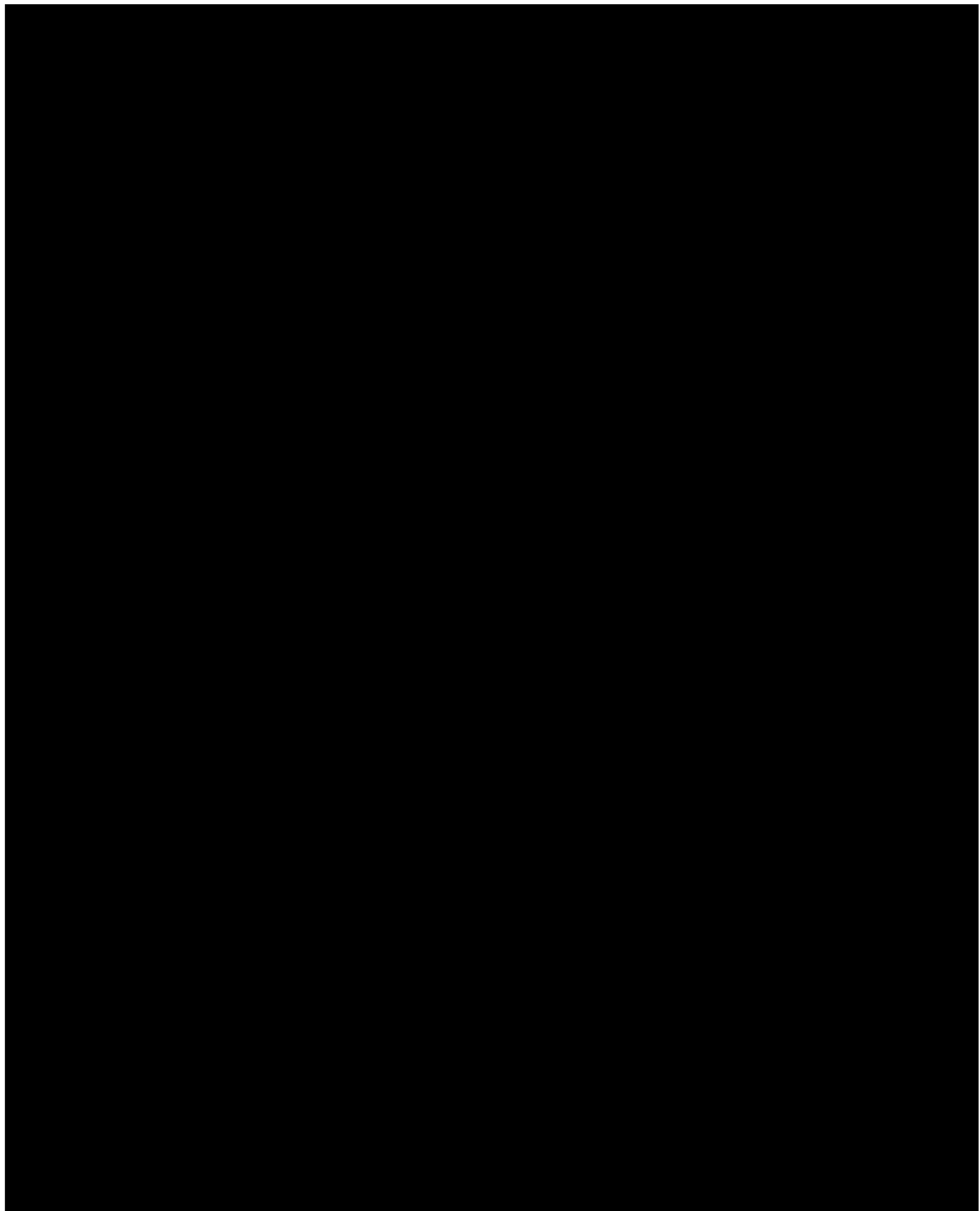
1.4 Regional USDW Characterization and Hydrogeology [40 CFR 146.82(a)(3)(vi), 146.82(a)(5)]

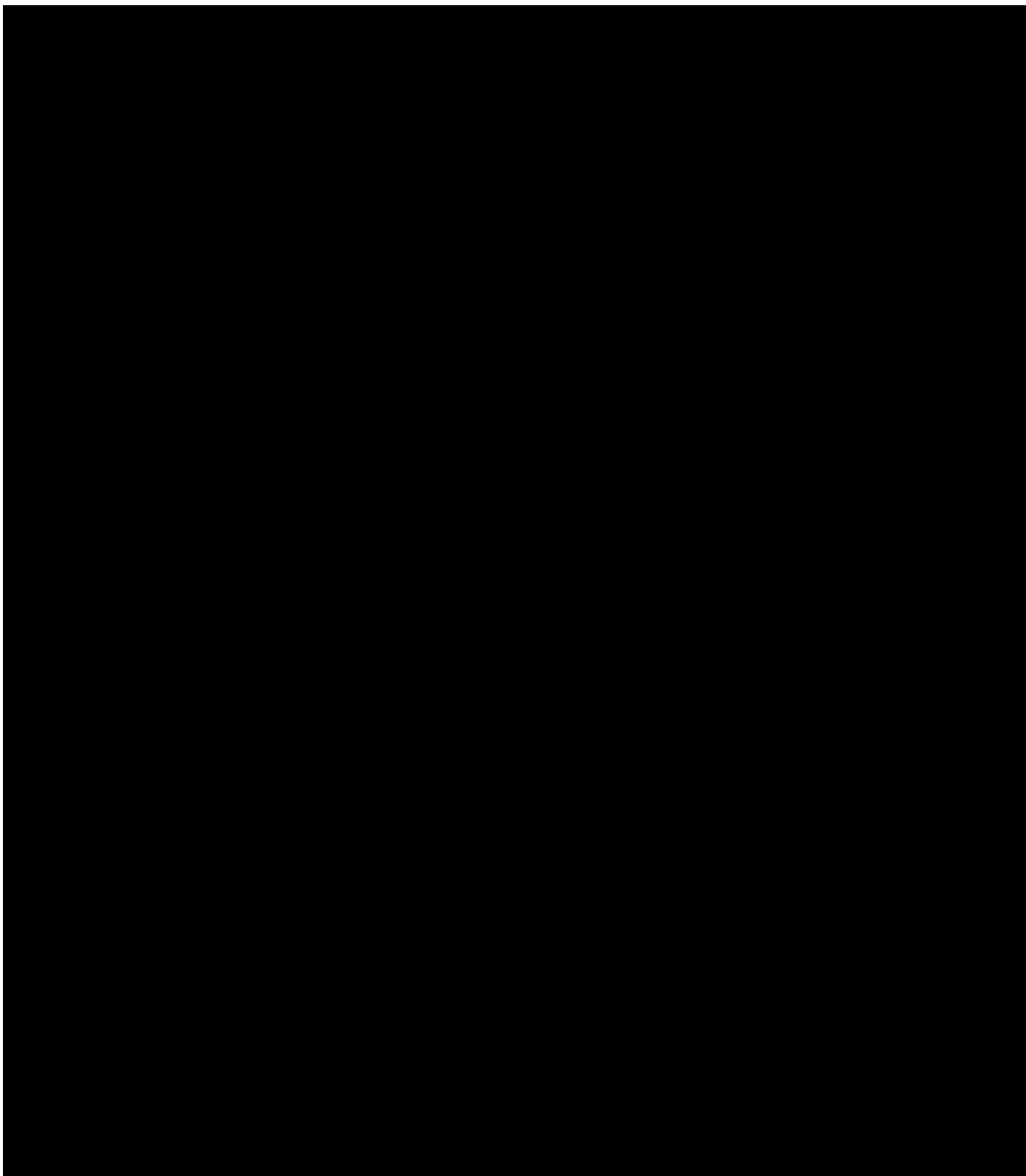
This section describes the general vertical and lateral limits of all Underground Sources of Drinking Water (USDW), water wells and springs within the AoR, their positions relative to the injection zone, and the direction of water movement, where known.

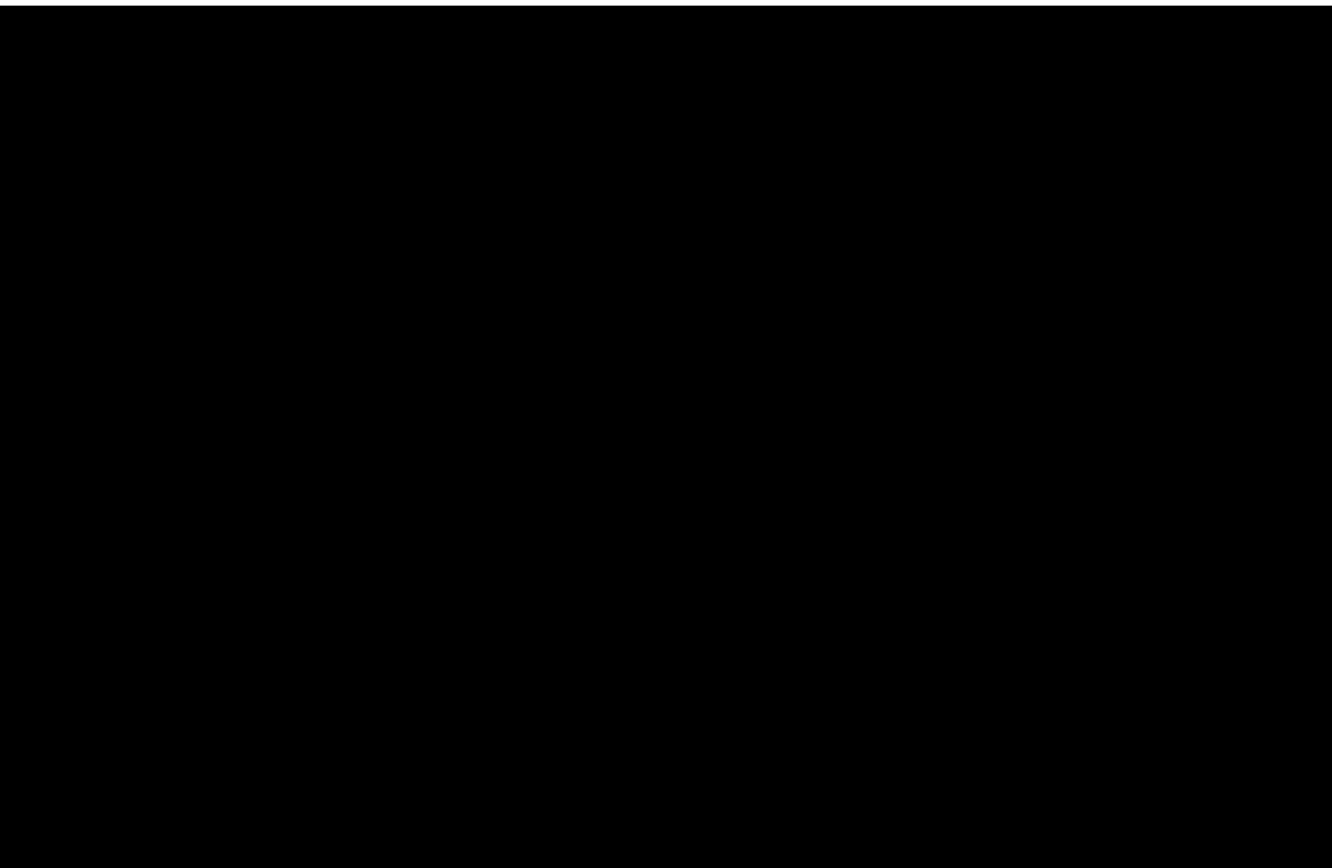
The Texas Railroad Commission Ground Water Advisory Unit (RRC GAU) has set the base of USDW [REDACTED] (GAU Determination letter, **Section 13, Appendix I**) The [REDACTED]

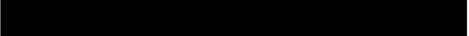
The 2011 Aquifers of Texas report and 2016 Texas Aquifers report by the Texas Water Development Board (TWDB) identified two potential aquifers in the vicinity of the [REDACTED]

In Upton County, of the two [REDACTED]



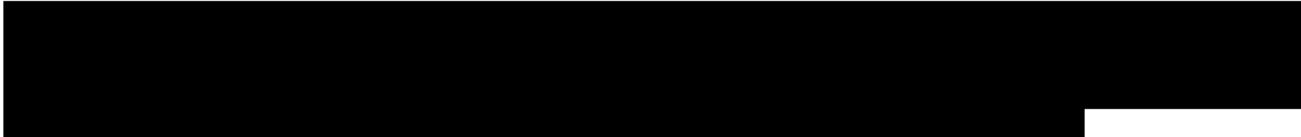




1.4.1 



The Antlers sand dips southeasterly at an average rate of about 10 ft per mi. In most of the



[REDACTED]

[REDACTED]

County).

A histogram of total dissolved solids (TDS) for

[REDACTED]

In addition to other

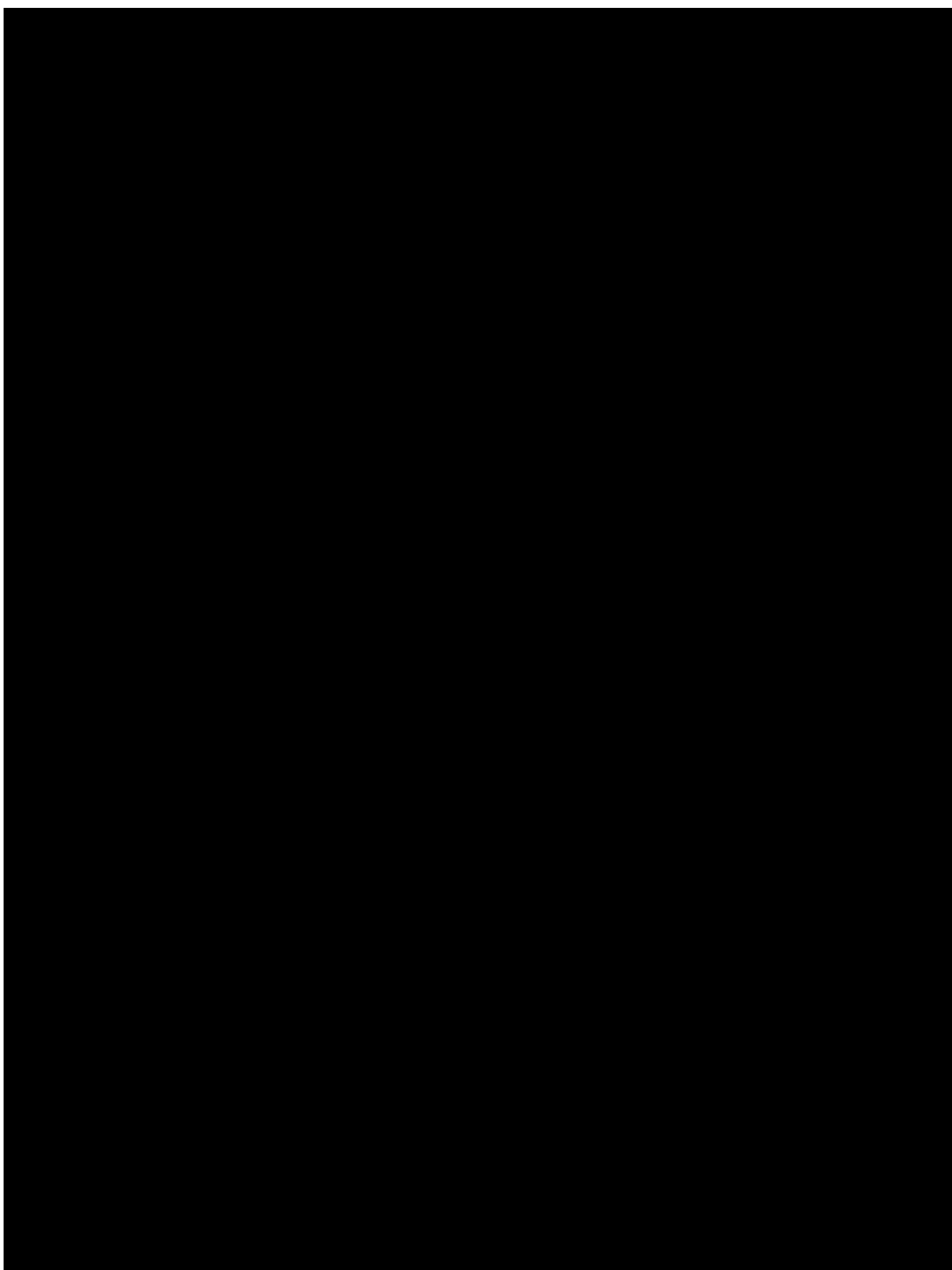
[REDACTED]

[REDACTED]

Hydraulic characteristics that influence the effectiveness of an aquifer to yield to water a pumping well include transmissivity and storage coefficient.

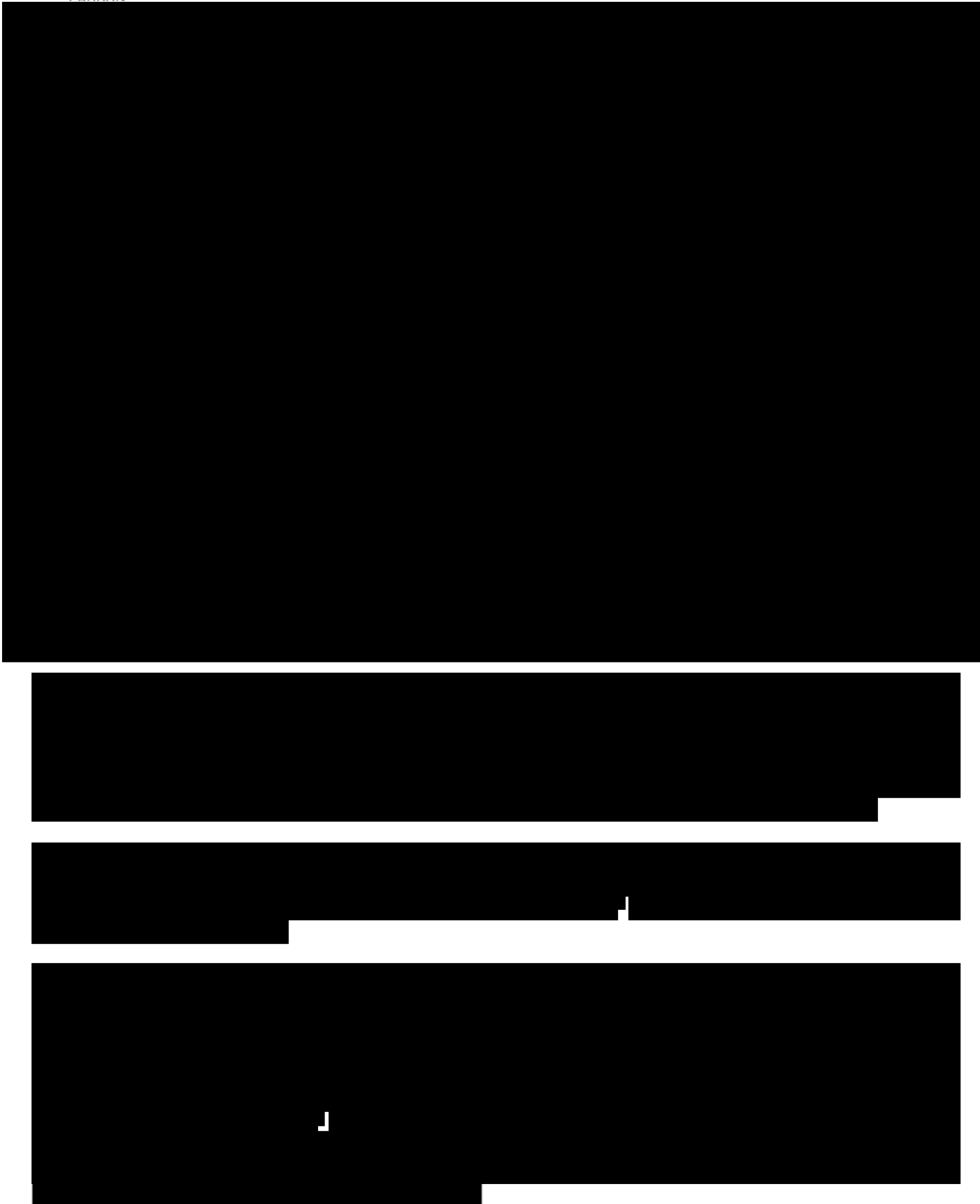
The highest average water analyte is [REDACTED]

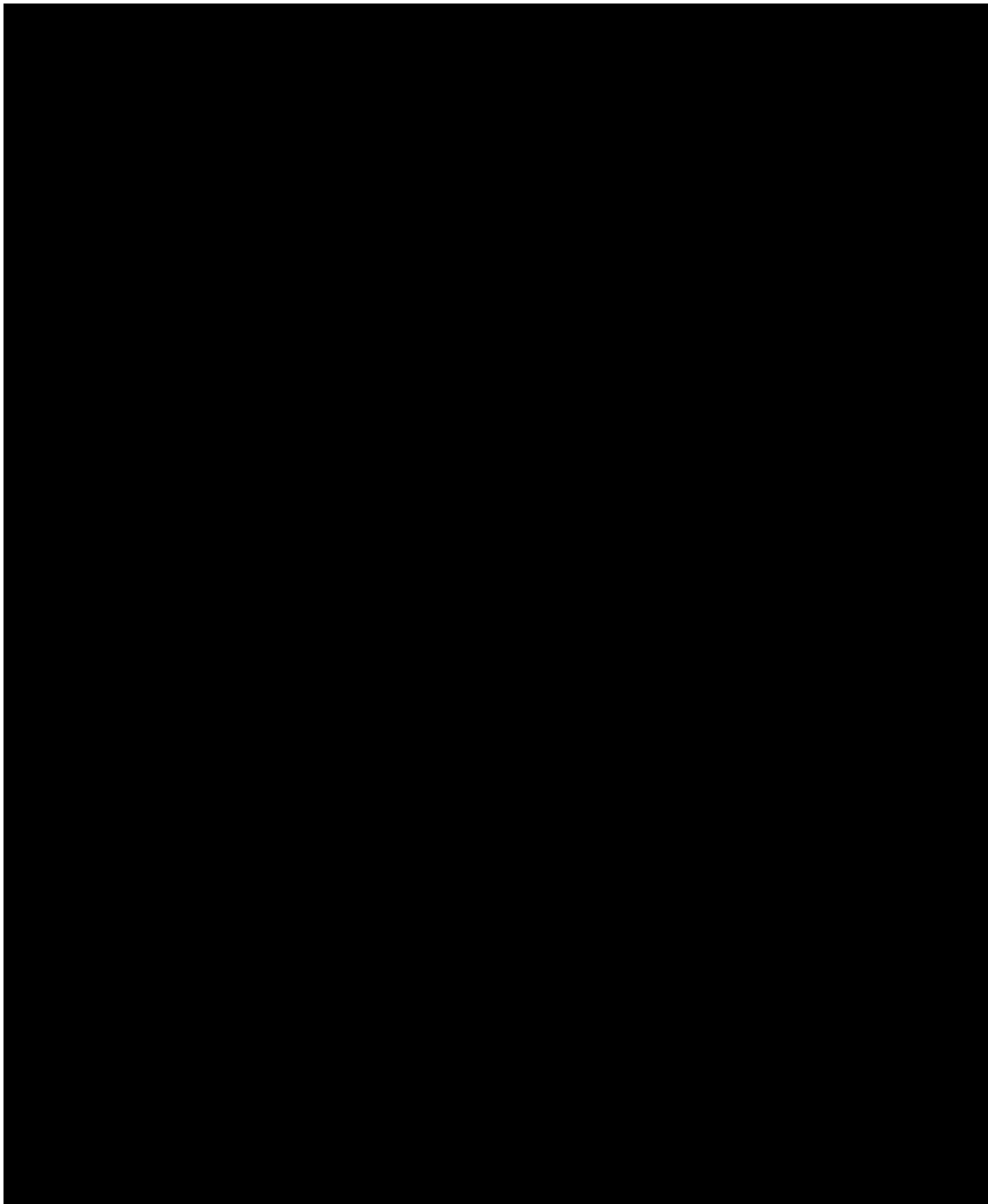
[REDACTED]

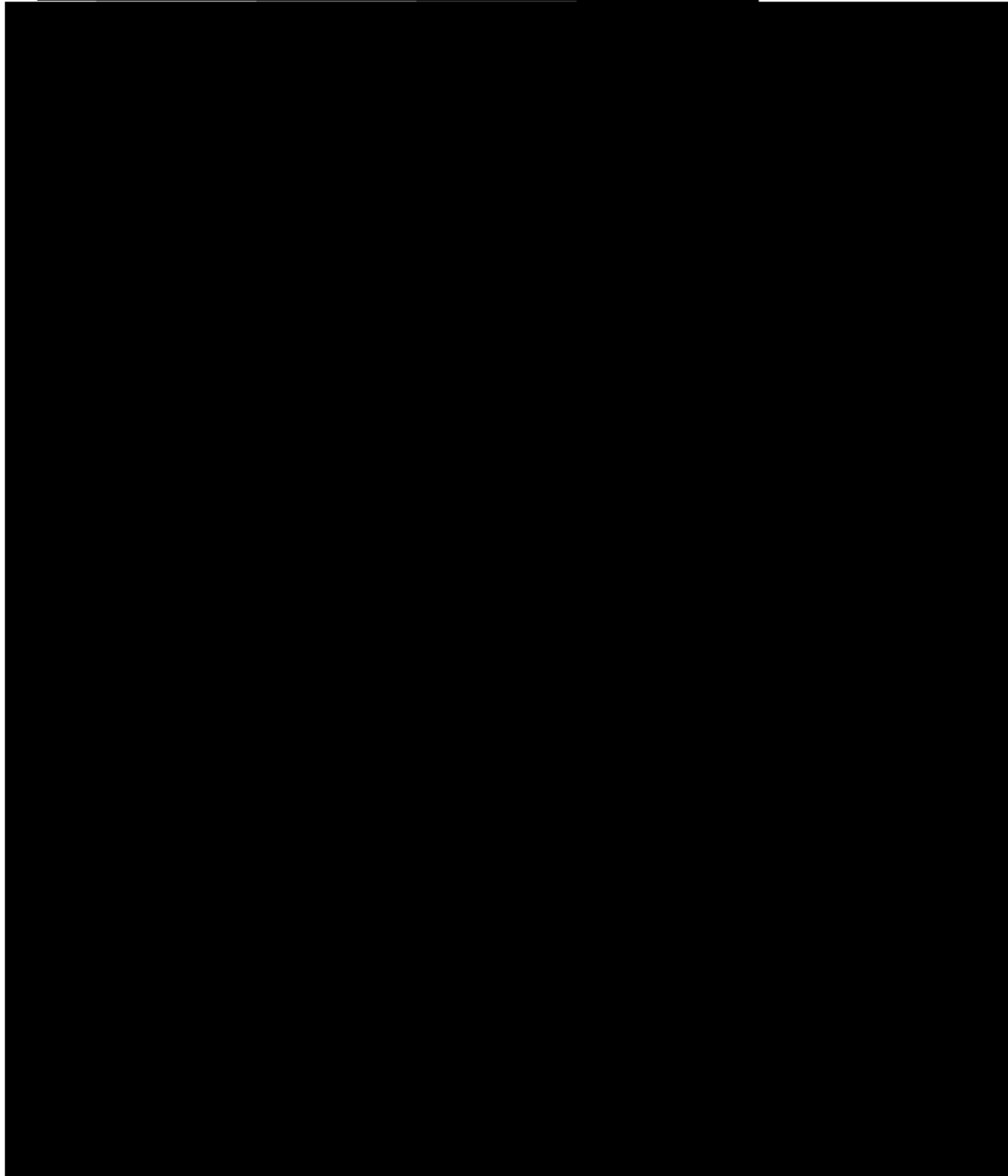


1.4.2









Regionally, the [REDACTED]

[REDACTED]

[REDACTED]

As reported in the literature, this water testing show [REDACTED]

[REDACTED]

from

Oklahoma [REDACTED]

1.4.3 [REDACTED]

Red Star notes Midland CCS #2 location. For additional information on monitoring wells see Section 1.3 or Section 6

1.4.4 RRC GAU and TWDB Data

The Texas Railroad Commission Ground Water Advisory Unit (GAU) has set the base of freshwater at 350 ft for all oil and gas production wells [REDACTED]

[REDACTED] The depths in this paragraph come from a review of the GAU determinations in RRC records for nearby oil and gas wells.

Milestone submitted an additional request to the GAU (dated 10/18/2024) for a determination of base of USDW; the GAU determined a base depth of [REDACTED]

[REDACTED] (GAU Determination letter, Section 13 Appendix I).

The TWDB has two continuously monitored wells in Upton County to the east of the site near Garden

[REDACTED]

[REDACTED]

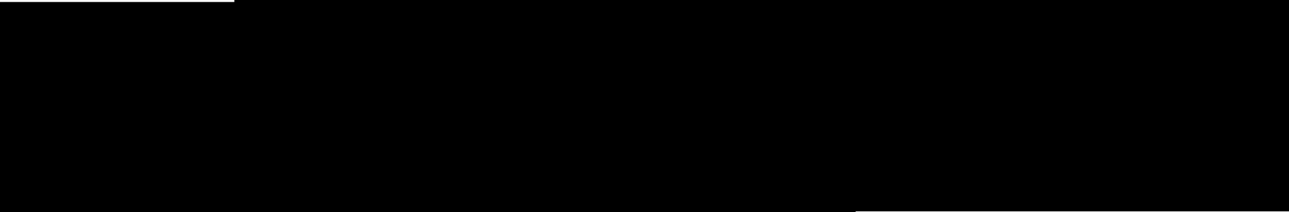
[REDACTED]

1.4.5 Springs and Surface Water

There are [REDACTED] in Upton County.



There are several [REDACTED]



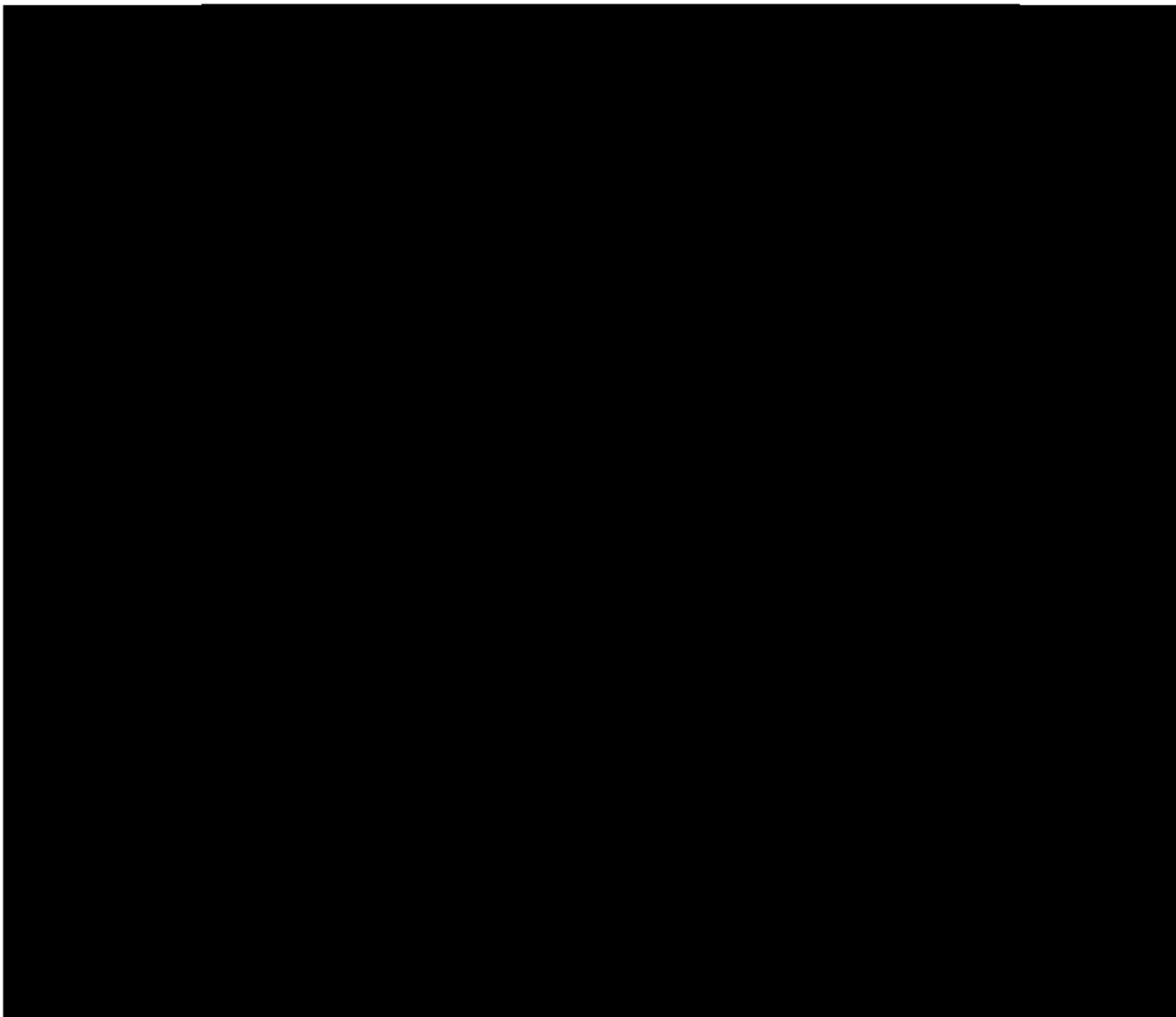
1.5 Regional Geology [40 CFR 146.82(a)(3)(vi)]

The proposed Injection Well is located in the southern portion of the Midland Basin within the larger Permian Basin, as seen in **Figure 1-23**. The Midland Basin is the major eastern structural subdivision of the Permian Basin and is contained by the Central Basin Platform to the west, the Northwest Shelf to the north, the Ozona Arch to the south, and the Eastern Shelf to the east.

The proposed injection units



Note: A more detailed treatise on Permian geology and regional background information is located in **Section 13 Appendix K**. Please consult for detailed depositional, lithologic and structural information on all formations within the injection zone and top seals. This section of the permit is intended to briefly summarize the extensive volume of work that has been published on the Permian and Midland Basins over the past 120 years. However, the brevity in this section of the permit application, intended for ease of reading, should **not** be construed as a lack of material or extensive research.



1.5.1 Stratigraphy

The proposed [REDACTED]

A generalized stratigraphic column for the Midland Basin

(right most) is shown in **Figure 1-24**.



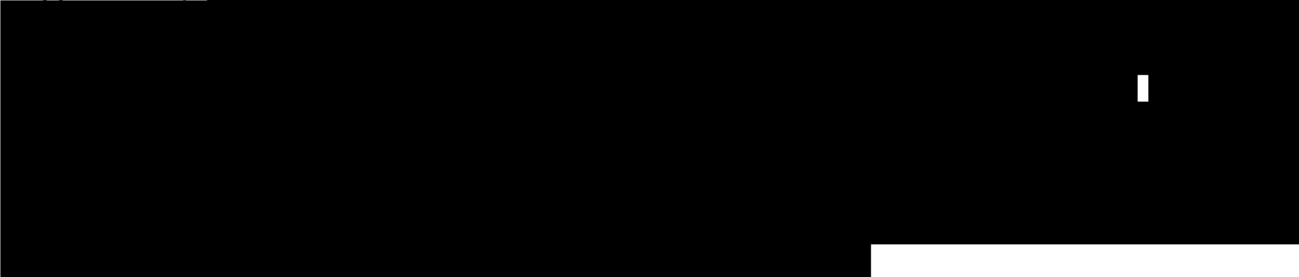
Next is the San Andres formation, a prodigious wastewater injection zone that has been used continuously in the region since at least 1978, followed by the Leonardian aged Spraberry and Dean formations.

Below the Dean is the Wolfcamp formation. The Spraberry and Wolfcamp formations are currently being drilled for oil and gas wells in the AoR. The majority of the wells producing from these formations are horizontal although there are also legacy vertical wells.

Below the Wolfcamp starts the Pennsylvanian section of rock. The Pennsylvanian aged Cisco and Canyon form a sequence of argillaceous shales and the Strawn and Atoka are predominantly carbonate benches. Following this, the Upper Mississippian Barnett Shale is present, which is equivalent to the Barnett Shale in the Fort Worth Basin. This is underlain by the organic Woodford Shale (**Figures 1-24, 1-25**). [REDACTED]



Next, is the Undifferentiated Devonian section which alternates between packstone and chert (S. Ruppel, 2008). [REDACTED]

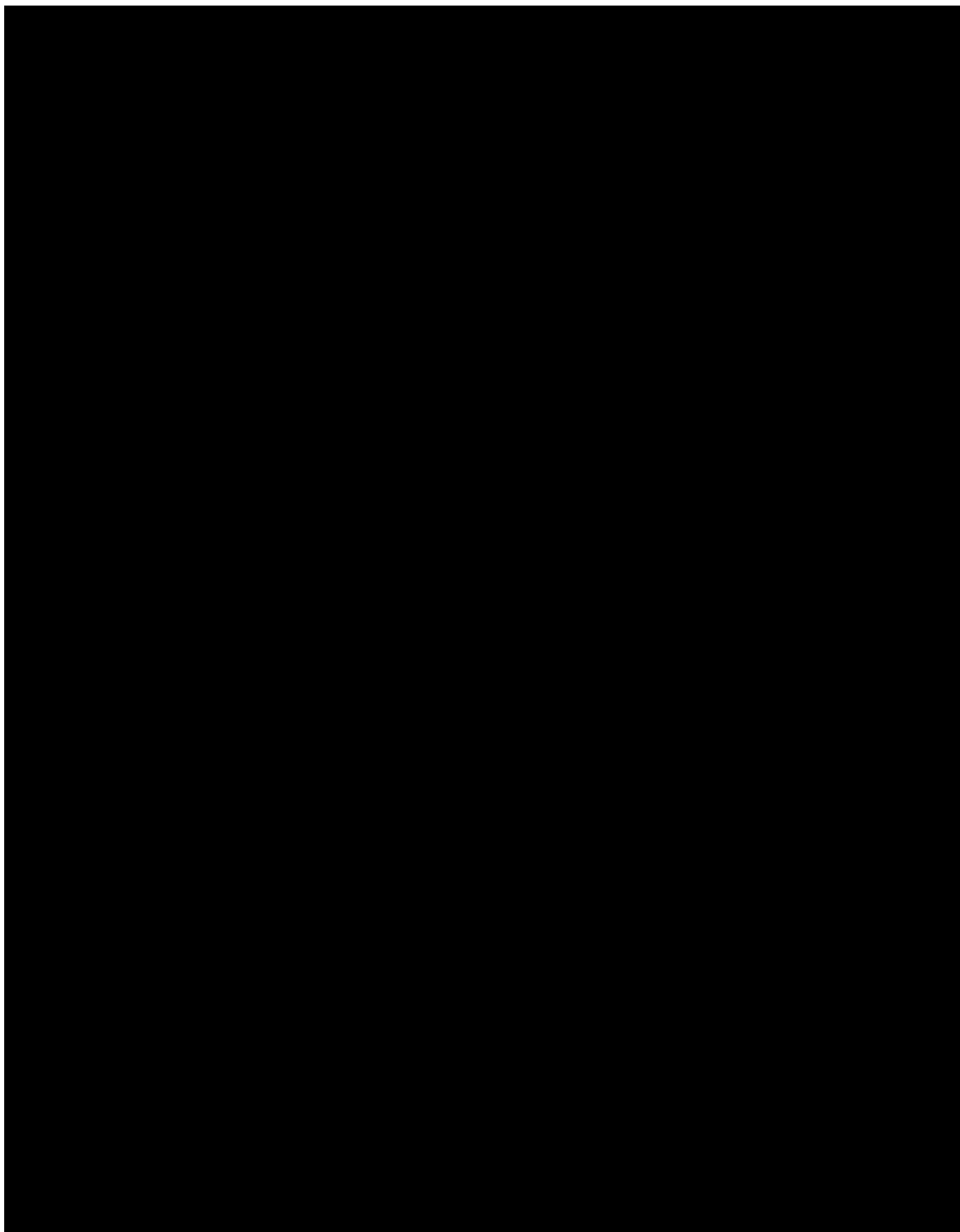


Finally, at the base of the section right above basement, is the Cambrian-aged Bliss sand. It is [REDACTED]



Stratigraphic charts found in **Figures 1-24 and 1-25** with [REDACTED]





At the Facility, [REDACTED]

[REDACTED]

[REDACTED]

1.5.2.1 Mississippian Shale (Barnett) – [REDACTED]

The interval of Mississippian age with high gamma ray is referred to as the Barnett Formation (see type log in **Figure 1-42/Figure 1-82**). The Barnett sits above a Mississippian carbonate which is in turn underlain by the Woodford shale (**Figures 1-24, 1-25**) in most parts of the basin. The Barnett is generally overlain by carbonate rich strata usually termed “Pennsylvanian Limestone” (or Lime) and often referred to as “The Atoka.”

The Mississippian is one of the most poorly known depositional successions in the Permian Basin. This is largely due to the fact that only small volumes of oil and gas have been produced from these rocks and there has thus been little interest in collecting data to interpret them. This has recently changed due to the successful development of the Barnett formation in the nearby Fort Worth Basin as a reservoir of natural gas (Montgomery, 2005; Ruppel and Kane 2008). Also contributing to poor understanding of the Mississippian section is the fact that it often washes out on well logs due to smectite rich clays.

Total Mississippian thickness varies widely across the Permian Basin area. A maximum thickness of more than 2,200 ft was reported by Craig and Connor (1979) in parts of Reeves and Ward Counties, Texas (see **Section 13, Appendix K** for additional maps on regional thickness). Mississippian can be <500 ft thick in areas of New Mexico where it transitions to a carbonate facies.

The mineralogy of the Mississippian shales is primarily quartz, calcite, smectite, and illite in roughly equal abundance. Higher gamma ray intervals increase clay and quartz minerals at the expense of carbonate minerals. Organic matter is present and indicated by intervals of high gamma ray and lower density. The shales are generally very fine grained with no distinguishable grains without the aid of electron microscopes.

Thus, the Mississippian is characterized by thick smectite-rich shales. [REDACTED]

[REDACTED] There is a minor carbonate member right above the Woodford that is probably Meramacian to Kinderhookian in age. This carbonate is the eastward extension of the undifferentiated Mississippian Lime.

[REDACTED] In the Permian Basin, lithologic, electric log, and sparse faunal data indicate that the Woodford unconformably overlies rocks ranging in age from Devonian to Ordovician (Lloyd, 1949). The Woodford is overlain disconformably by Mississippian limestone and Barnett Shale (Lloyd, 1949; Wright, 1979) (**Fig.1-24**).

Ellison (1950) divided the Woodford formation into three units using radioactivity, log response, and lithology. The Upper Woodford Shale is defined as brownish-black pyritic fissile shale with few resinous spores and abundant chert. It generally has medium gamma ray response and lower organic matter and clay content. The Middle Woodford Shale is characterized by the highest readings of gamma ray and the most abundant spores. It is generally high in clay and organic matter. The middle unit is also the most widespread unit of the Woodford Shale. The Lower Woodford Shale is characterized as a siliceous shale with few spores, medium chert content, lowest gamma ray and the highest resistivity of the three units.

The composition of the Woodford primarily consists of organic matter and illite, and the silt-sized fraction consists of mostly dolomite, quartz, pyrite, mica, feldspar, glauconite, biogenic pellets, spores, and radiolarians. Other types of fossils, including conodonts, brachiopods, trilobites, sponge spicules, and vertebrate debris, were found locally, but only rarely.

In terms of texture, parallel laminae are the most characteristic feature of black shale. Other distinguishing features include abundant pyrite, fine grain size, black color, and high radioactivity. The black color is caused by high concentrations of pyrite (as much as 13 vol %) and organic carbon (up to 35% by volume) and high radioactivity is caused by tetravalent uranium bound in the organic matter (R. Comer, 1991), (Haecker, 2016).

In the Midland Basin,

The Woodford, at its thickest, is 135 ft in north-central Martin County. Areas greater than 100 ft thick are located in Dawson, Gaines, Andrews, and Martin Counties. Between the thick areas lie an east-west trend of relatively thin Woodford (50 to 100 ft). Another narrow thin trend (<50 ft) lies in southern Martin and southeastern Andrews Counties (Figure 1-26).

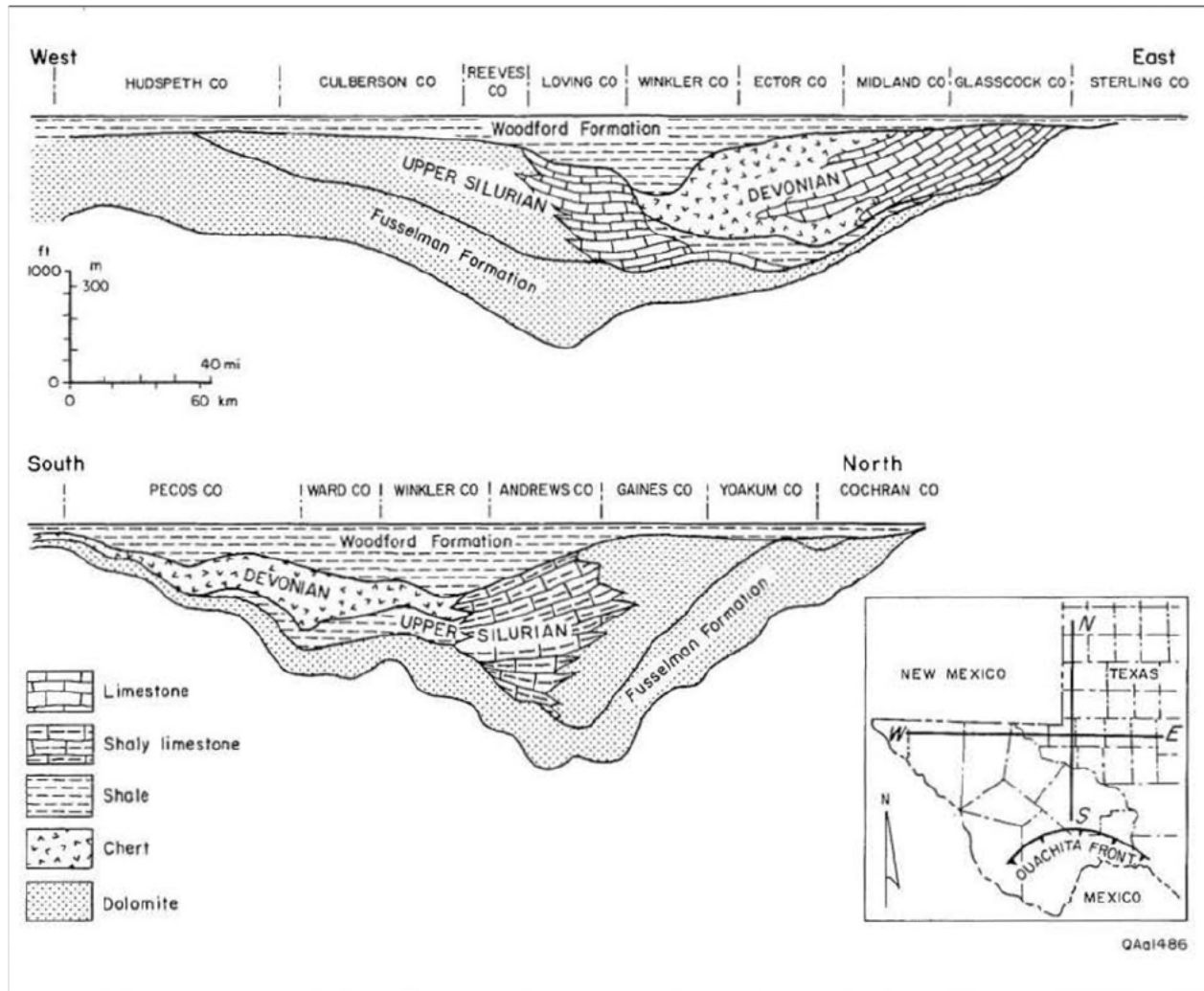


Figure 1-26: Woodford Schematic Cross Section

Schematic Cross Section of the Woodford and below Stratigraphy. (Ruppel and Holtz, 1994)

The interval

Devonian aged undifferentiated packstones and cherts are often referred to as 'Devonian' in the remainder of this document, the Woodford is not included in this lithologic grouping even though the lower Woodford is also Devonian in age. The unconformity at the base of the Woodford is used as a lithologic boundary despite using *Devonian* age to name of the deeper rocks.

Throughout most of west Texas, undifferentiated Devonian rocks comprise two distinct facies: (1) skeletal carbonates, primarily pelmatozoan packstones and grainstones, and (2) bedded, commonly spiculitic, chert (Saller and others, 1991). Chert is most abundant in the basin depocenter. In this region, the general stratigraphic succession consists of basal laminated dark cherts and lime mudstones that pass upward into laminated to massive spiculitic cherts overlain by skeletal lime packstones. In other words, generally packstone is found near the Woodford-Devonian unconformity, and chert deeper in the interval (Ruppel et al., 2008).

The Wristen Group is argillaceous and organic with the Frame and Wink members present in the southern Permian Basin and the carbonate rich Fasken member present in the northern Permian Basin. The Fusselman and Montoya Formations are composed of shallow water carbonates, principally ooid grainstones and pelmatozoan packstones.

Open and closed fractures are common in both chert and carbonate facies; however, cherts at Three Bar Field contain two to six times as many fractures as associated limestones. In addition, fractures are more abundant close to identified fault zones (Ruppel and Hovorka, 1995).

Reservoir quality porosity is typically associated with chert facies as opposed to the carbonate facies, and chert of a distal and discontinuous nature has been noted in Upton County in core description.

The Fusselman formation and Montoya Group are carbonate rich and generally lower porosity than the chert facies above.

Mineralogy of the undifferentiated Devonian is primarily quartz in the chert intervals and calcite in the packstone intervals with some illite present. The Silurian-aged Wristen Group is generally finer grained and may contain organic matter. The Wristen Group, Fusselman Formation and Montoya Group are known to contain trace amounts of dolomite as well.

The Packstone facies is generally fine grained and light gray in color, while the chert facies are generally darker grey and easily distinguishable in core sample.

The Simpson Group is a low permeability group of Ordovician shales and sands [REDACTED]

[REDACTED] It is characterized by multiple formations. It has three (3) sandstone formations and three (3) shale formations, alternating in sequence. Shale is present on top then corresponding sand, then it repeats. The three sandstone members of the Simpson Group—the Connell, Waddell, and McKee—occur at the base of the Oil Creek, McLish, and Tulip Creek formations, respectively, from oldest to youngest. Detailed information on each formation can be found in **Section 13, Appendix K**.

Sandstones make up only approximately 5 percent of the total thickness of the Simpson Group in west Texas and southeastern New Mexico. Not all sandstones are likely present in all areas owing to their depositional setting facies changes updip and downdip.

Little-to-no fracturing is expected within the shale members of the Simpson Group forming an effective intrazonal seal of low vertical permeability rock.

The thickness of the Simpson Group ranges from 450-50 ft thick in the Midland Basin. The Bromide and the Tulip Creek pinch out as the formation thins. The Simpson is thickest in the western part of the Midland Basin in Crane County and thins to the east in Reagan County. [REDACTED]

[REDACTED]
[REDACTED]
[REDACTED] This may include the Cambrian Bliss Sand, although it is unclear whether it is unconformably eroded or not from available well logs.

The Ellenburger Group of the Permian Basin is part of a Lower Ordovician carbonate platform sequence that covers a large area of the United States (Kerans, 1989). It is well known for being one of the largest shallow-water carbonate platforms in the geologic record (covering thousands of square miles (sq. mi) and as much as 500 mi wide in west Texas. Extensive cave collapse features (karsting) lead to pervasive fracturing that occurred shortly after deposition. This fracturing enhances the permeability of the formation. Additional details are found in **Section 13, Appendix K**.

The Ellenburger is extensively fractured due to three stages of karsting that occurred repeatedly for millions of years as sea level rose and fell over an area that covered the entire Permian Basin. When sea level was lower than the carbonate platform, karst features would form. **Figure 1-27** illustrates the various stages of cave collapse. First water infiltrates and dissolves carbonate, after a void is created, the above ceiling collapses into the void due to gravity and weight. Finally, the entire chamber collapses and is compacted. These features are called cave collapse breccias or simply breccias and the process is referred to as brecciation. This process happened shortly after deposition and then the rock was subsequently dolomitized (Loucks, 2019).

Dolomitization favors preserving open fractures and pores because it is mechanically and chemically more stable than limestone. Pores within dolomites are commonly preserved to deeper burial depths and higher temperatures than those of pores in limestone. Also, limestone breccia clasts tend to undergo extensive pressure solution at their boundaries and lose all interclast pores whereas dolomite breccia clasts are more chemically and mechanically stable with burial (R. Loucks, 2007, 2019). Thus, even at extreme depths, pores and fractures are expected to be open and prevalent.

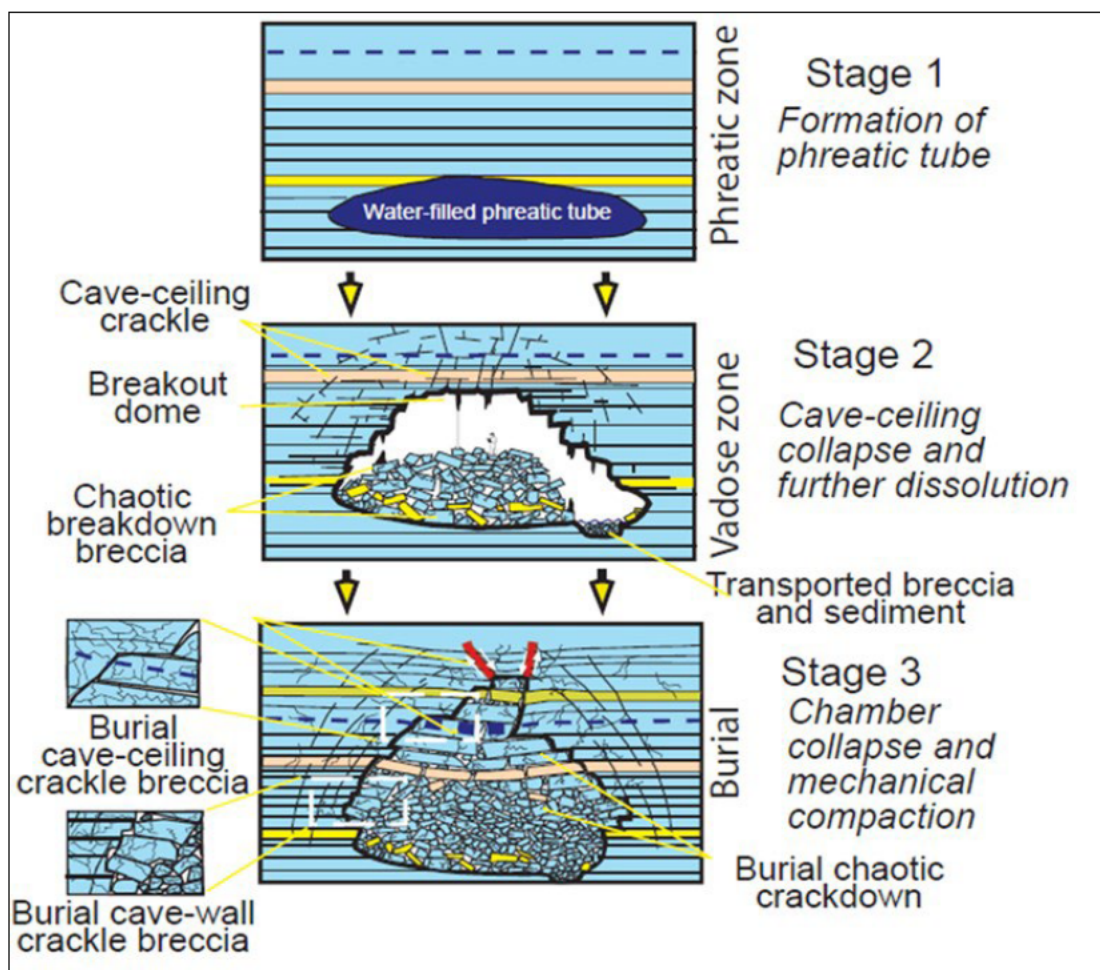


Figure 1-27: Cave Collapse Schematic

Process of Cave collapse that forms paleo cave breccias. First, water infiltrates the subsurface via hydrodynamic processes. Then, after a sufficient void is dissolved in stage 2, the continued burial and weight of overburden causes the cave to collapse (Loucks, 2023).

Pore networks in the Ellenburger are complex because of the amount of dolomitization, brecciation, and fracturing associated with karsting and regional tectonic deformation. Pore networks can consist of any combination of the following pore types, depending on depth of burial (Loucks, 1999): (1) matrix, (2) cavernous, (3) interclast, (4) crackle-/mosaic-breccia fractures, or (5) tectonic-related fractures (Figures 1-28, 1-29).

The Ellenburger's mineralogy is primarily composed of dolomite (>80% dolomite) but it may contain calcite, anhydrite, chert, gypsum and other minerals in small quantities at a core scale. Many minerals occur in minor quantities related to evaporite deposition or other chemical processes. Over 99% of the non-dolomite mineralogy is contained within the pervasive fractures.

The Ellenburger ranges from 2,500 ft to 500 ft thick in various parts of the Permian Basin.

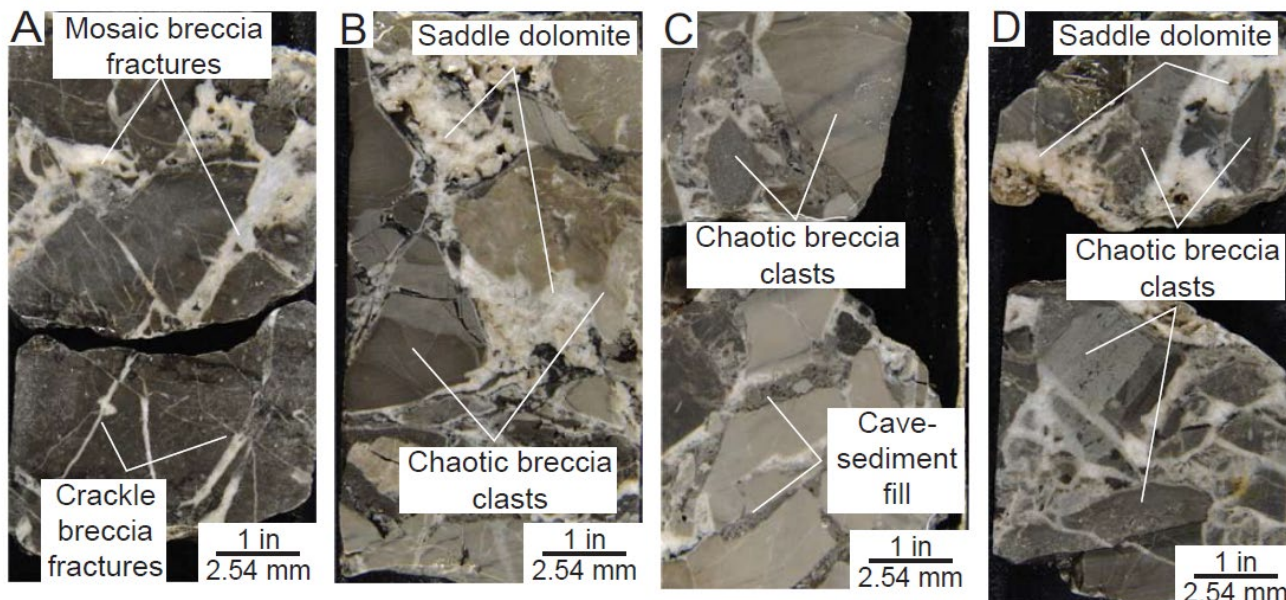


Figure 1-28: Meteoric karst breccias McElroy #1 Crane County, Texas.

Meteoric karst breccias from McElroy #1 core in Crane County, Texas. (Loucks, 2023)

Cave Facies	Interpretation	Description	Pore System/ Reservoir Quality
Undisturbed strata	Undisturbed host rock	Excellent bedding continuity for hundreds to thousands of feet.	Minor matrix and fracture pores. $\emptyset < 3\%$ to 5% K < few millidarcys
Disturbed strata	Disturbed host rock	Bedding continuity is high but folded and offset by small faults. Commonly overprinted with crackle and mosaic brecciation.	Minor matrix pores and crackle to mosaic fracture pores. $\emptyset < 5\%$ K is as much as tens of millidarcys
Highly disturbed strata	Collapsed host rock (cave-roof and cave-wall rock) over passages	Highly disturbed, very discontinuously bedded strata with pockets and layers of chaotic breccia. Small-scale folding and faulting are common. Commonly overprinted with crackle and mosaic brecciation.	Localized pockets or layers of breccia might have porosities in the range of 5% to 15% and permeabilities in the tens to hundreds of millidarcys.
Coarse chaotic breccia	Collapsed-breccia cavern fill	Mass of very poorly sorted, granule- to boulder-sized chaotic breccia clasts 1 to 10 ft long. Commonly clast supported but can contain matrix material. Ribbon- to tabular-shaped body as much as 45 ft across and hundreds of meters long.	Abundant interclast pores. Porosity can exceed 20%, and permeability can be in the darcys.
Fine chaotic breccia	Transported-breccia cavern fill	Mass of clast-supported, moderately sorted, granule- to cobble-sized clasts with varying amounts of matrix. Clasts can be imbricated or graded. Ribbon- to tabular-shaped body as much as 45 ft across and hundreds of feet long.	Abundant interclast pores. Porosity can exceed 20%, and permeability can be in the darcys.
Sediment fill	Cave-sediment cavern fill	Carbonate and/or siliciclastic debris commonly with sedimentary structures.	Siliciclastic fill is commonly tight. Carbonate fill might be permeable.

Figure 1-29: Ellenburger Formation Core Facies

Identified facies from core in the Ellenburger formation. After R. Loucks 2007, 2023

1.5.6 Major Geologic Features and Description on Tectonic History

The Permian Basin is composed of several sub-basins, each with its own unique characteristics (**Figure 1-23**). The Delaware Basin is located in the western part of the Permian Basin and is known for its thick organic-rich source rocks and stacked reservoirs, making it a significant oil and gas producing region. The Midland Basin is located in the eastern part of the Permian Basin and is characterized by relatively few faults and fractures.

The Central Basin Platform is a relatively flat area that separates the Delaware and Midland Basins and contains several oil and gas fields, including the famous Yates Field (among the most prolific oilfields in the world³). The Northwest Shelf is the northernmost portion of the Permian Basin and is primarily a gas-producing area, while the Eastern Shelf is located in the southeastern part of the basin and contains a mix of oil and gas fields. Overall, the Permian Basin is a complex and diverse petroleum province with a long history of hydrocarbon production and several crustal blocks with different tectonic histories.

Hills (1970) used subsurface data to suggest the possibility of extensive lateral displacement along pre-Permian faults in the Permian Basin. Hills' primary objective was to determine the direction of tectonic forces responsible for regional deformation. Hills interpreted two tectonic systems. The first consists of folds and faults possessing orientations of N35W (folds) and N55-80E (right lateral faults), and N50-65 W (left lateral faults). The age of this deformation is thought to be early Late Mississippian to late Middle Pennsylvanian. There also are a series of NNW-trending faults that appear to be right lateral systems with larger displacement that formed synchronous with the other faults. It is this system of conjugate faults that has been interpreted to control the jagged geometry of the Central Basin Platform, especially along its eastern margin (**Figure 1-30**) (T. Hoak et al. 1998).

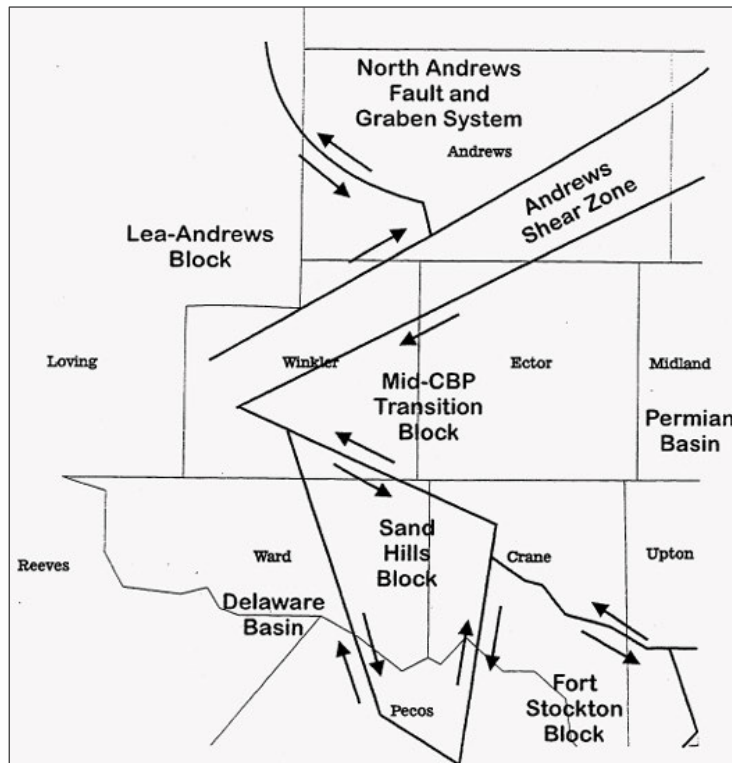


Figure 1-30: Interpreted Crustal Blocks

Interpreted crustal blocks from Gardiner (1990). After (T. Hoak et al. 1998). Midland CCS #2 Well location off eastern edge of map, hence no red star.

³ Texas State Historical Association (TSHA), an independent nonprofit since 1897

A second, later deformation phase as interpreted by Hills (1970), is marked by the relaxation of stress and normal fault motion reactivation of older fault systems. The timing of this deformation is interpreted to be middle-to-late Permian in age and fault displacements relatively minor.

Finally, during the Tertiary, the western margin of the Permian Basin was uplifted, and Basin-and-Range tectonism commenced in this area. This deformation has apparently been restricted to the western Delaware Basin and the basin margin (T. Hoak et al. 1998).

Hills (1985) describes the eastern boundary of the Midland Basin as possessing little evidence of tectonism. Instead, the Eastern Shelf is largely a stratigraphically controlled boundary with rocks of the Pennsylvanian-Permian-age carbonate shelf dipping gently westward into the basin.

The Midland Basin area is a large area (>-6,000 square miles) that is dominated by small NE and NW-trending faults and related folds. All structures are similar in style but smaller in size to those seen in the Mid-CBP Transition Zone. The majority of uplift occurred prior to the Mississippian with isolated fault block movement during Barnett-Strawn time. Since that time, the region has experienced regional subsidence. Gardiner (1990) outlined the boundaries of six "crustal" blocks that are roughly 40 mi on their longest dimension (**Figure 1-30**). The boundaries of these blocks represent major discontinuities that separate zones of distinct or different structural orientations and /or structural styles.

The Mid-CBP Transition Block is an area of ~ 600 square mi dominated by NW-trending reverse faults in the northern area (including Gandu Unit) and NW-trending reverse faults in the southern area. Both areas contain less dominant NE-trending normal faults. There is a NE-trending sag corresponding to the center of the area. A map of Ellenburger structure (**Figure 1-31**) demonstrates that the majority of deformation occurs along faults that form the boundaries of Gardiner's crustal blocks. The centers of the blocks are relatively undeformed. Erosional limits are markedly affected by the block boundaries and are used to delineate the chronology of block development and interaction.

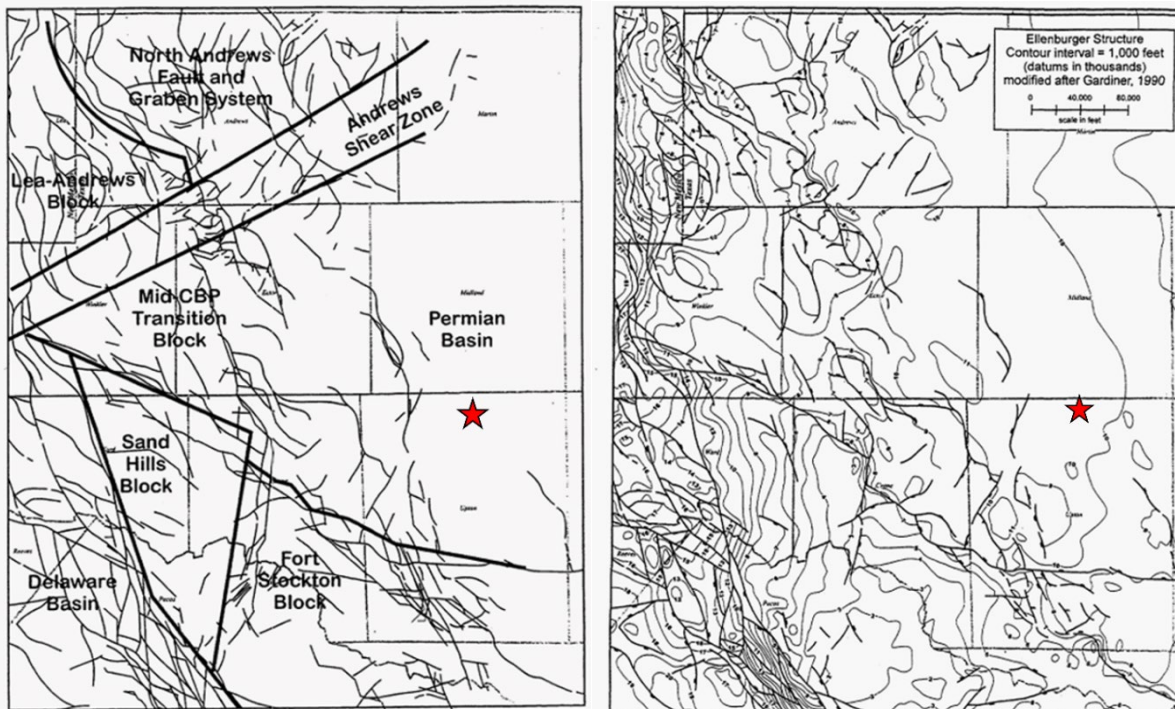


Figure 1-31: Interpreted Crustal Blocks

(Left) Interpreted crustal blocks from Gardiner (1990). With Ellenburger faults superimposed on top of different wrench faulting regimes. (Right) Ellenburger Structure Map with Faults. Red Star - Midland CCS #2 Well.

Building on earlier work, Horne et al., 2024 reported that the Midland Basin contains several new previously unknown fault systems. The main system in the Midland Basin is a N-NW/S-SE trending system that is primarily reverse and forms fault bounded uplifts with propagation folds in Crane, Ector and Andrews Counties. This fault system bounds the eastern edge of the Central Basin Platform. The dips of these faults are 65 degrees \pm 5 degrees. Crosscutting this main system is an E-NE basement rooted fault system aligned with the leading edge of the Metaproterozoic-age (1200-1000 MA) Grenville front that extends from Loving County, Texas to Abilene, Texas. This regional fault pattern extends from the eastern margin of the Central Basin platform into the Midland Basin with the scale of deformation observed gradually diminishing eastward. The E-NE faults are primarily strike-slip with additional minor reverse movement. The faults are high angle with dips of 80 degrees, \pm 10 degrees. Horne et al. 2024 interpreted the data from 3D seismic surveys, horizontal log steering data, and sparse 2D/3D seismic surveys. (Figures 1-32, Fig. 1-33) (Horne et al., 2024).

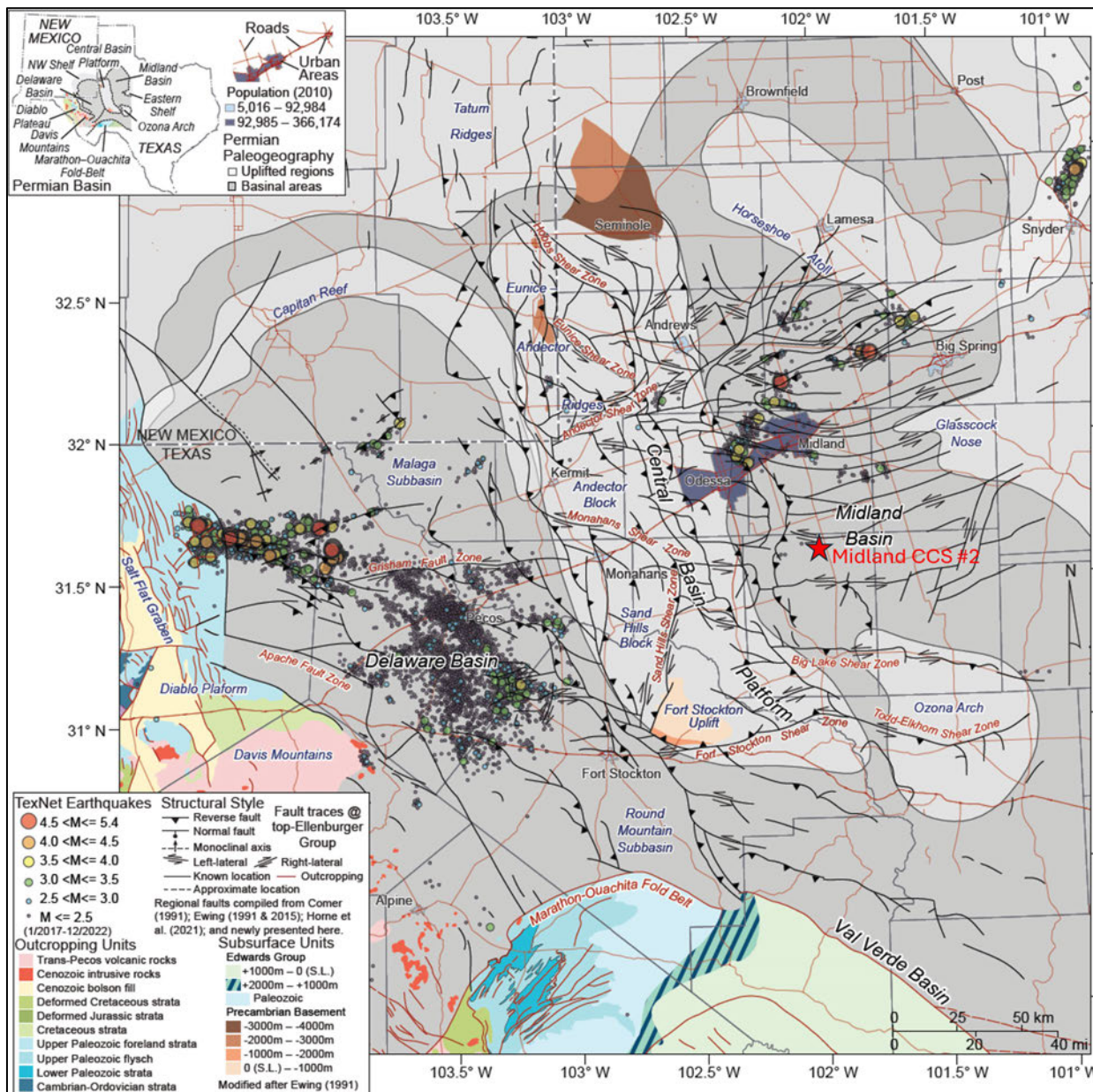


Figure 1-32: Permian Basin Structural Blocks and Major Fault Systems, Horne et al., 2024

Generalized paleogeographic map of the Permian Basin, highlighting the different tectonic provinces labeled in blue. Earthquake dots are supplied from TexNet Earthquake Catalog. Notable fault zones are labeled in Red. Red Star - Midland CCS #2 Well. Sourced from Horne et al., 2024

N-NW/S-SE reverse faults (black and red) are generally ~10 KM (6.2 mi) in length while E-NE (gold and green) strike slip faults can extend up to 50 KM (31 mi) to the eastern edge of the basin (**Figure 1-33**). In all cases, the faults interpreted are likely several smaller faults in aggregate forming a fault system. 3D seismic reflection datasets also show that NNW-SSE and NNE-SSW striking reverse faults became activated in the Pennsylvanian and deformation continued through to the early Wolfcampian (early Permian), but dip-slip motion dissipated after middle Pennsylvanian Strawn deposition (Horne et al., 2024).

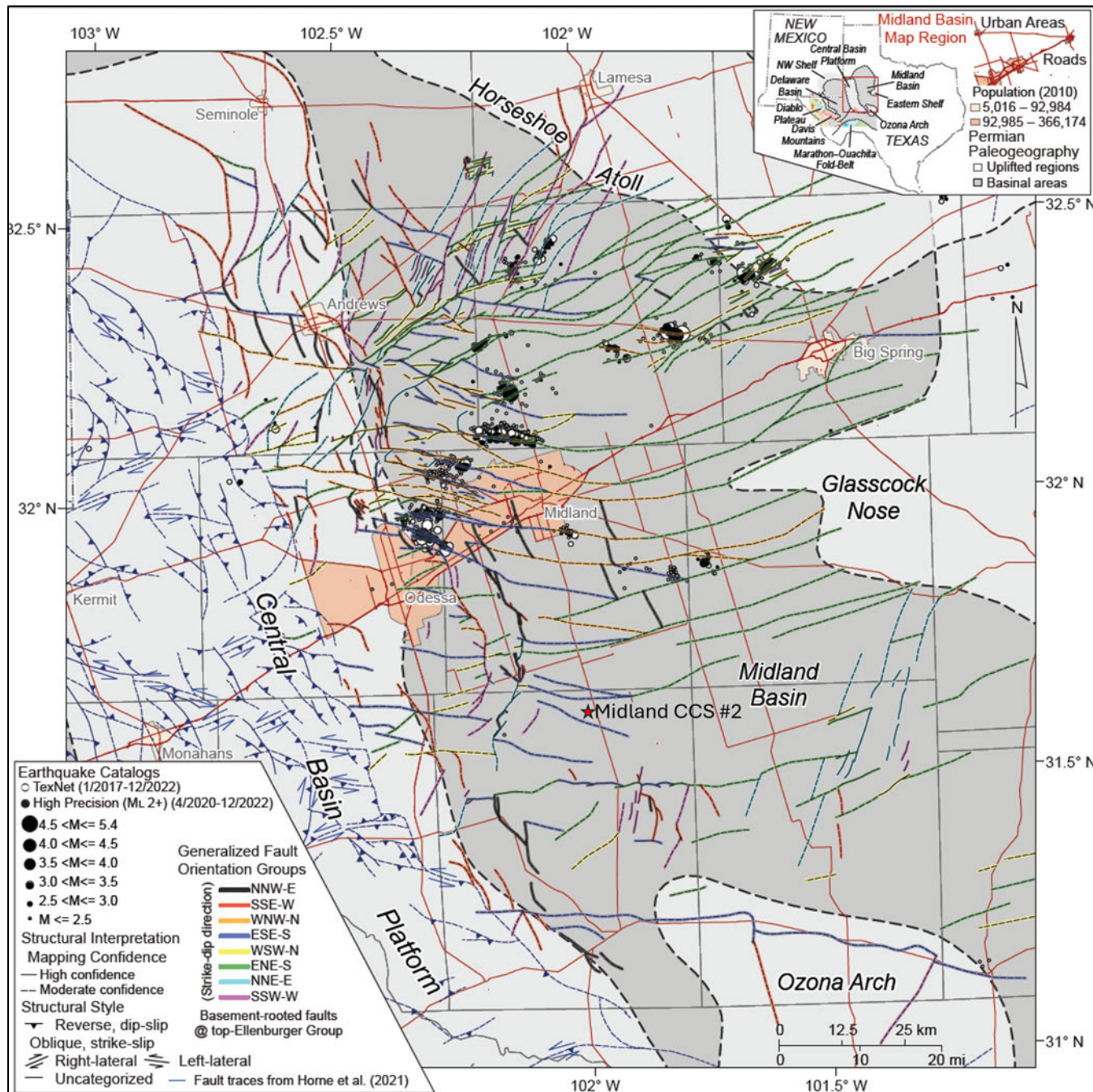


Figure 1-33: Midland Basin Faults, Horne et al., 2024

Interpreted regional faults in the Midland Basin, these are basement rooted faults at the Top Ellenburger surface. Note the different generalized fault orientation groups. Red Star - Midland CCS #2 Well. Sourced from Horne et al., 2024

1.6 Local Geology Introduction

The following **Sections 1.7** through **1.12** discuss the local geology around the proposed Well.

- **Section 1.7** – Structural Geology - Thickness, Lithology
- **Section 1.8** – Faults and Fractures – Faults and Fractures, Seismic History, Regional Stress
- **Section 1.9** – Petrophysical Characterization – Porosity, Permeability, Salinity, Cap Pressure
- **Section 1.10** – Geomechanics – Stress Magnitude, Orientation, Strength, Ductility, Pressure
- **Section 1.11** – Geochemistry – Brine-CO₂ Interactions, Mineral-CO₂ interactions
- **Section 1.12** – Mineral Resources – Petroleum production from Ellenburger or Devonian

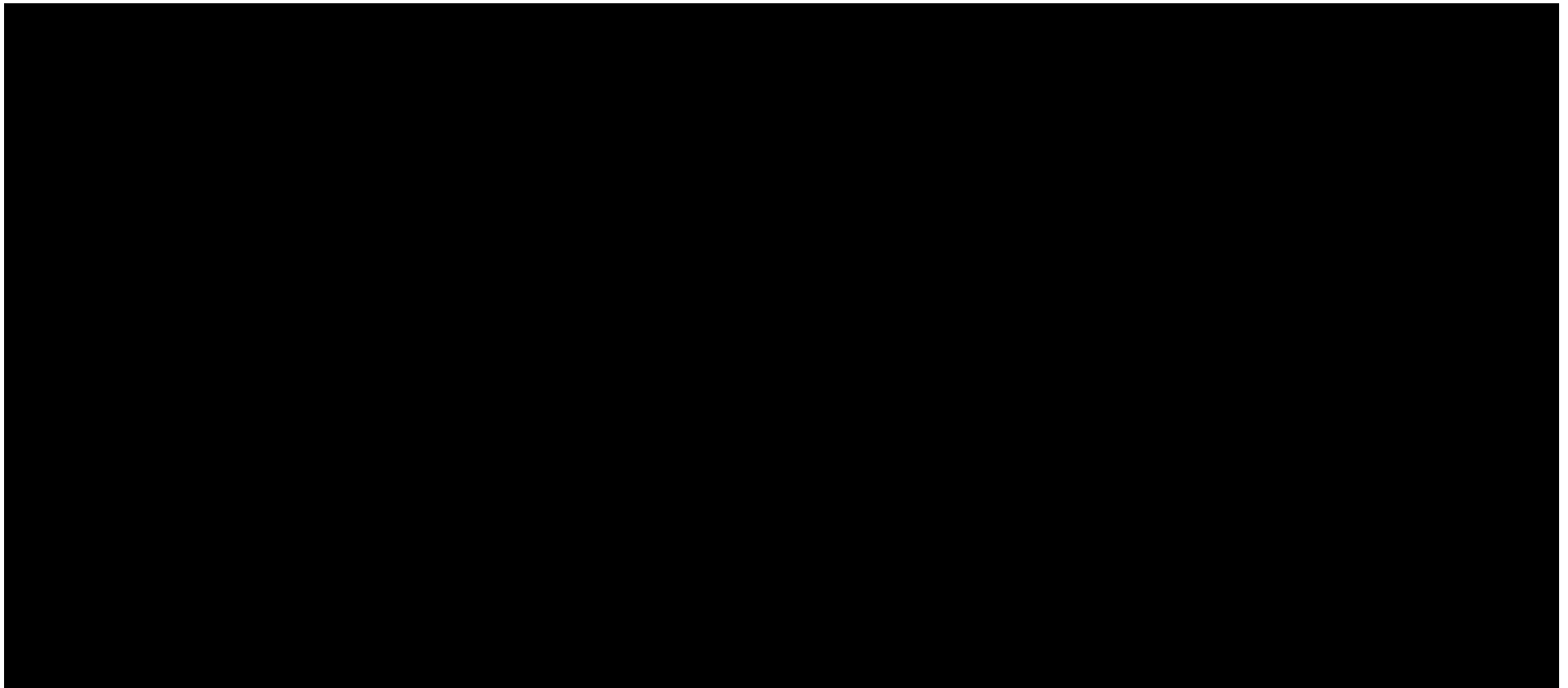


1.7 Structural Geology [40 CFR 146.82 (a)(3)(iii)]

The purpose of **Section 1.7** is to demonstrate that within the AoR the structure is laterally continuous with predictable with very low dip (<5 degrees). This section provides data regarding the depth, thickness, structure and lithology of the injection and confining zones.

The injection interval is defined from its base: 100 ft above the basement; to its top: the top of the



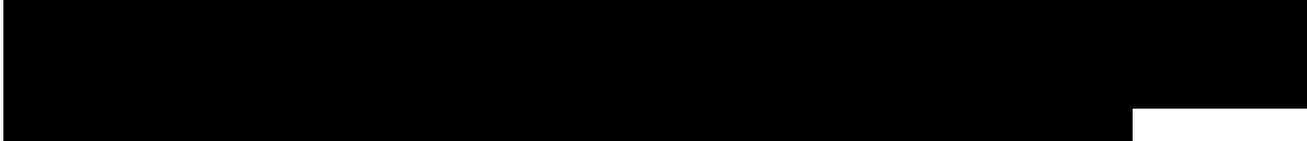


Most formations below the Strawn are regionally extensive, conformable and cover both Upton and Midland Counties. The Simpson Group pinches out to the east, in Reagan County (**Figure 1-39**) and some variations in thickness of the Atoka, Simpson Group and Wristen Group are observed across the area (**Figures 1-35 through 1-41**)

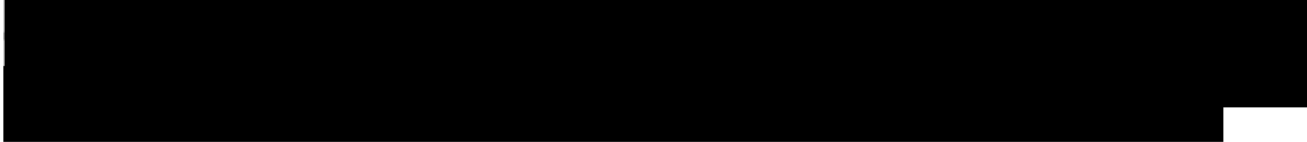


Figures 1-35 through 1-41 illustrate the subsea depths from the top of the Barnett to the Basement. Basement has been estimated through the few well penetrations available in the area, correlated to seismic data, and then gridded. Basement is expected to occur at range relative to AoR below ground level based on offset logs and grids.

The depth of the base of USDW per the RRC Ground Water Advisory Unit correspondence with



Indeed, there are a myriad of zones that are impermeable between the USDW base and the injection unit. The first is the Artesia Group at a depth of ~1750 ft which has several anhydrite layers. Next, the Wolfcamp Shale (9,124 ft), Cisco (10,128 ft) and Canyon shales (10,494 ft) are barriers. After that, the Atoka (11,503 ft) also forms a barrier



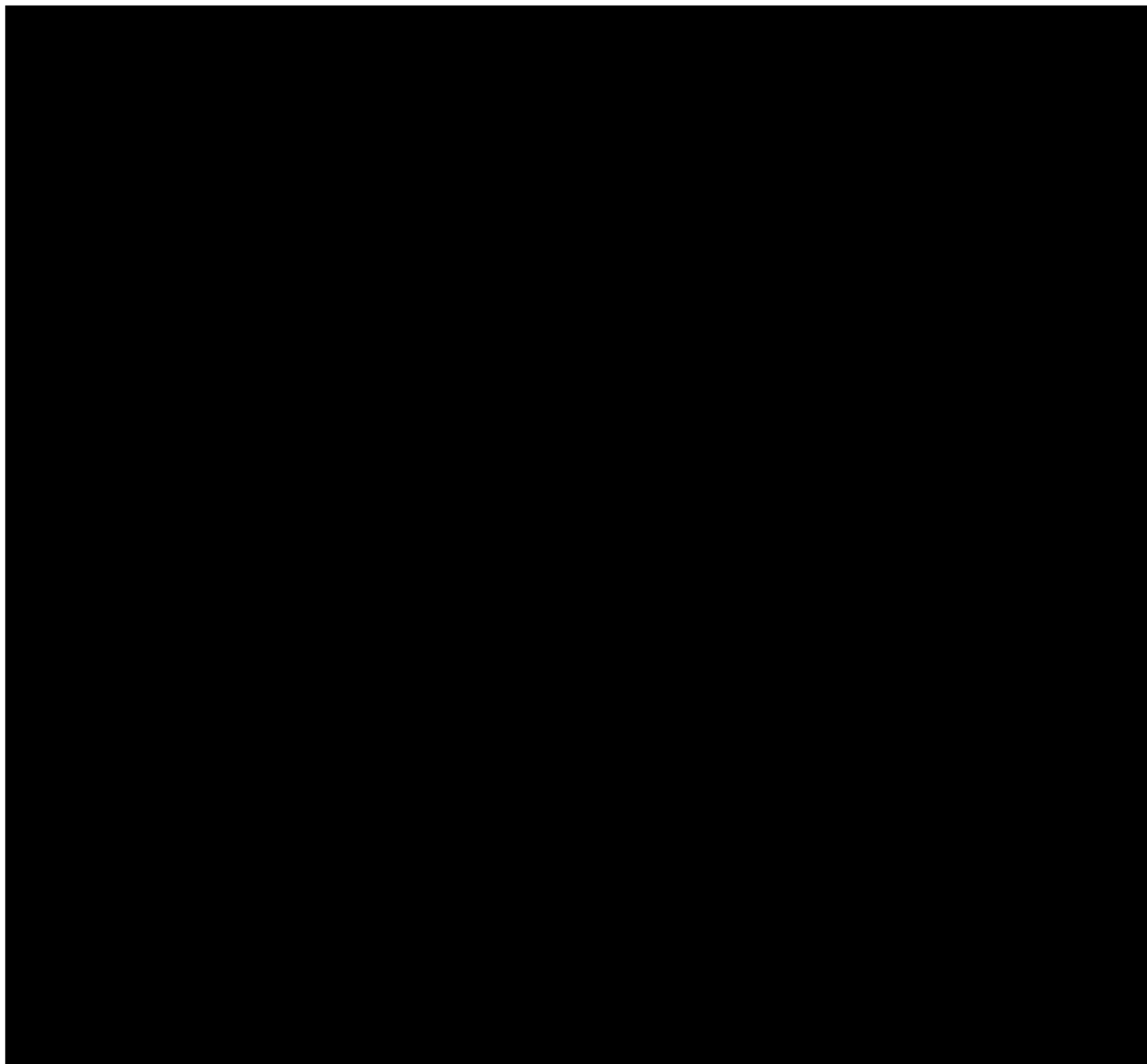
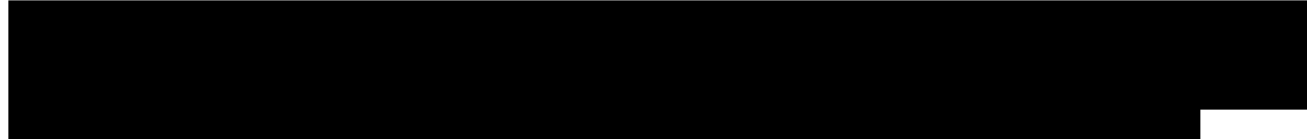
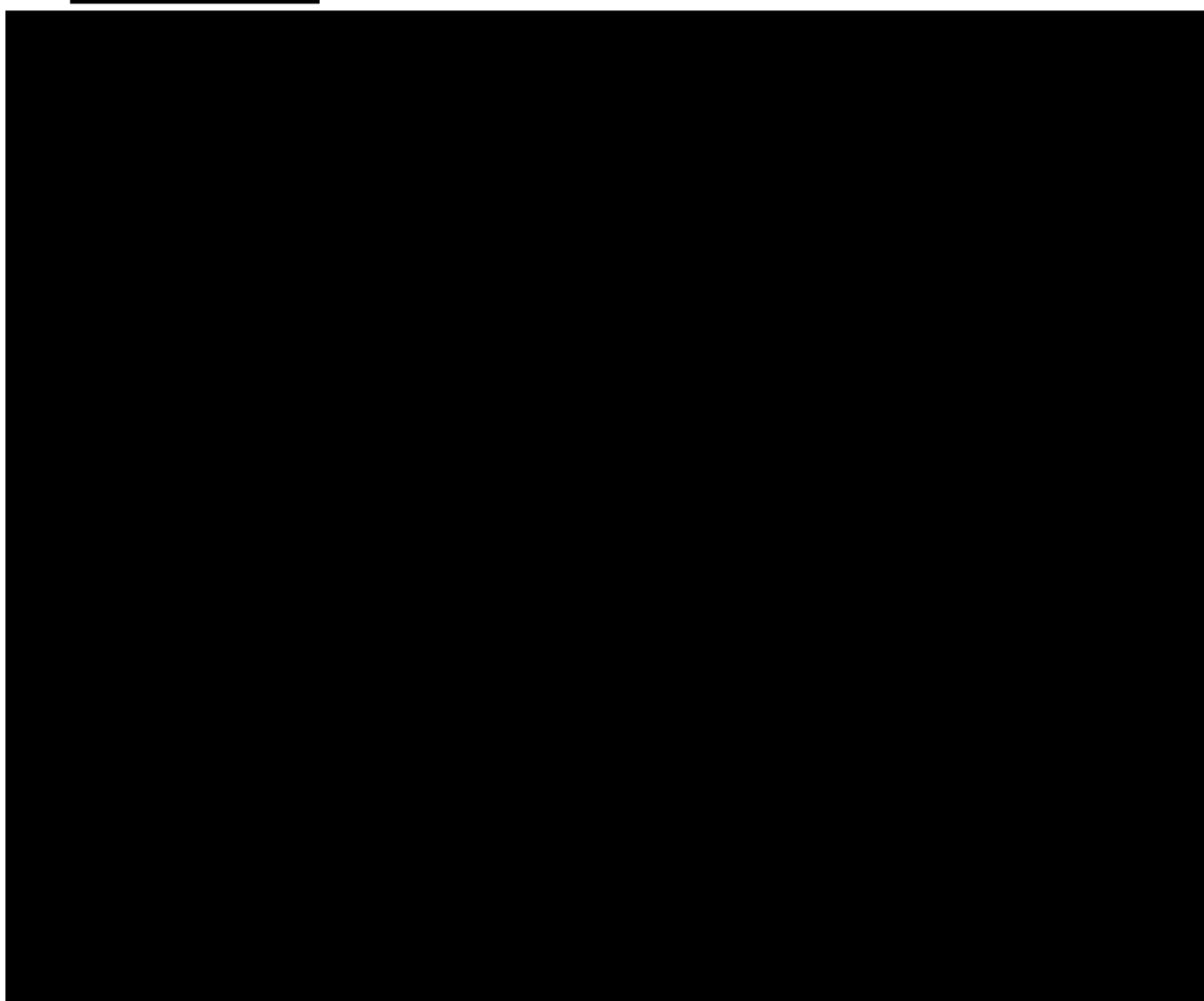


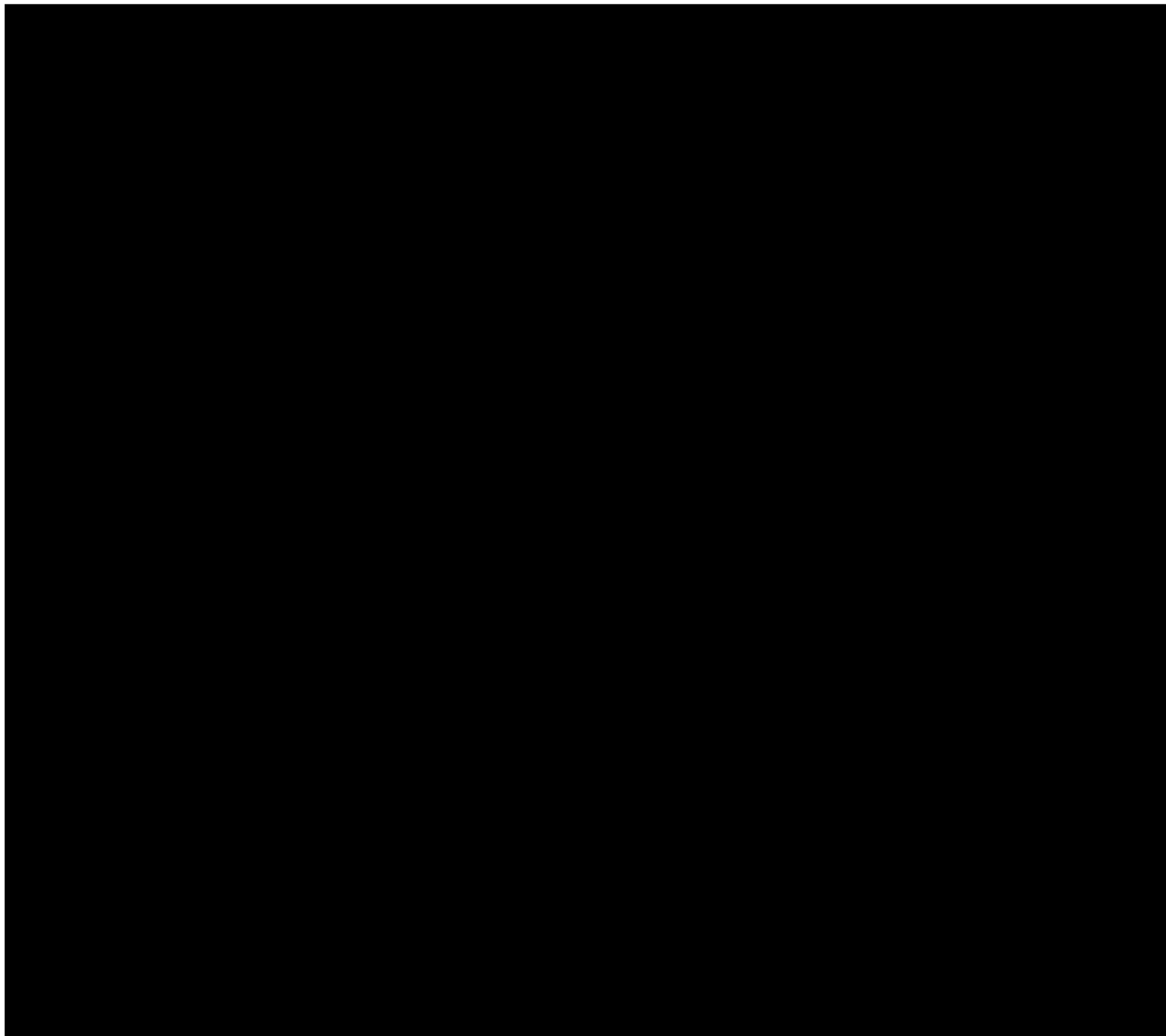
Figure 1-35 represents a structure map of the top of the Barnett shale. The Barnett shale consists of mudrock, carbonate lenses, and shales. [REDACTED]

[REDACTED]

[REDACTED]

[REDACTED]





The Devonian structure map is illustrated in **Figure 1-37**.



The Simpson is expected to be -10,139 ft TVD SS at the proposed Well location. The structure of [REDACTED]

[REDACTED]

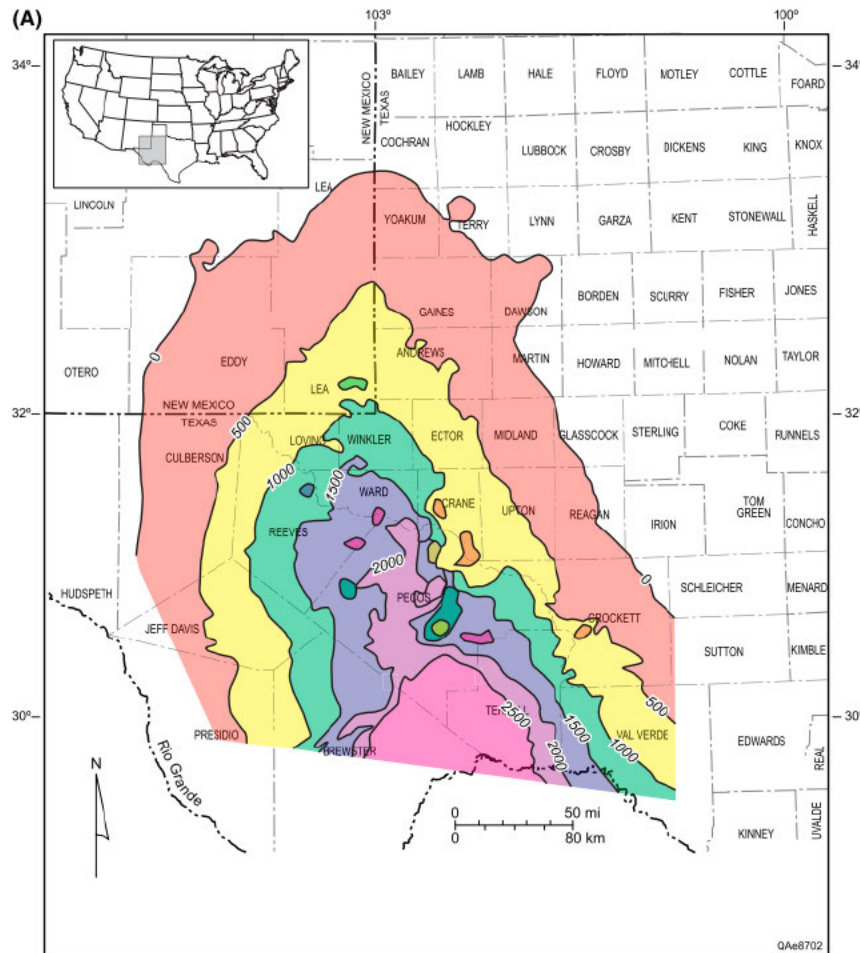
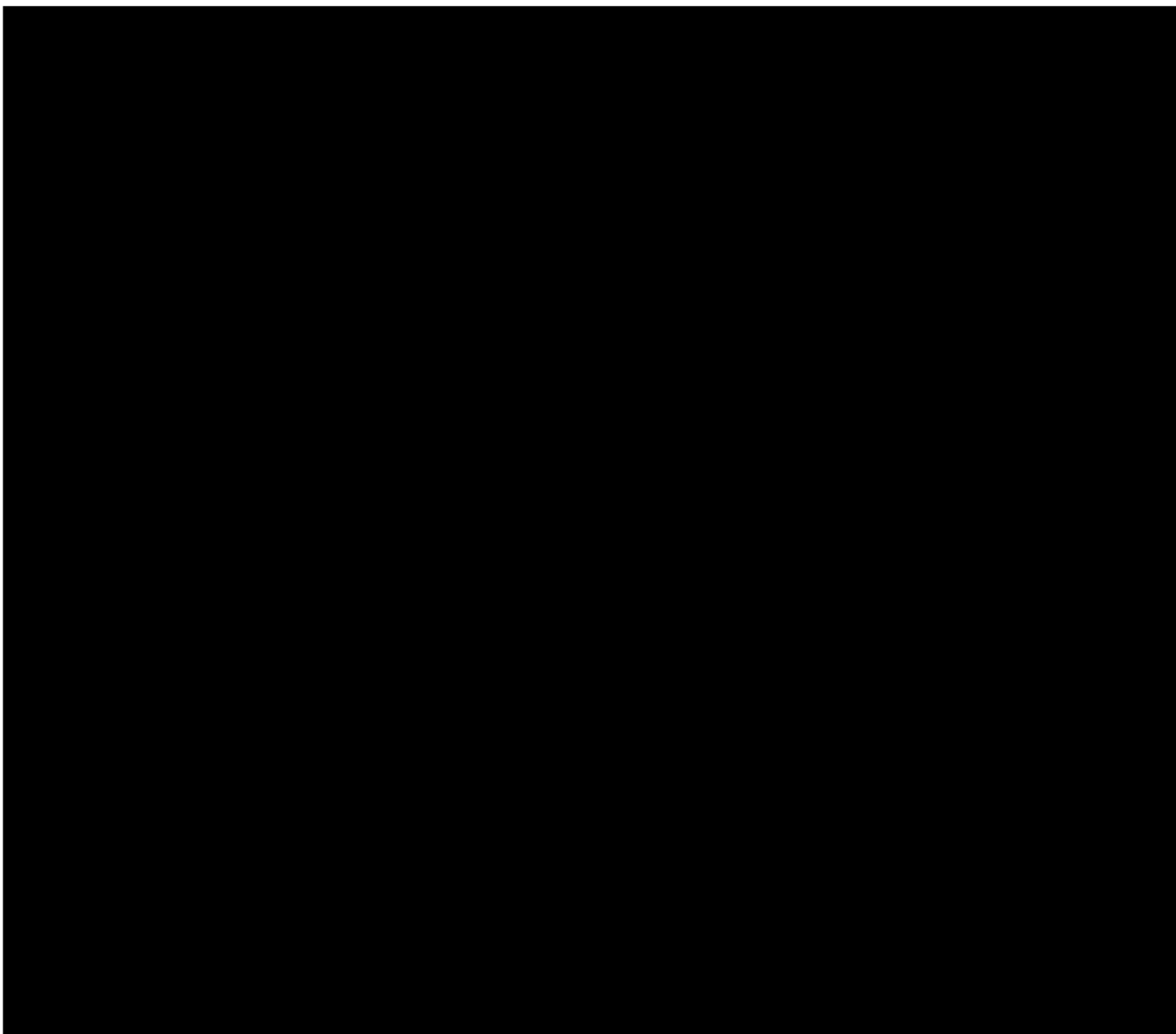


Figure 1-39: Regional Isochore Map of Simpson Group

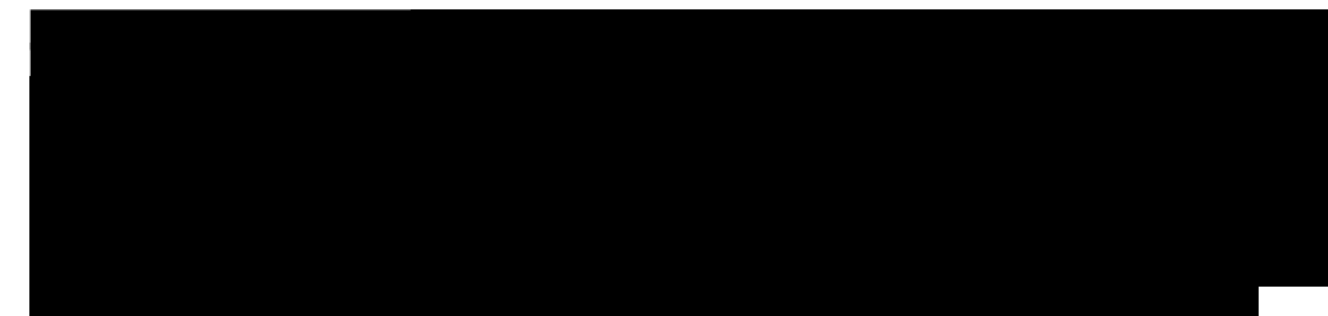
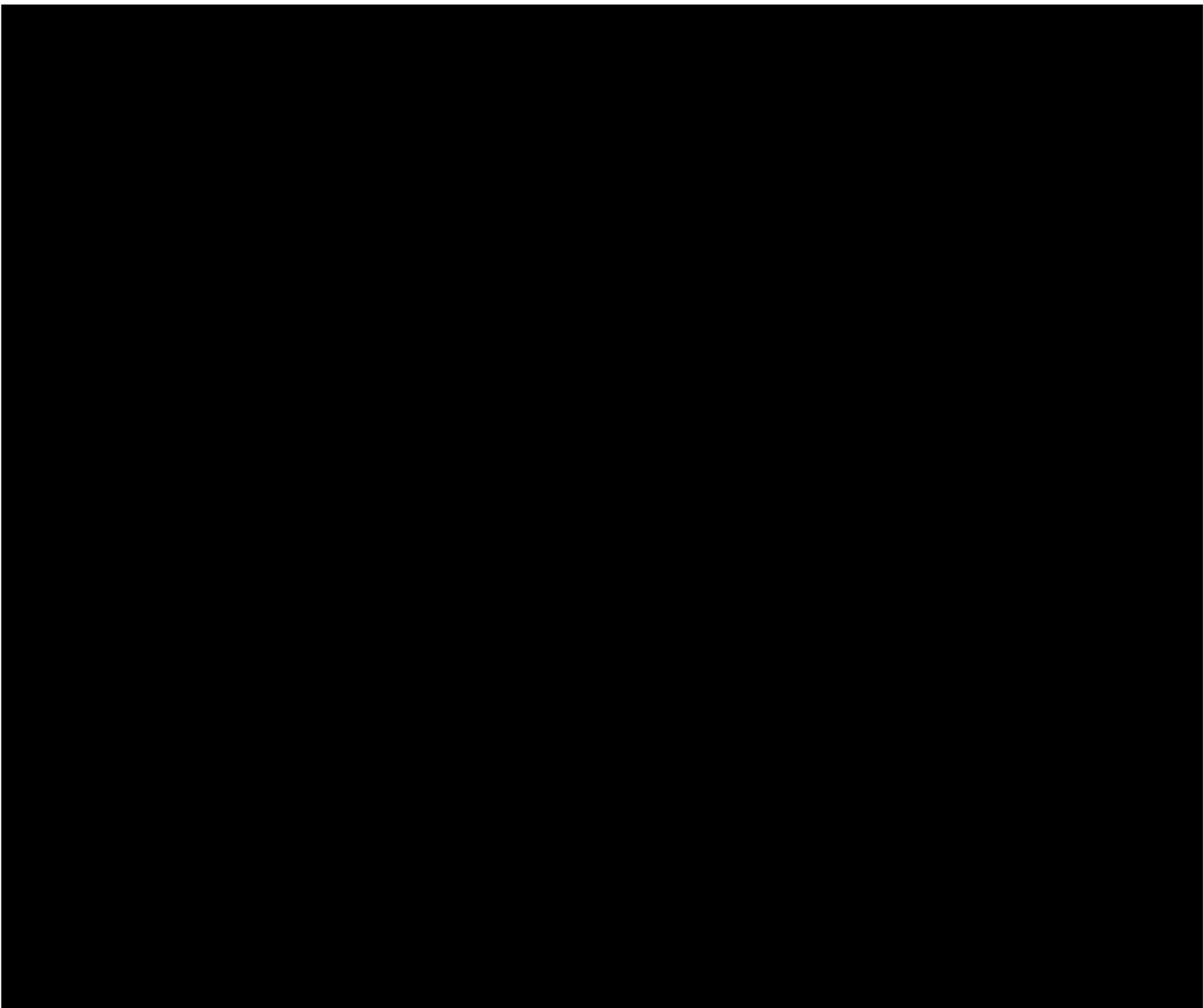
(Fairhurst et. al., 2021) Isochore map of the Simpson Group (contour interval = 500 ft) modified from Fairhurst (2015). The axis and western margin of the Simpson isochore of the Tabosa Basin are similar to the axis of the current Delaware Basin. The eastern margin through central Martin, southwestern Glasscock, and eastern Regan Counties includes only the western half of the current Midland Basin. Individual beds display thinning onto the margins, and there are indications of erosion along these margins.

The upper members of the Simpson Group are subcropping from south to north in from Upton to Midland County.



The Ellenburger Group's structure is illustrated in Fig. 1-40.





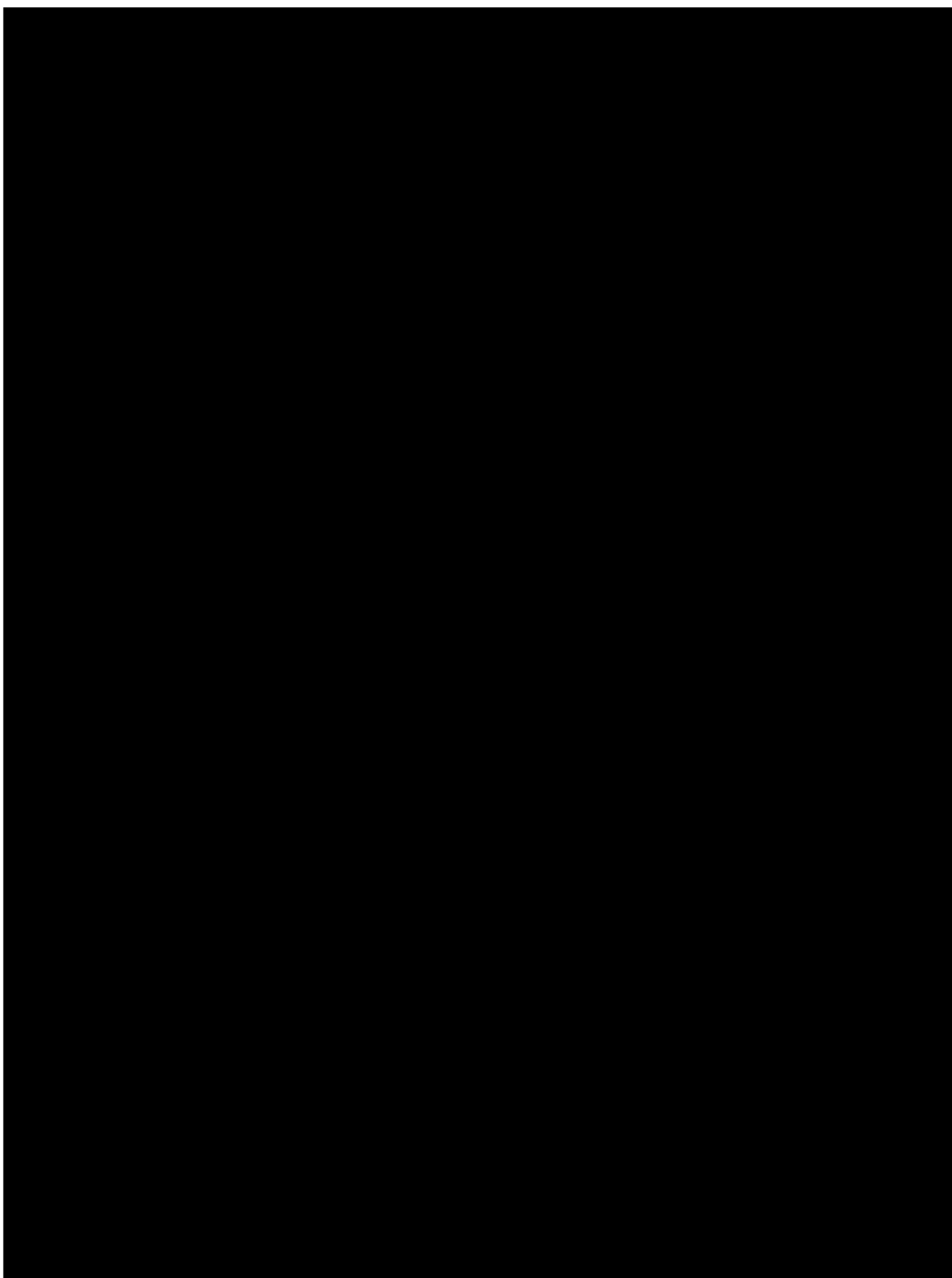


1.7.2 *Thickness*

1.7.2.1 *Log From Surface to Basement*

Figure 1-42 illustrates an example type log of the local area with relevant thicknesses listed for each formation.

A large rectangular area of the page has been completely blacked out, indicating that the original content has been redacted.



1.7.2.2 Thickness Maps for Injection Units

Figures 1-43 to 1-46 illustrate the true vertical thicknesses for [REDACTED]

[REDACTED]

Figure 1-43 illustrates a map of the [REDACTED]

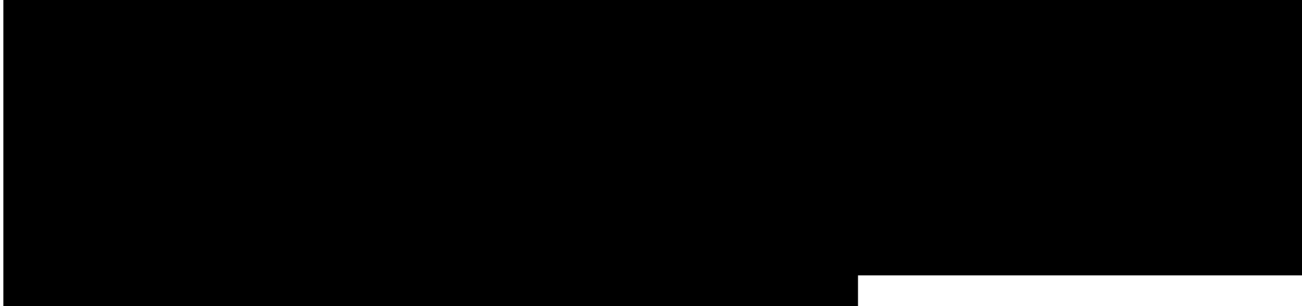
[REDACTED]

[REDACTED]

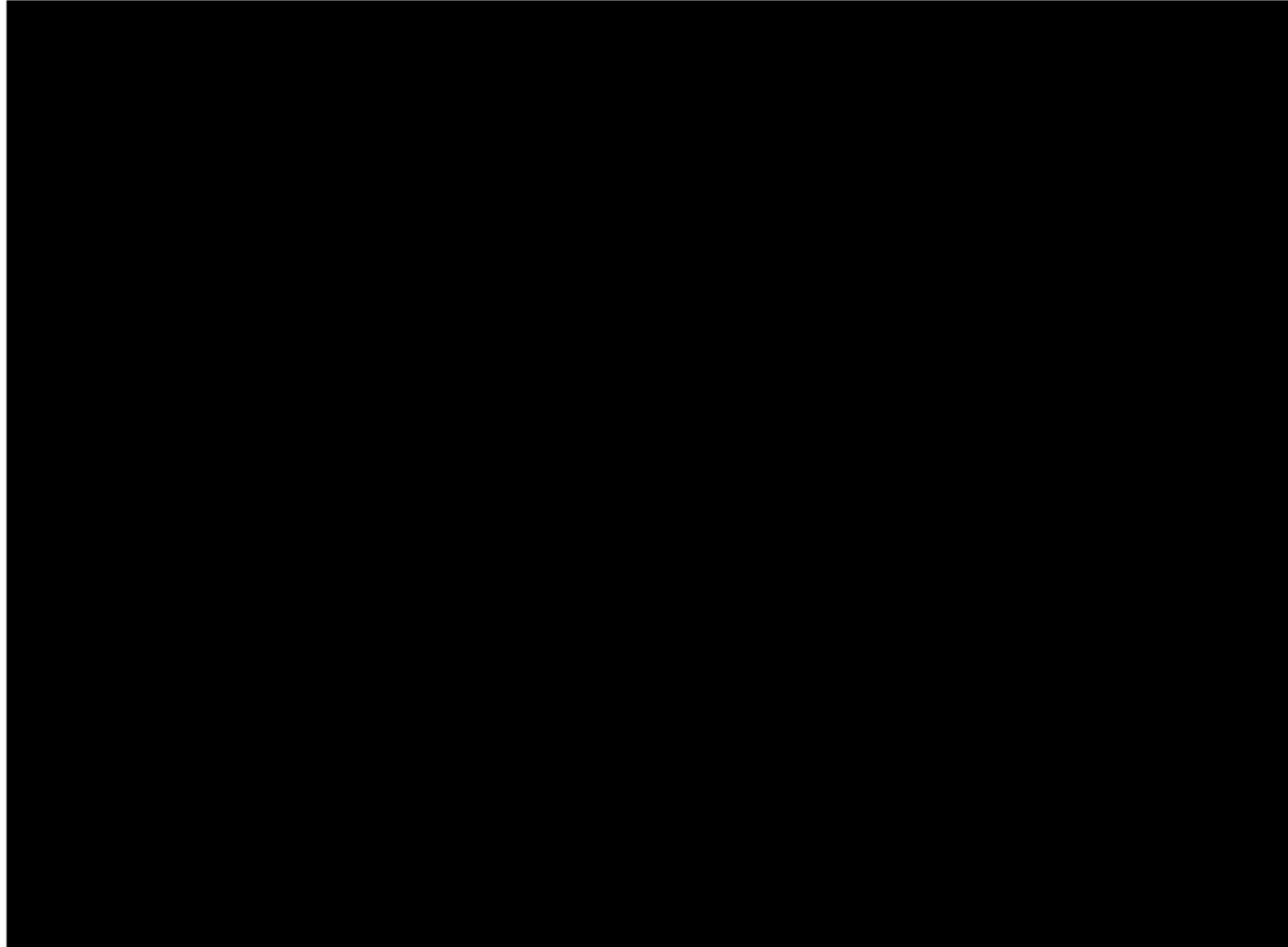
[REDACTED]

[REDACTED]





1.7.2.3 





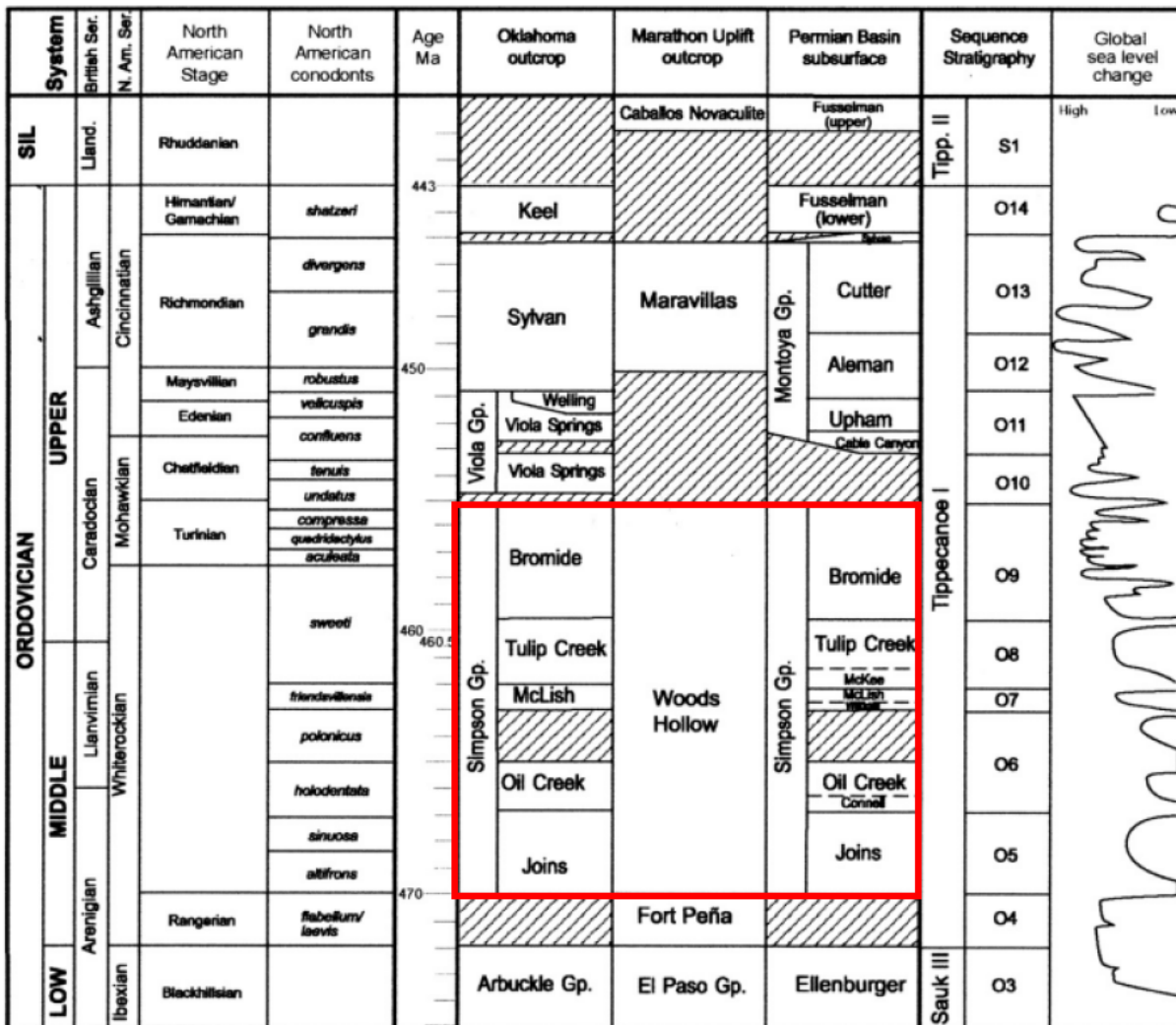
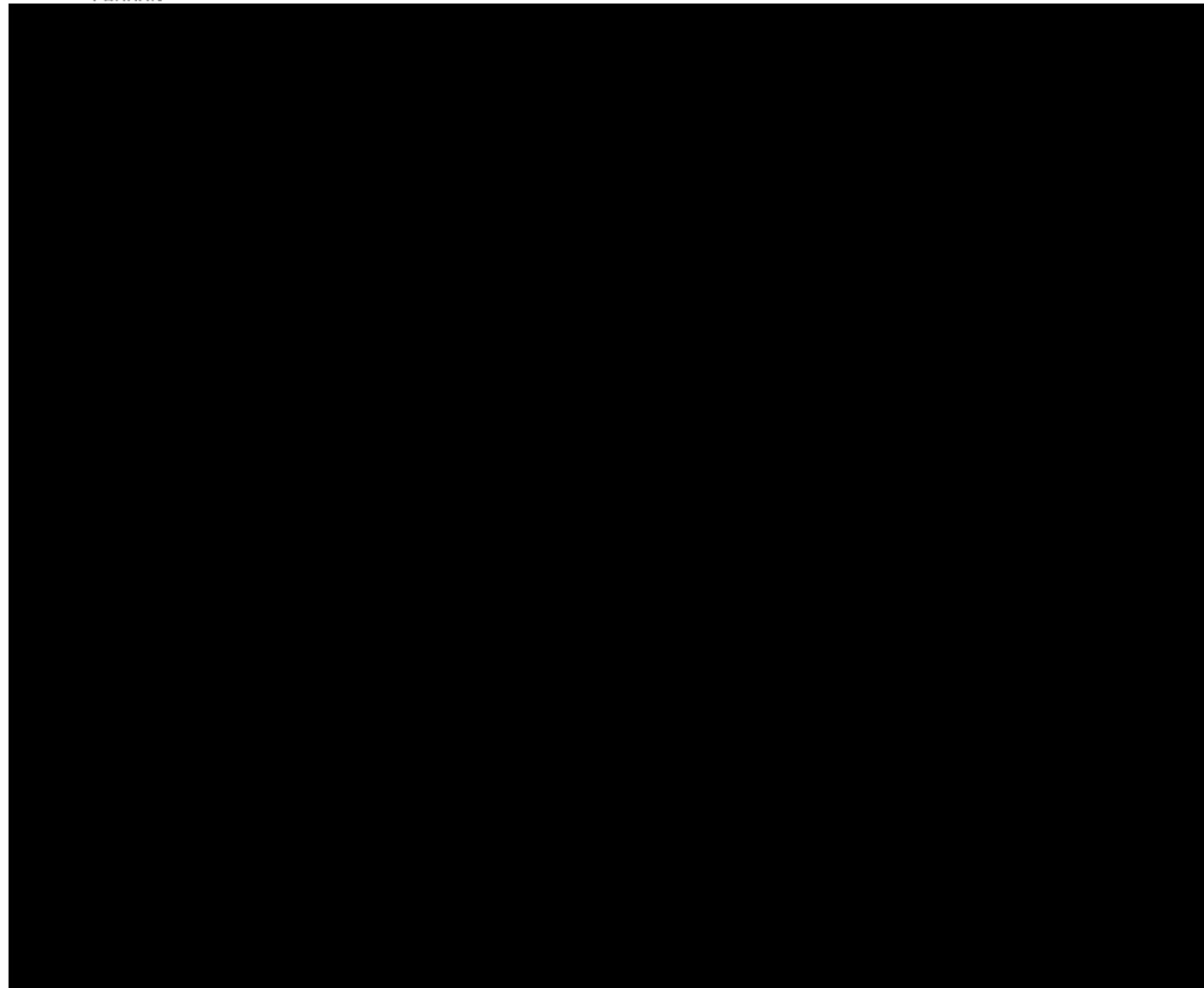


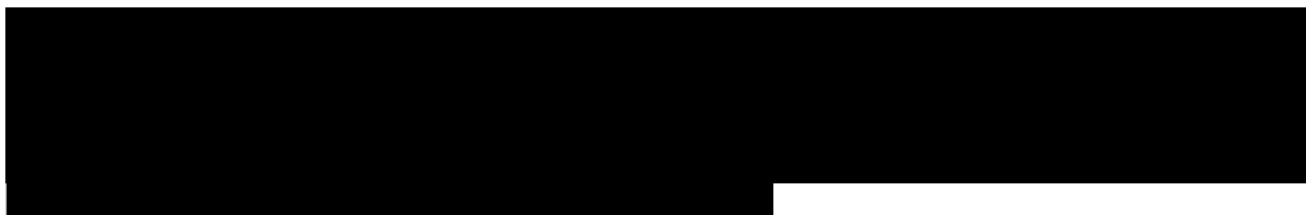
Figure 1-47: Detailed Stratigraphic Column illustrating the Simpson Group
Detailed stratigraphic column illustrating the individual formations that make up the Simpson Group. (Modified from Fairhurst et. al., 2016)



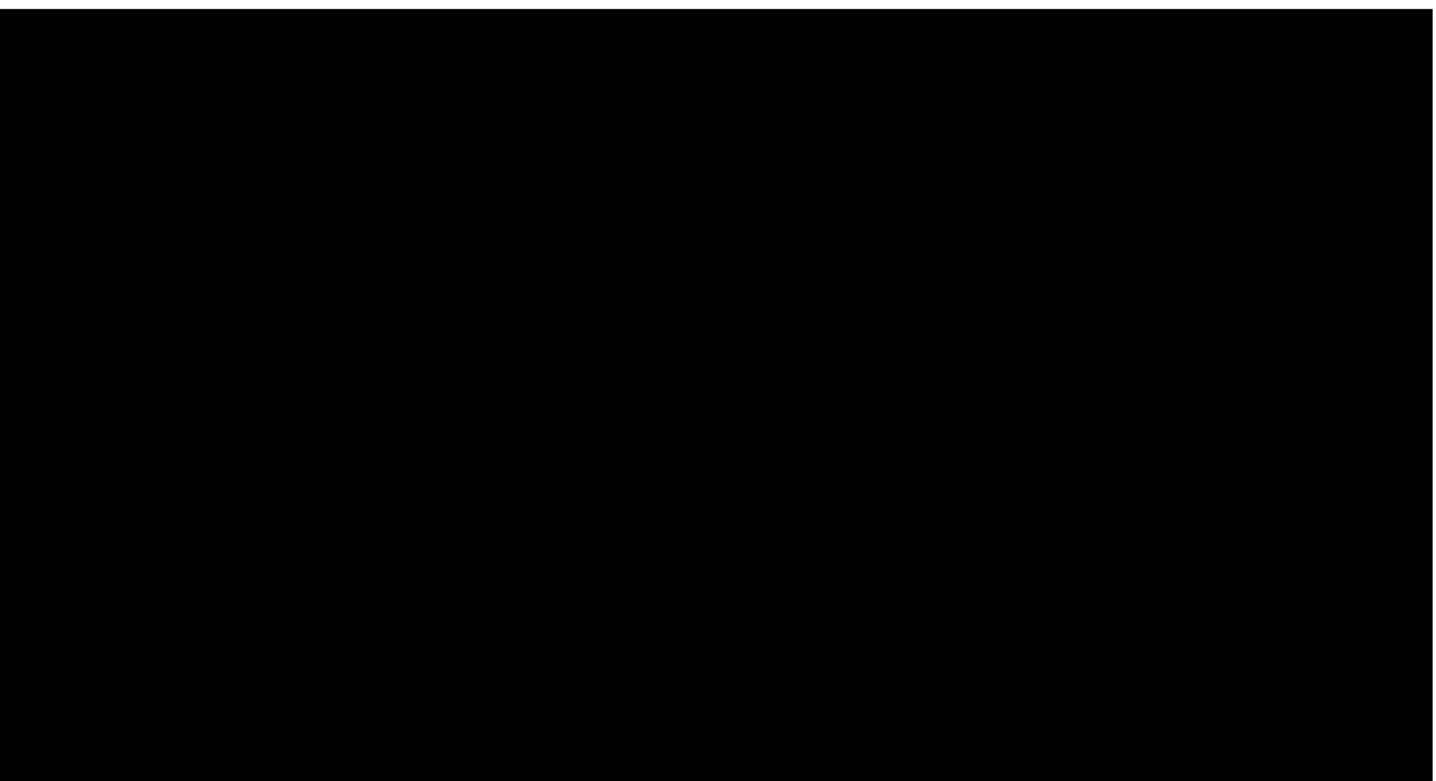
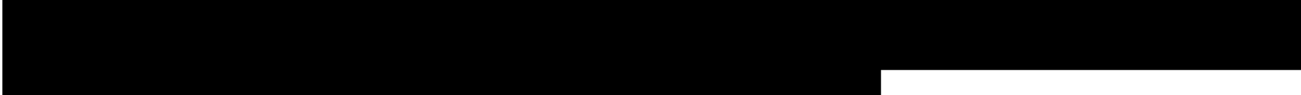
1.7.3 Cross sections

A base map showing the paths of



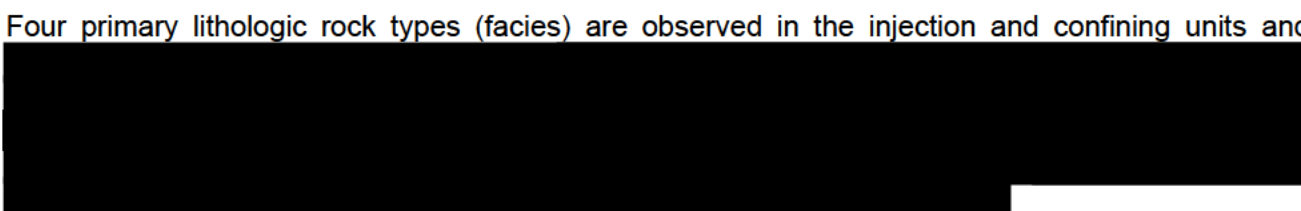


In reference to the north-south cross section B-B' in **Figure 1-51**, there are several observations worth



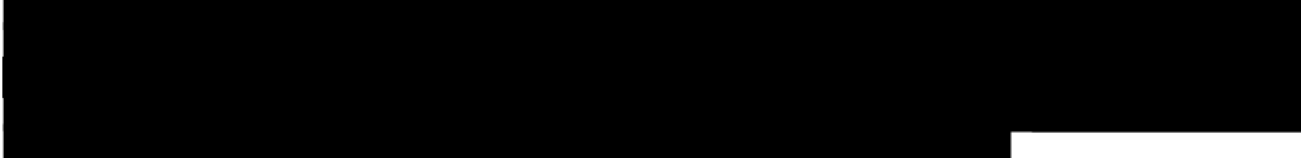


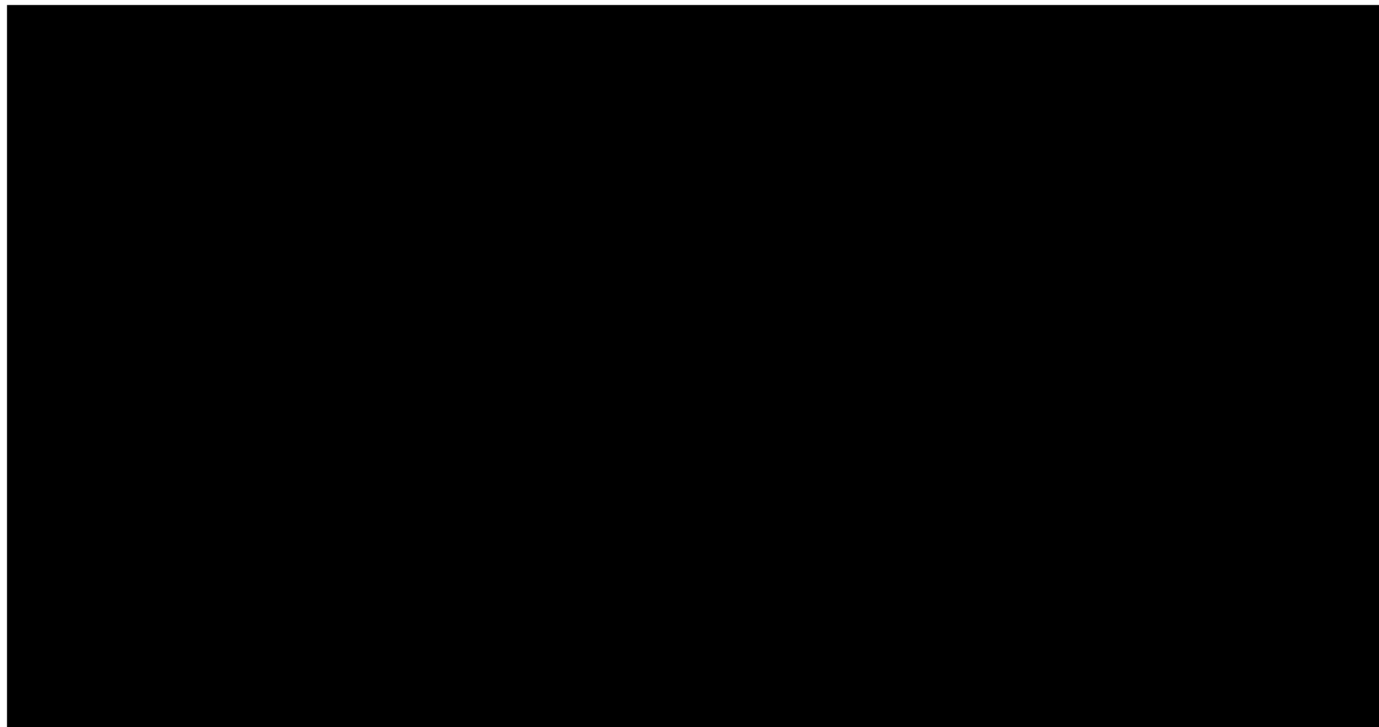
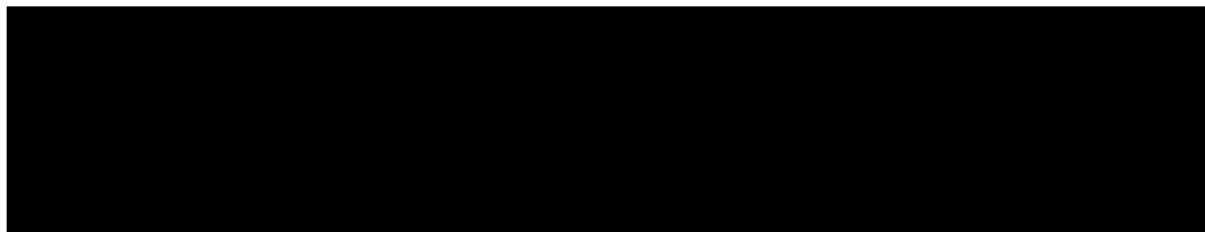
On both cross-sections, multiple faults are visible; however, no faults penetrate through the top of the



1.7.4 *Lithology*

Four primary lithologic rock types (facies) are observed in the injection and confining units and





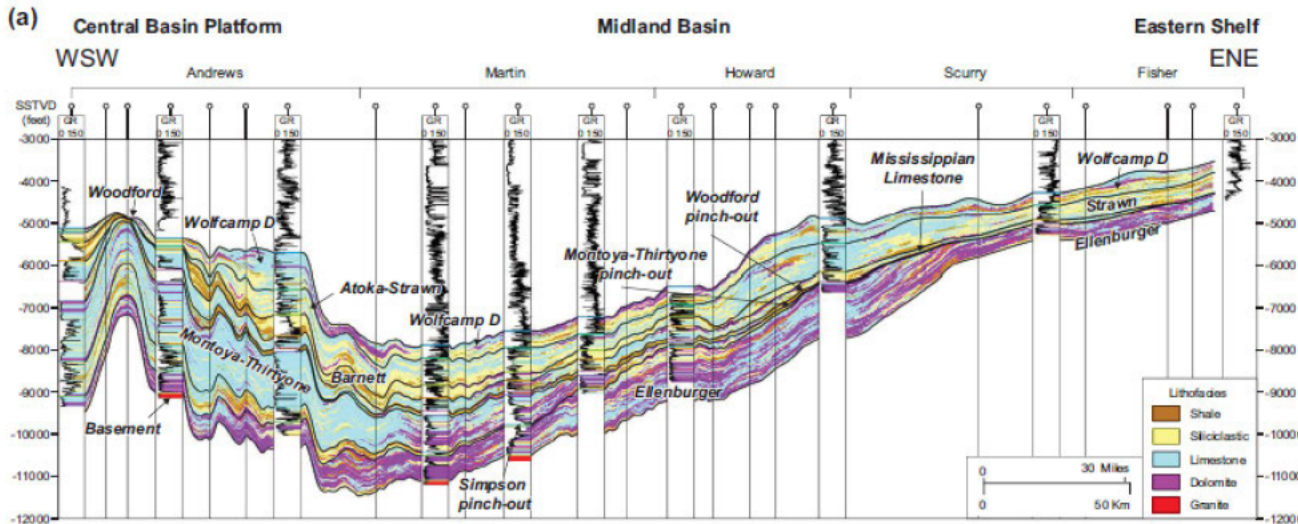


Figure 1-53: Facies Cross Sections (Calle et. al., 2024)

Lithofacies distribution from the northern shelf to the structurally compartmentalized Ozona arch.

No significant lateral change in facies proportions is predicted with the AoR, particularly within the

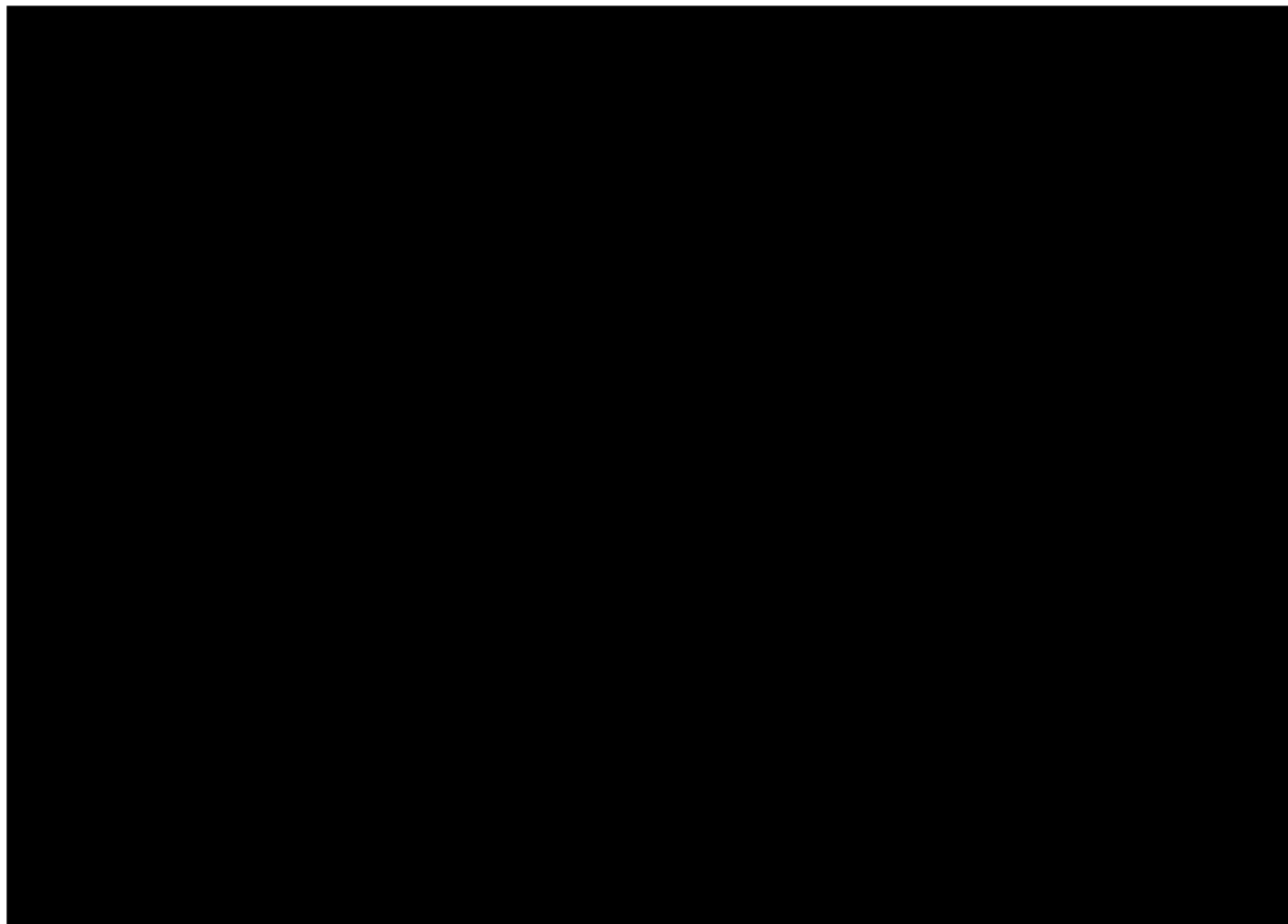
1.8 Faults and Fractures [40 CFR 146.82 (a)(3)(ii)]

This section addresses data regarding faults and fractures in the seals and injection units as well as the seismic history of area. It further documents the regional stress field for the southern Midland Basin and shows fault slippage analyses for nearby faults.

1.8.1 Faulting

This section will address the regional and localized interpreted data regarding the faulting present that affects this area and the Well AOI.

With respect to the regional faulting, the Bureau of Economic Geology (BEG) has performed extensive regional research in the Permian Basin. In this section, we will reference figures and citations from the BEG and their regional analysis in the Midland Basin. In addition to the regional data and analysis,



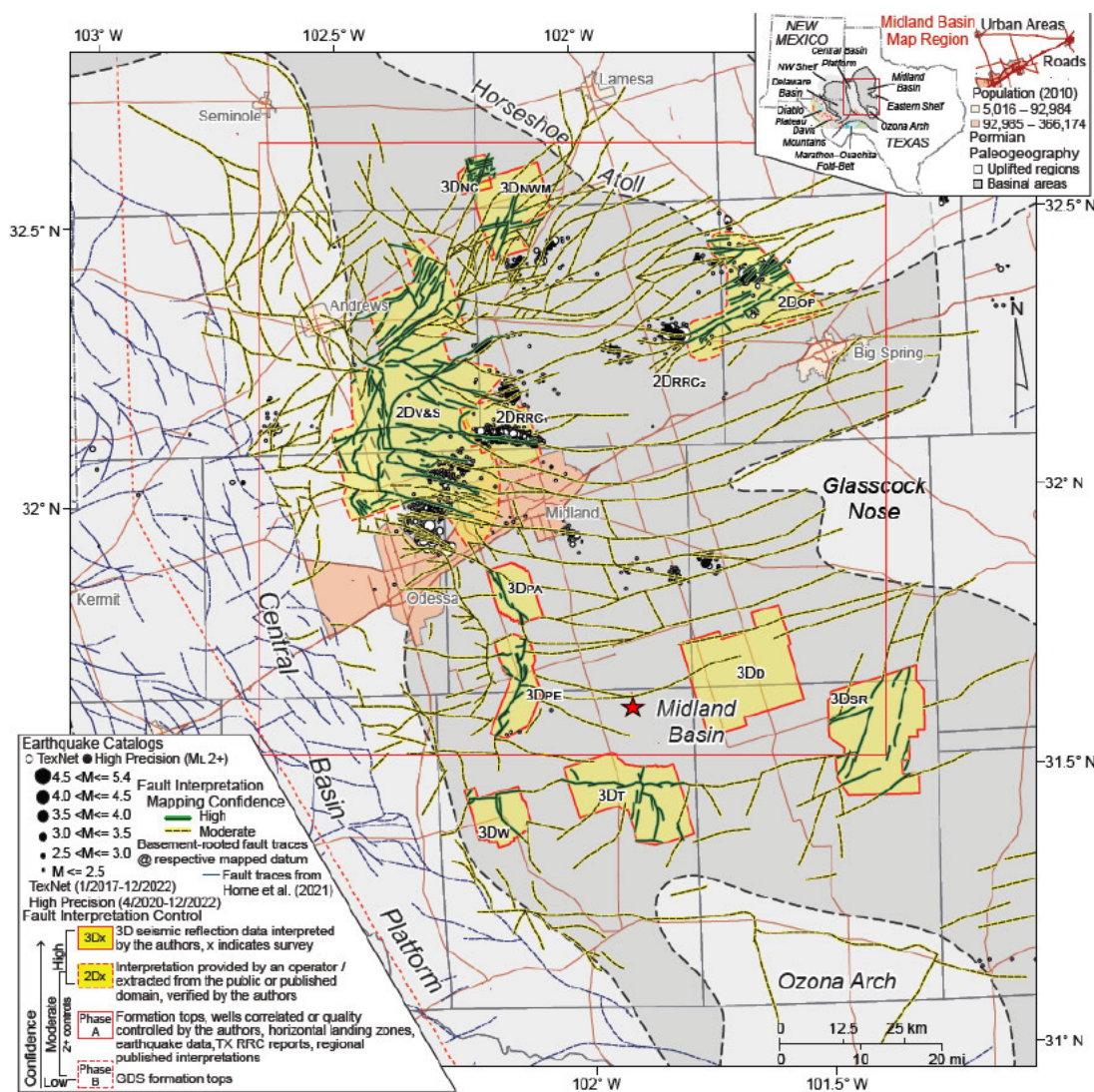
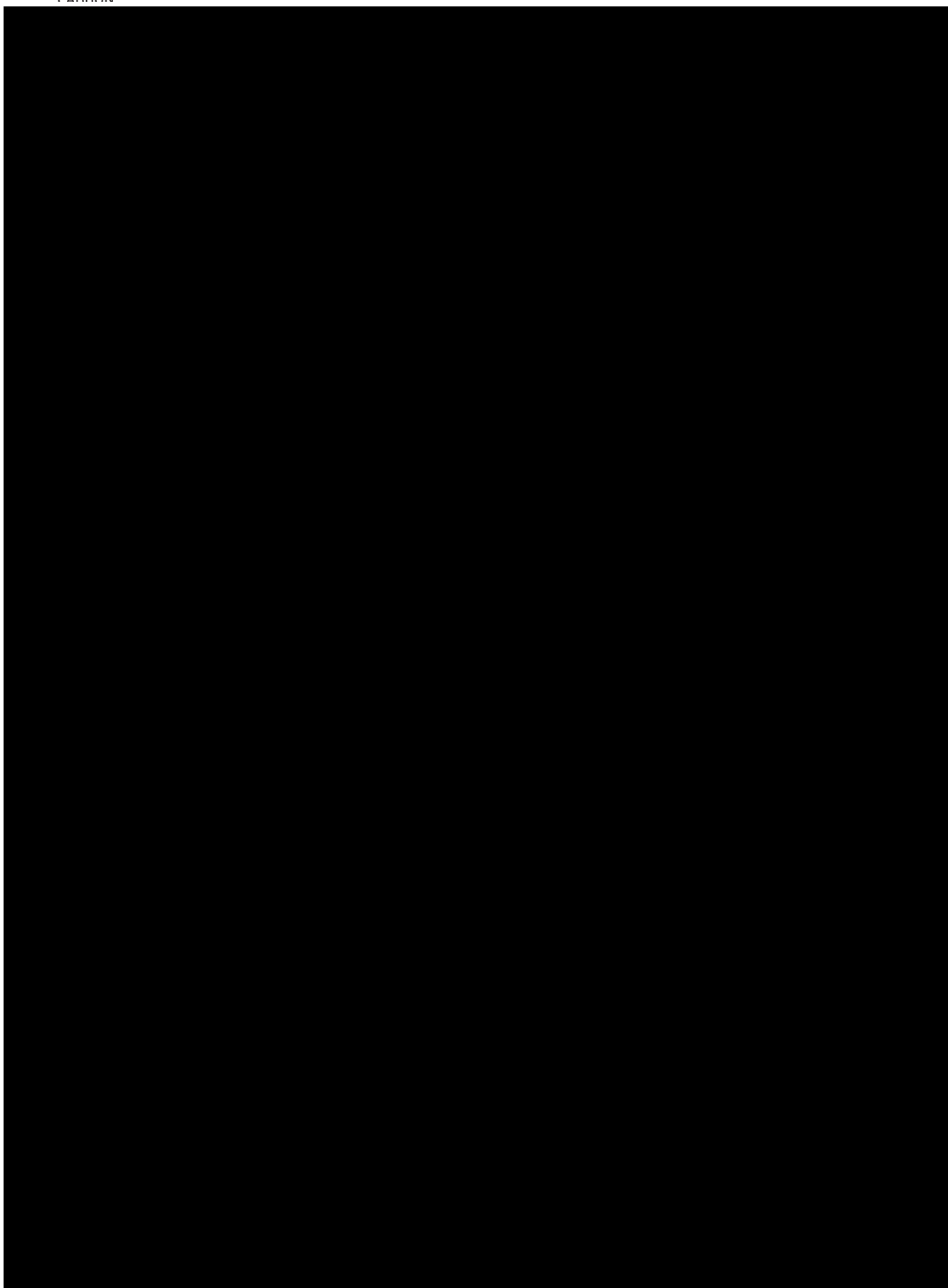


Figure 1-55: Horne et. al., 2024 – Summary Map of Data Sources

Map illustrating the data sources available for Horne et. al. interpretations and fault mapping confidence.

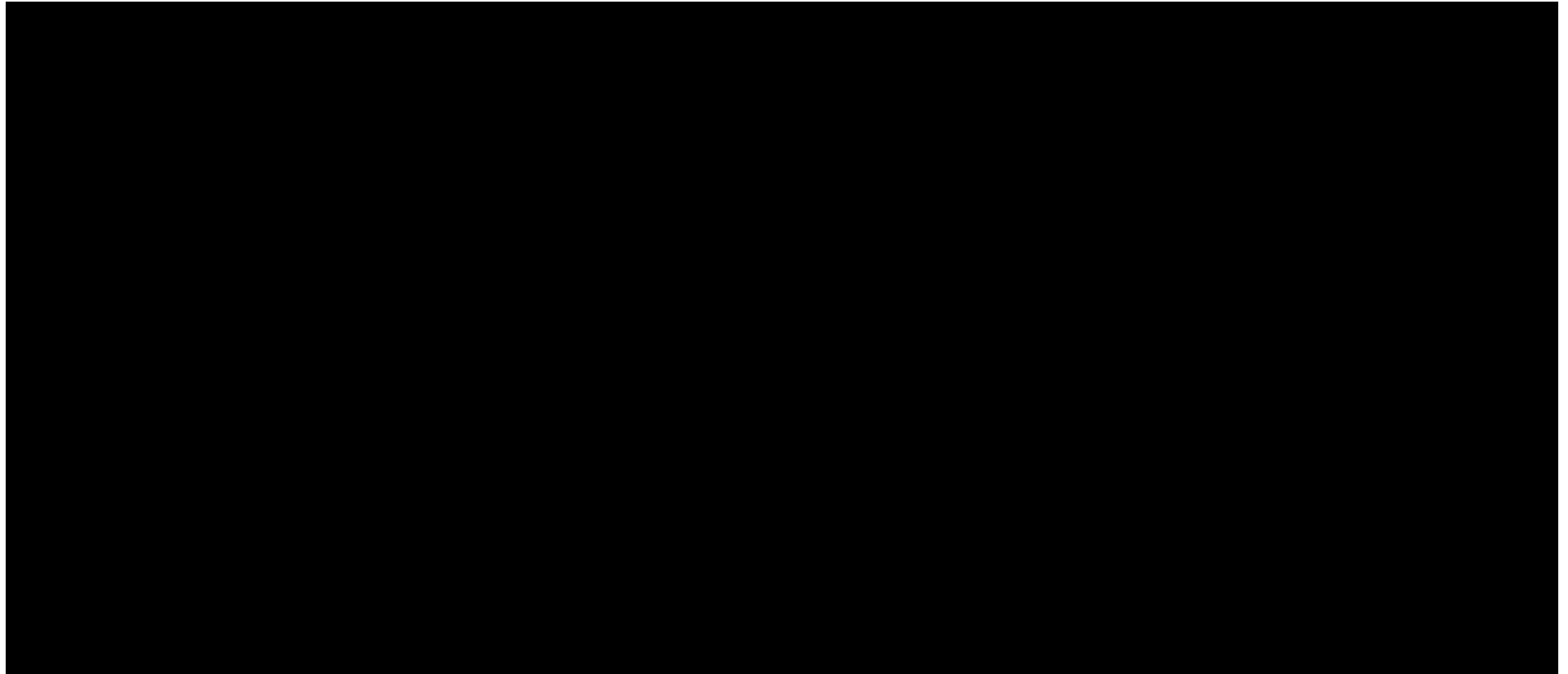


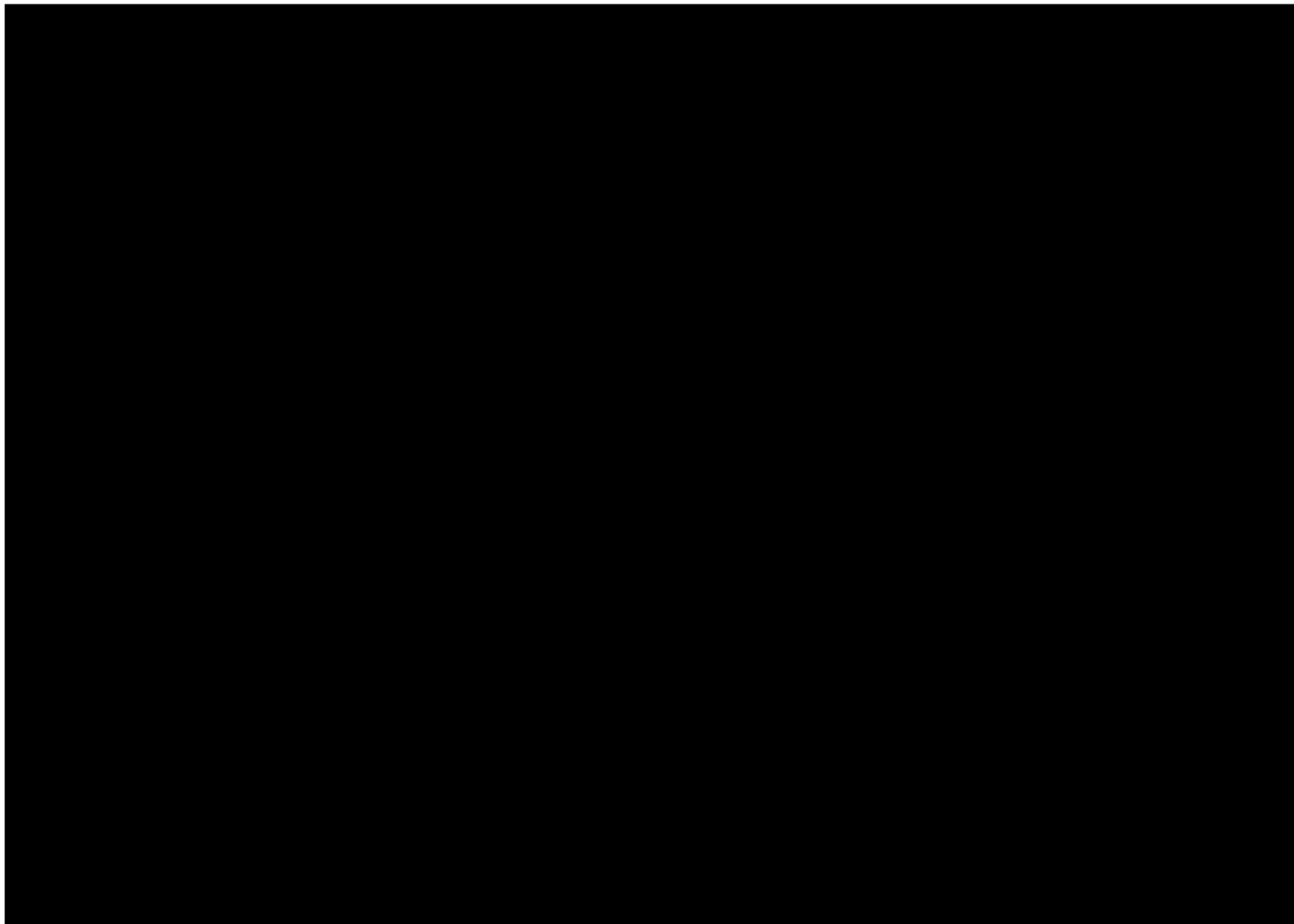


1.8.1.1 Fault Details

The following section will cover the detail of each fault in the AoR and nearby area. The map (**Figure 1-59**) illustrates the faults within the local area and Model and **Figure 1-60** illustrate the faults in additional 3D orientations. This includes a 3D representation of the geometry of each of the faults which are numbered relative to the descriptions below.







Fault #1 (F1): This is the northernmost fault in the system. It has a WSW-ENE orientation, and its



1.8.2 *Fractures*

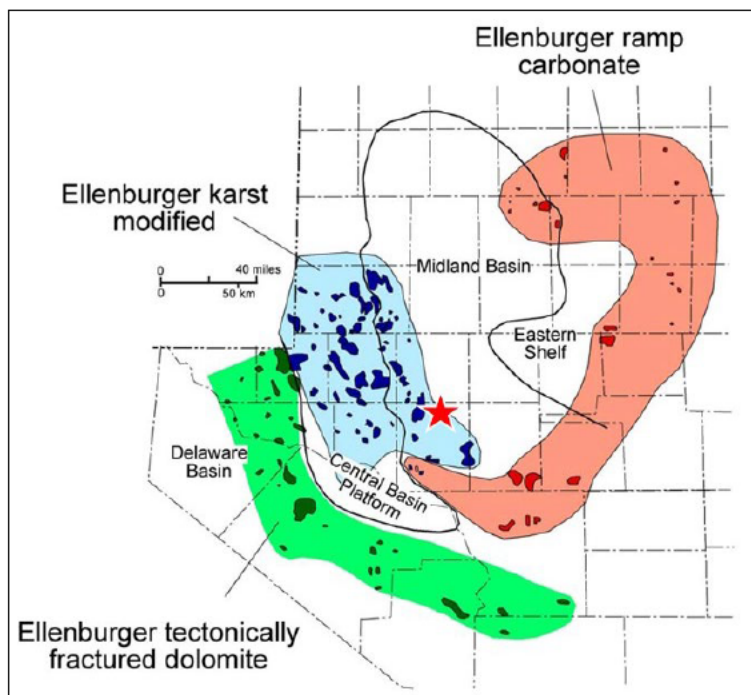


Figure 1-61: Ellenburger Group Reservoir Types

Distribution of Ellenburger Group Reservoir types by Holtz and Kerans (1992) showing Karst Modified areas. (Loucks, 2023) Red Star for Midland CCS #2 Well. Notice how the location is on the edge of the Karst modified area but still within it.



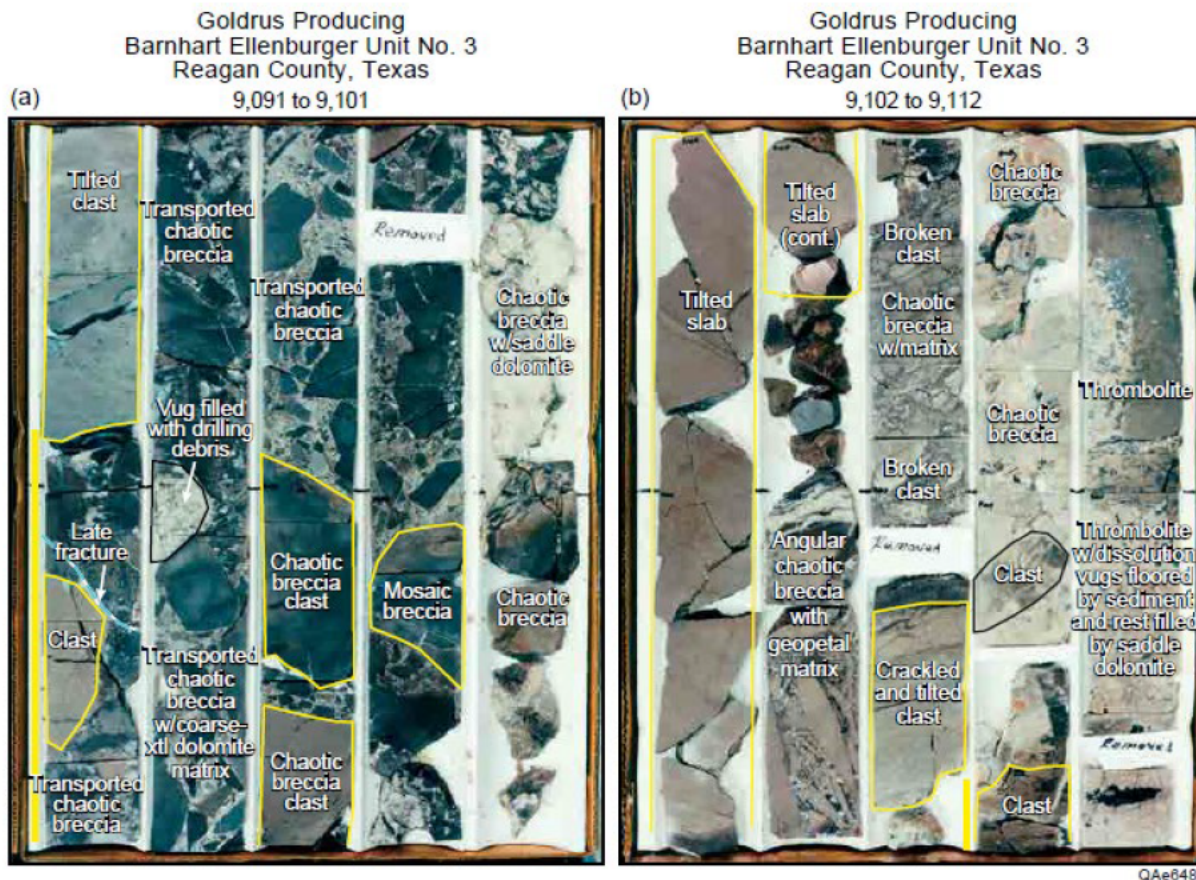


Figure 1-62: Ellenburger Paleocave Facies

Copied from Loucks and Kerans 2019, Example of several Ellenburger paleocave facies from Goldrus Producing Company Barnhart Ellenburger Unit No. 3 core in Reagan County, Texas. Larger clasts are outlined in yellow. (a) Debris-flow chaotic breccia in a paleocave passage. Notice that some clasts show crackle brecciation by compaction. (b) Large deformed blocks with crackle-breccia overprint at far-left column and far right



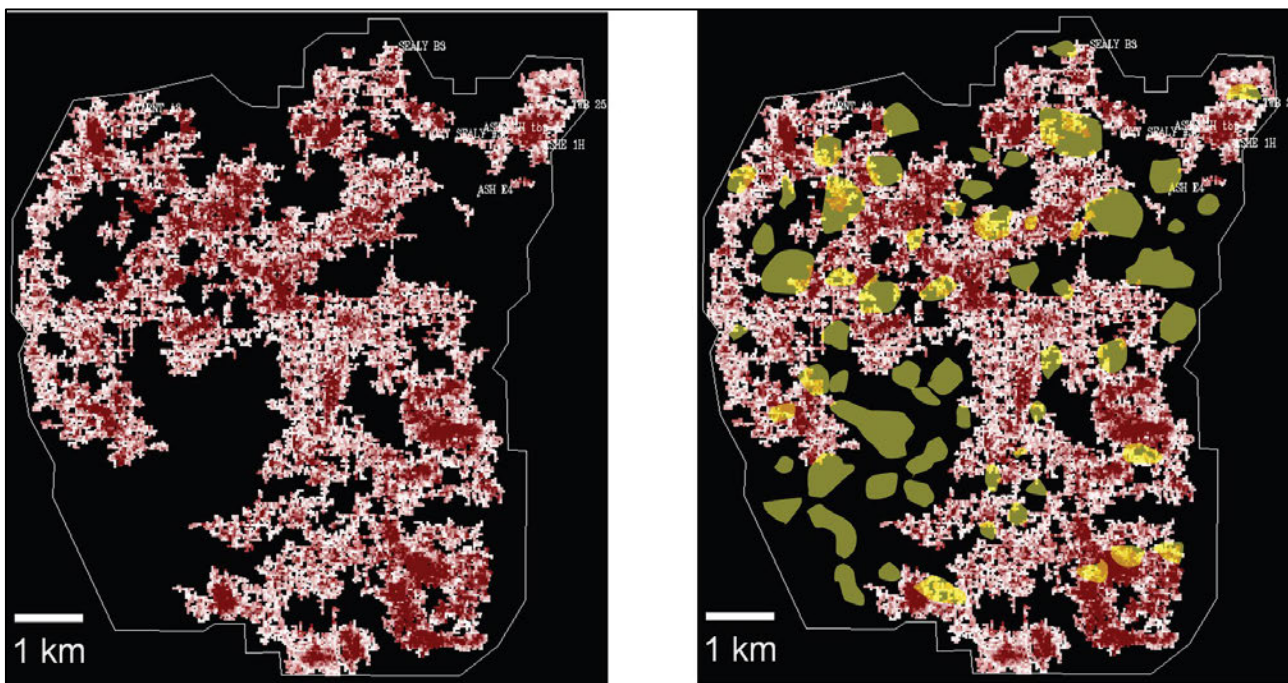


Figure 1-63: Intra-Ellenburger Horizon Amplitude Map

From McDonnell et al. 2007, amplitude map extracted from an intra-Ellenburger horizon. The horizon was mapped only where the reflection was distinct and continuous (assumed unkarsted host rock). (Left) Intervening low-amplitude, chaotic reflections are assumed to be paleocave collapse-brecciated zones. (Right) Overlay of circular sag structure locations shows that they correspond to chaotic Ellenburger zones (i.e., paleocave zones). This suggests a good correlation between collapse feature locations and their causal mechanism

1.8.3 Seismic History [146.82 (a) (3) (v)]

An important consideration in the design and development of all new injection well projects is the determination for the potential of injection activities to induce a seismic event. As shown in more detail below, there is a low probability [REDACTED].

Studies completed by the United States Geological Survey (USGS) indicate there is a low probability of earthquake events occurring in the Midland Basin of west Texas that would cause damage to infrastructure (**Figure 1-64**) (Geological Survey, 2024). According to the recent updates from the USGS, the proposed Well location is located in a region with the lowest probability of a damaging earthquake in the country.

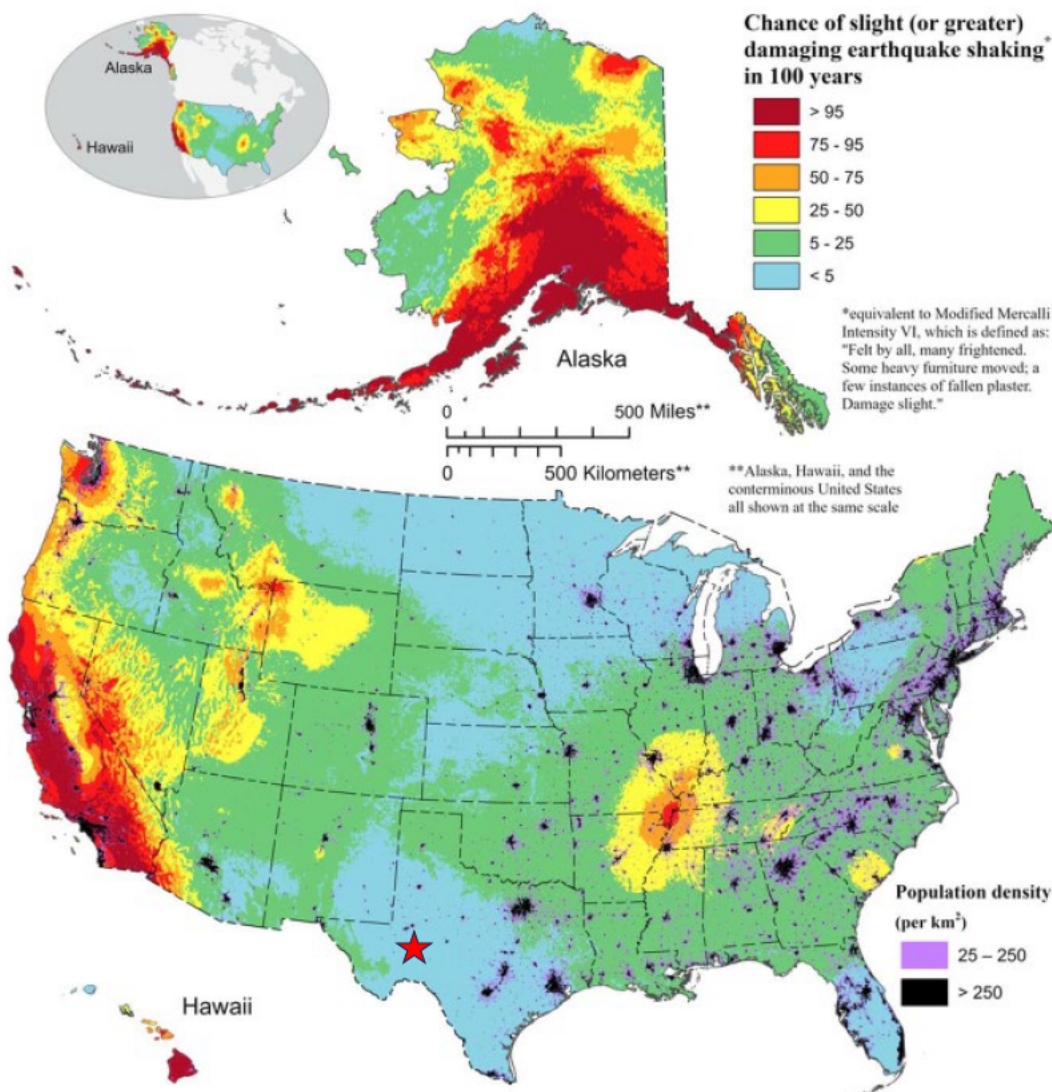


Figure 1-64: Frequency of U.S. Damaging Earthquakes

Probabilistic map showing how often scientists expect damaging earthquake shaking around the United States (U.S. Geological Survey, 2023). The map illustrates there is a low probability of damaging earthquake events occurring in west Texas area near Midland CCS #2 well (red star).

The USGS also recently updated the Seismic Hazard Map (Figure 1-65) in January of 2024. This report illustrates peak ground accelerations having a 2 percent probability of being exceeded in 50 years. The models are based on seismicity and fault-slip rates and take into account the frequency of earthquakes of various magnitudes. The map illustrates that the Midland CCS #2 location was within a region with one of the lowest hazard probabilities within the country.

The Permian Basin is a tectonically stable region of the North American Craton. Most of the relatively larger earthquakes in Texas are associated with the major geological faults and uplifts (Figure 1-66). The proposed Facility sits in the middle of Texas and far away from any of these relatively large historical earthquakes.

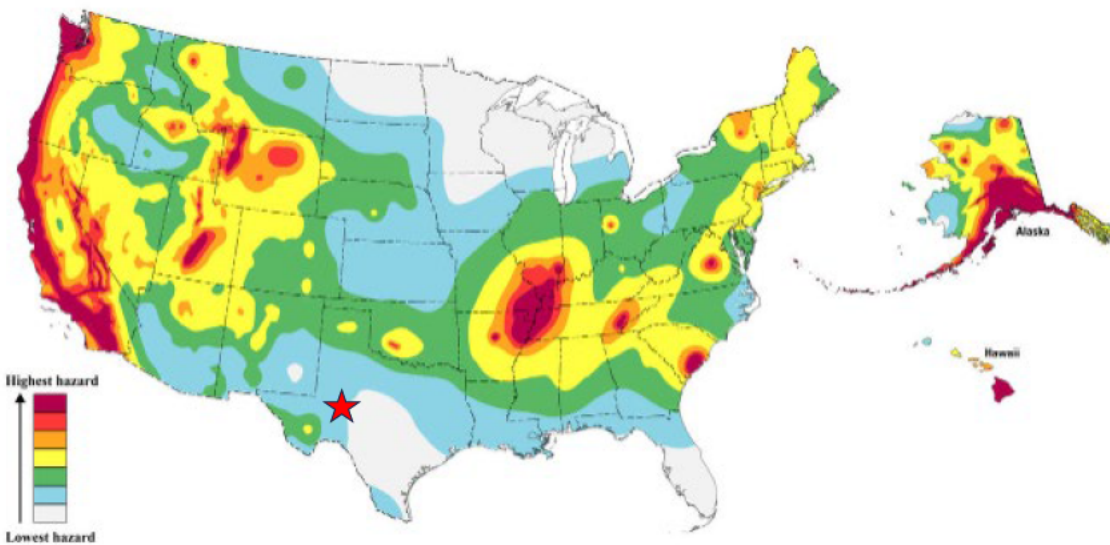


Figure 1-65: USGS Seismic Hazard Map

Hazard map is a simplified 2% in 50-year probability of exceedance map (U.S. Geological Survey, 2024). Red star illustrates the approximate location of Midland CCS #2 Well.

Texas has several distinct structural regions, each with different fault orientations, ages, and architecture (Figure 1-66).

The Basin and Range province of West Texas, in the center of the North American Craton, has fault systems related to past orogenic events and is currently being stressed by several mountain ranges to the west including the Franklin Mountains, the Guadalupe Mountains, the Sacramento Mountains and smaller ranges and the Ouachita-Marathon Thrust belt to the south. The Ouachita-Marathon thrust belt forms the northern terminus of the Balcones Fault Zone and is noted in purple. Mountain ranges are noted in red, yellow, and orange on the USGS map relating to damaging earthquakes.

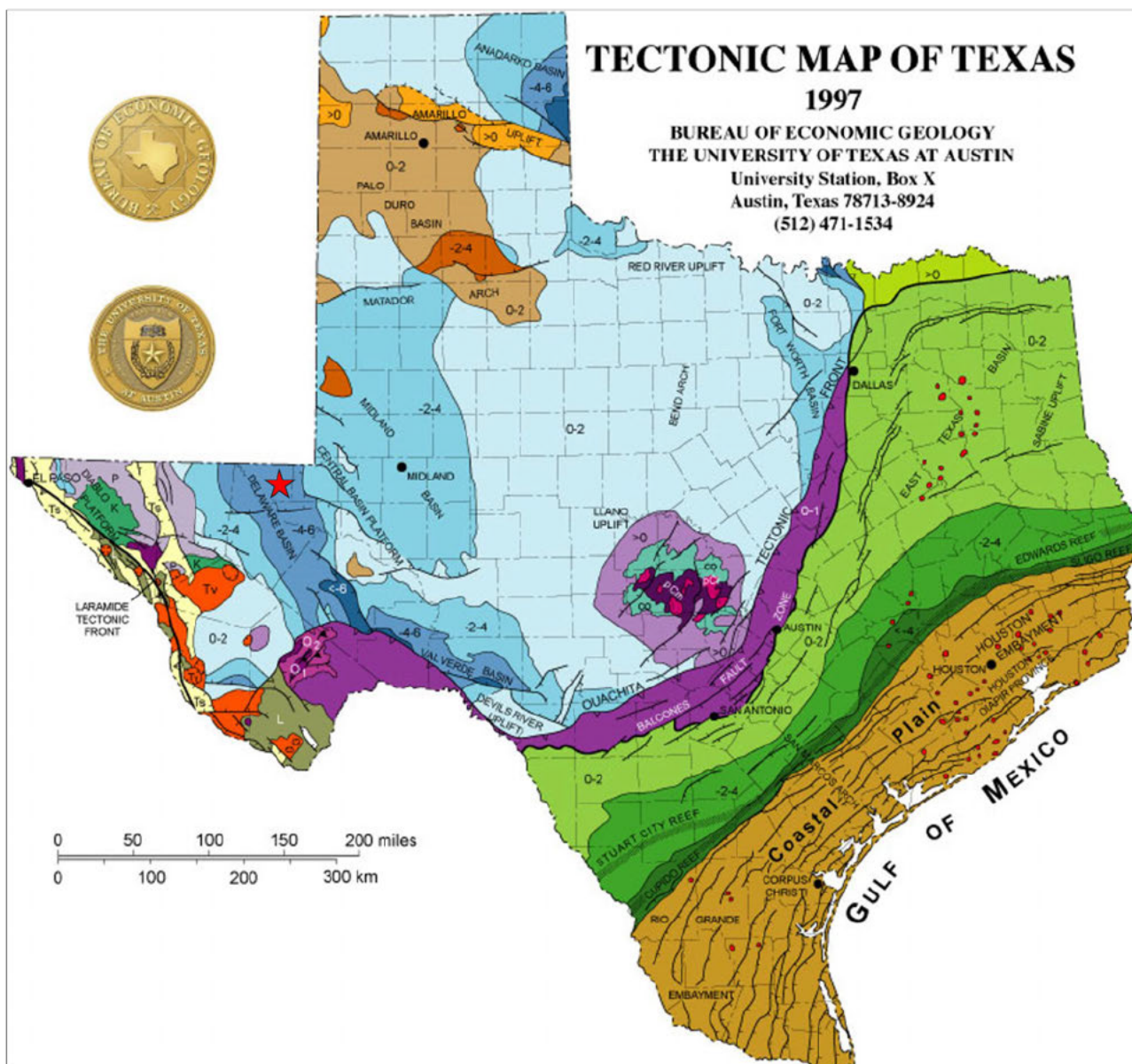


Figure 1-66: Tectonic Map of Texas

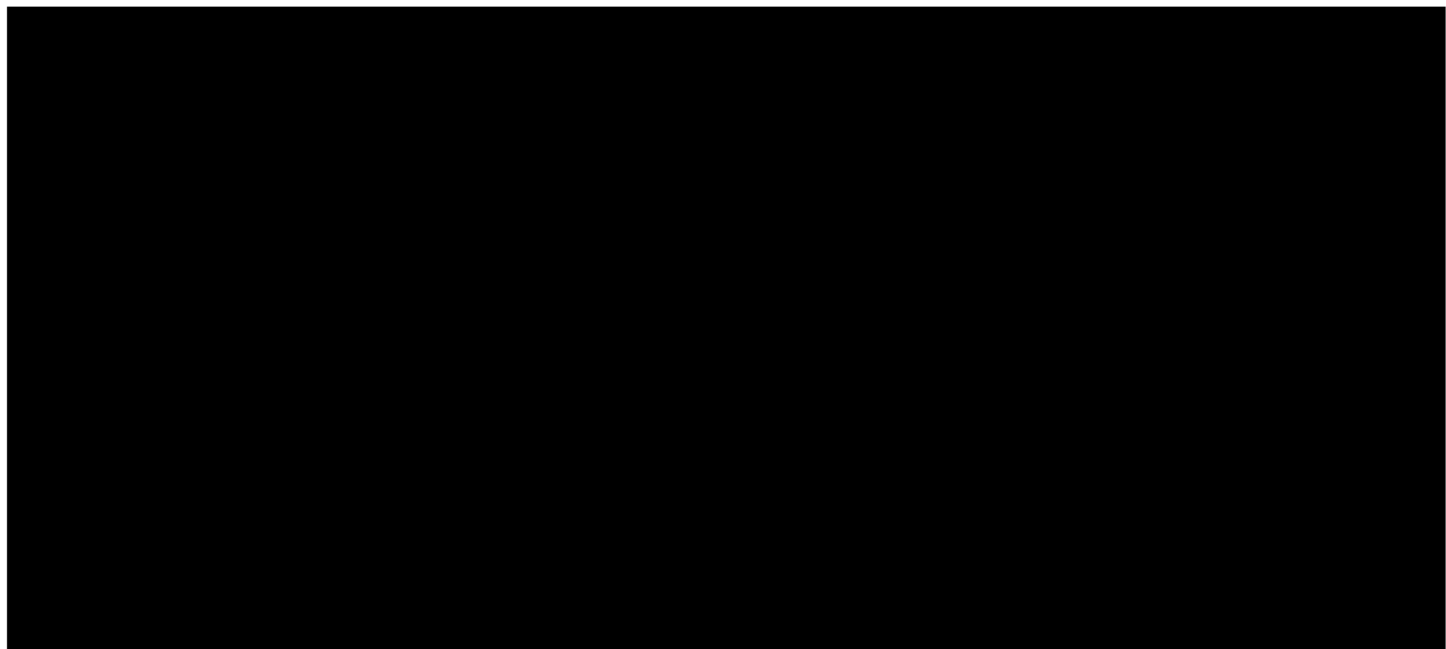
Tectonic map of Texas, BEG 1997 illustrating the major structural features of the state.

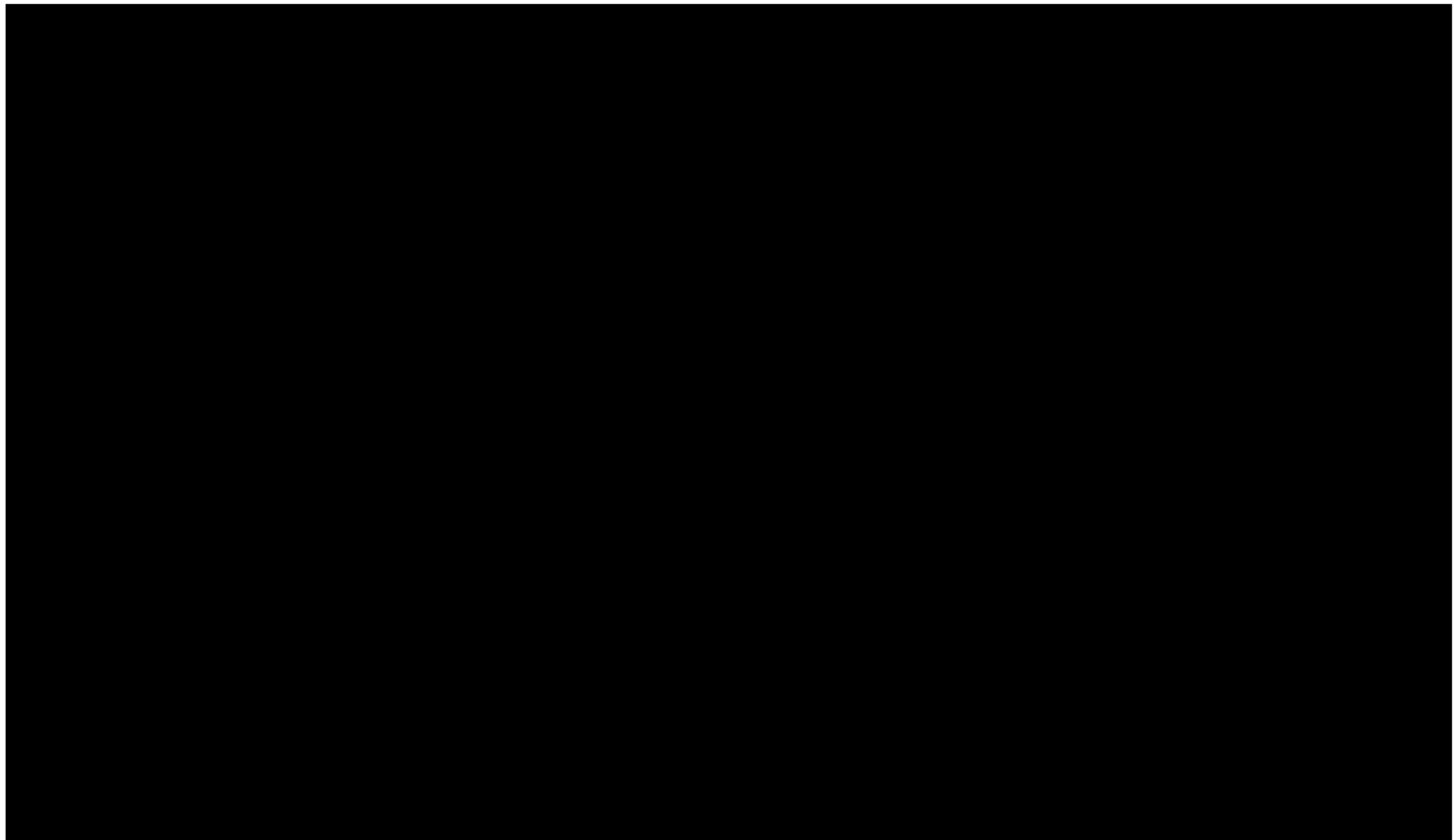
The local region of the Midland Basin has two Seismic Response Areas (SRA's) north of the location (Figure 1-67). The Gardendale Seismic Response Area and the Stanton Seismic Response Area. Both are associated with significant faulting and heavy SWD injection.





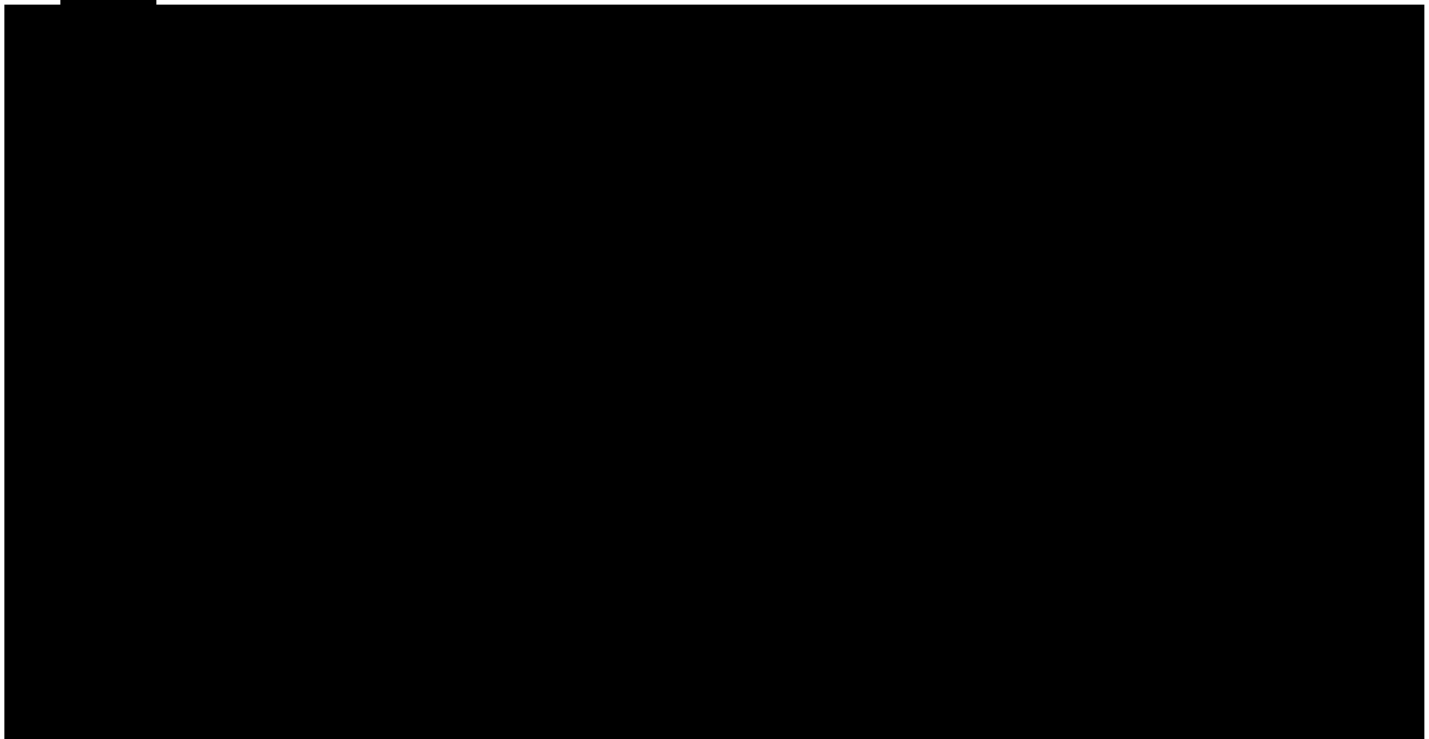
In the area close to the South Midland Facility, Texas Seismological Network and Seismology Research (TexNet) earthquake catalog search shows very little earthquake activity near the proposed injection site (**Figure 1-68**). According to TexNet, an earthquake catalog, there have been 10 earthquakes reported within a 10-mile radius since 2016, the inception of the [REDACTED]





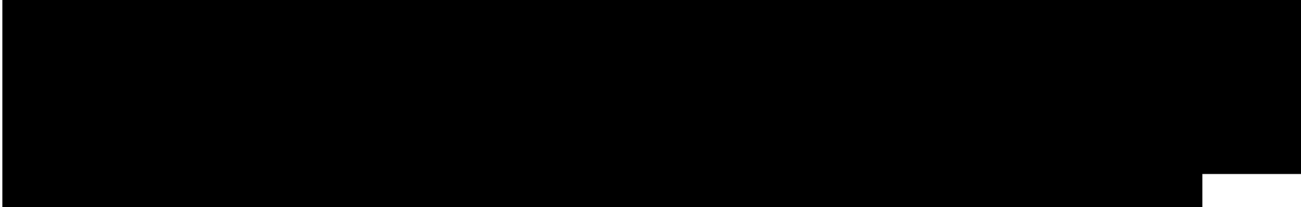
1.8.4 Regional Stress

The stress regime and maximum horizontal stress orientation is well-studied and understood in west Texas area. **Figure 1-71** displays the regional stress map.

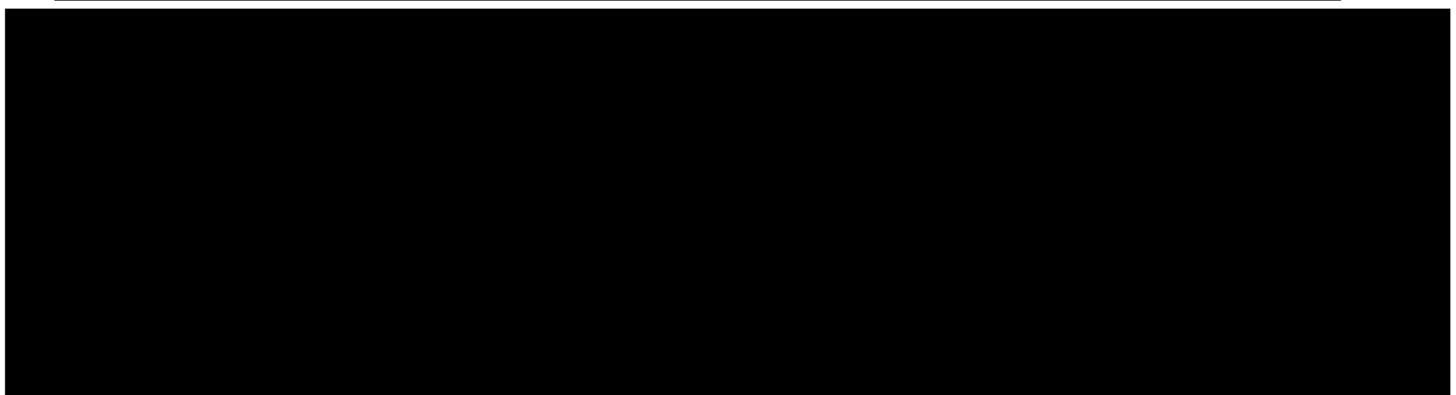
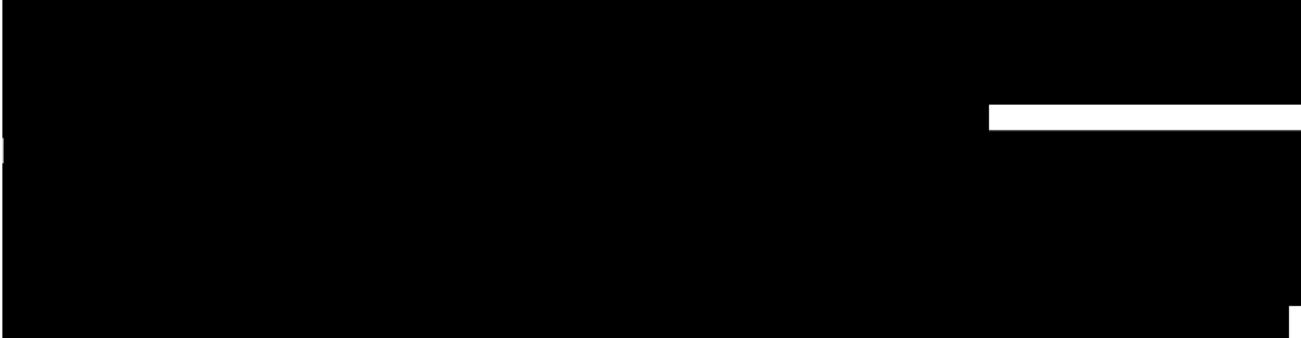


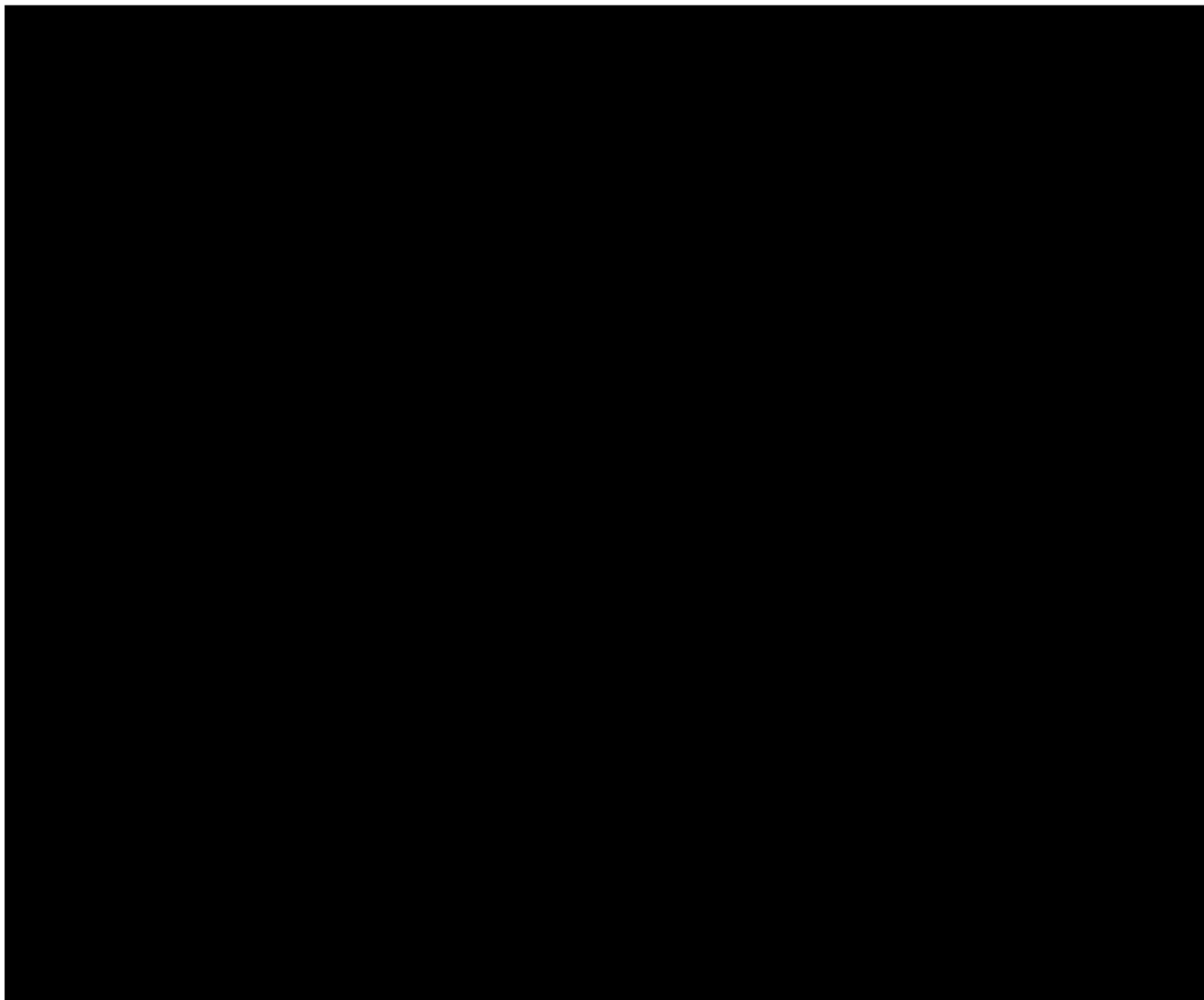
1.8.5 Fault Slippage Potential Analysis

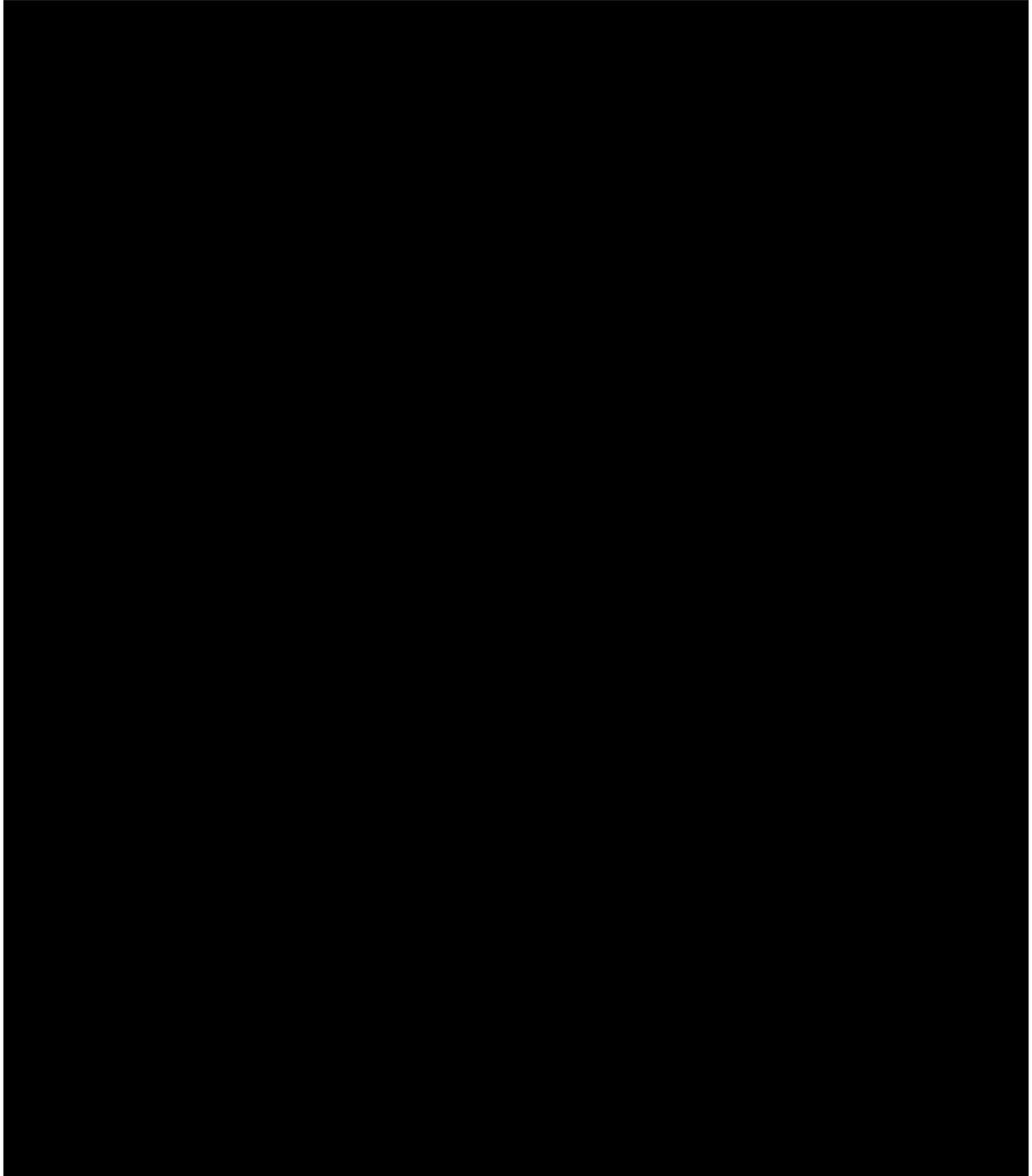
This section contains a fault slippage potential (FSP) analysis to examine the potential of fault movement caused by an increase in reservoir pressure due to CO₂ injection at the Well.

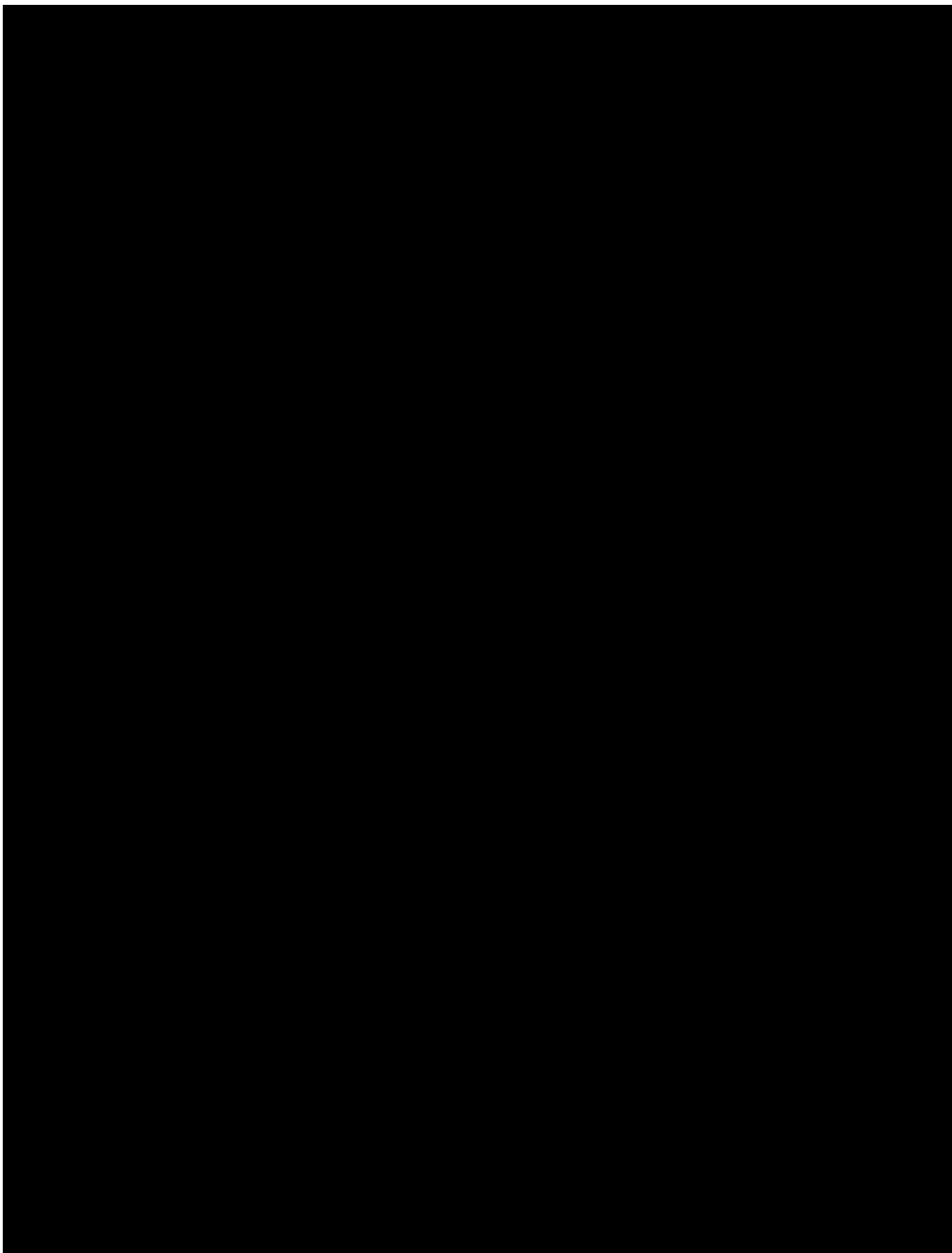


1.8.5.1









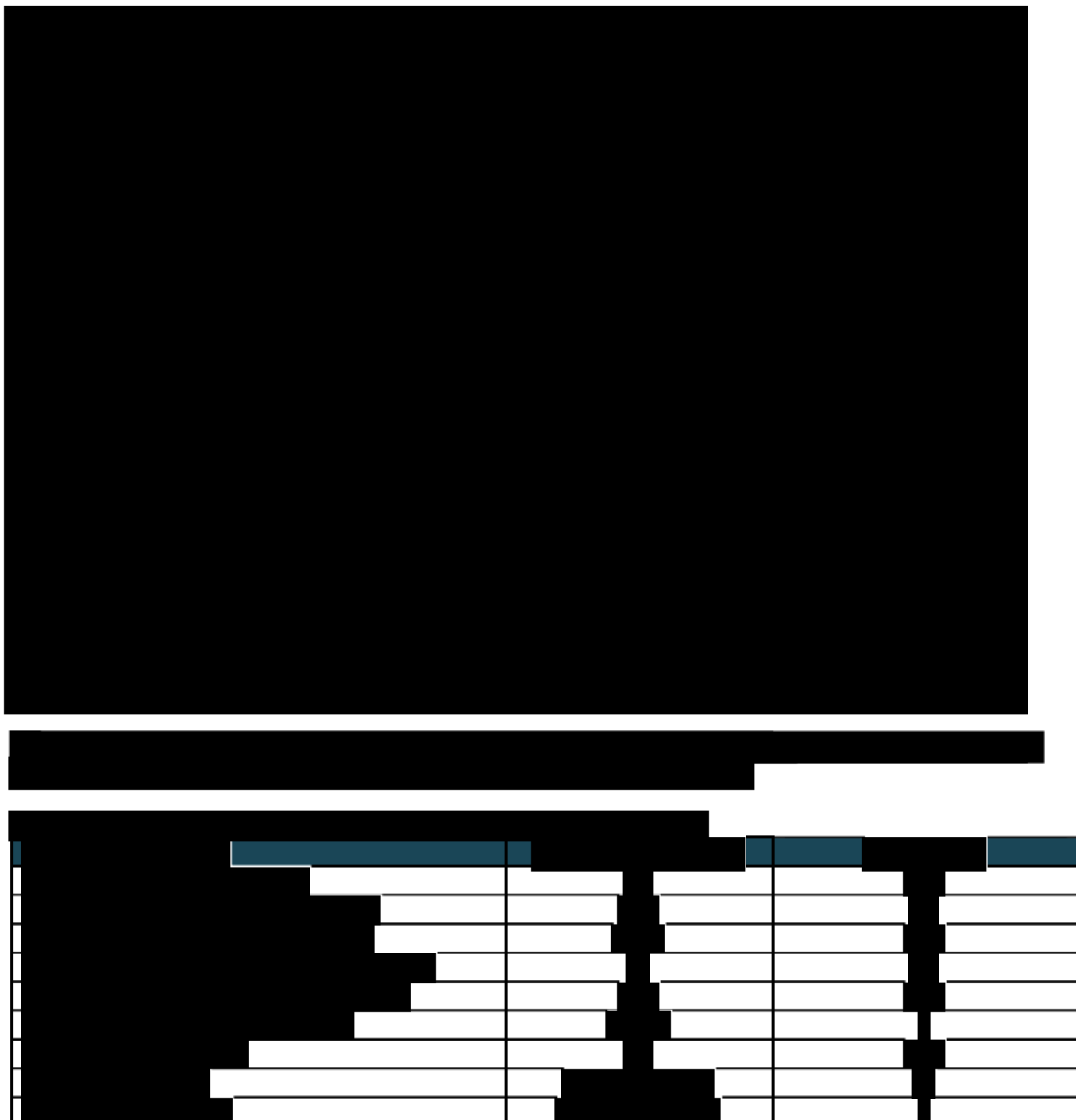
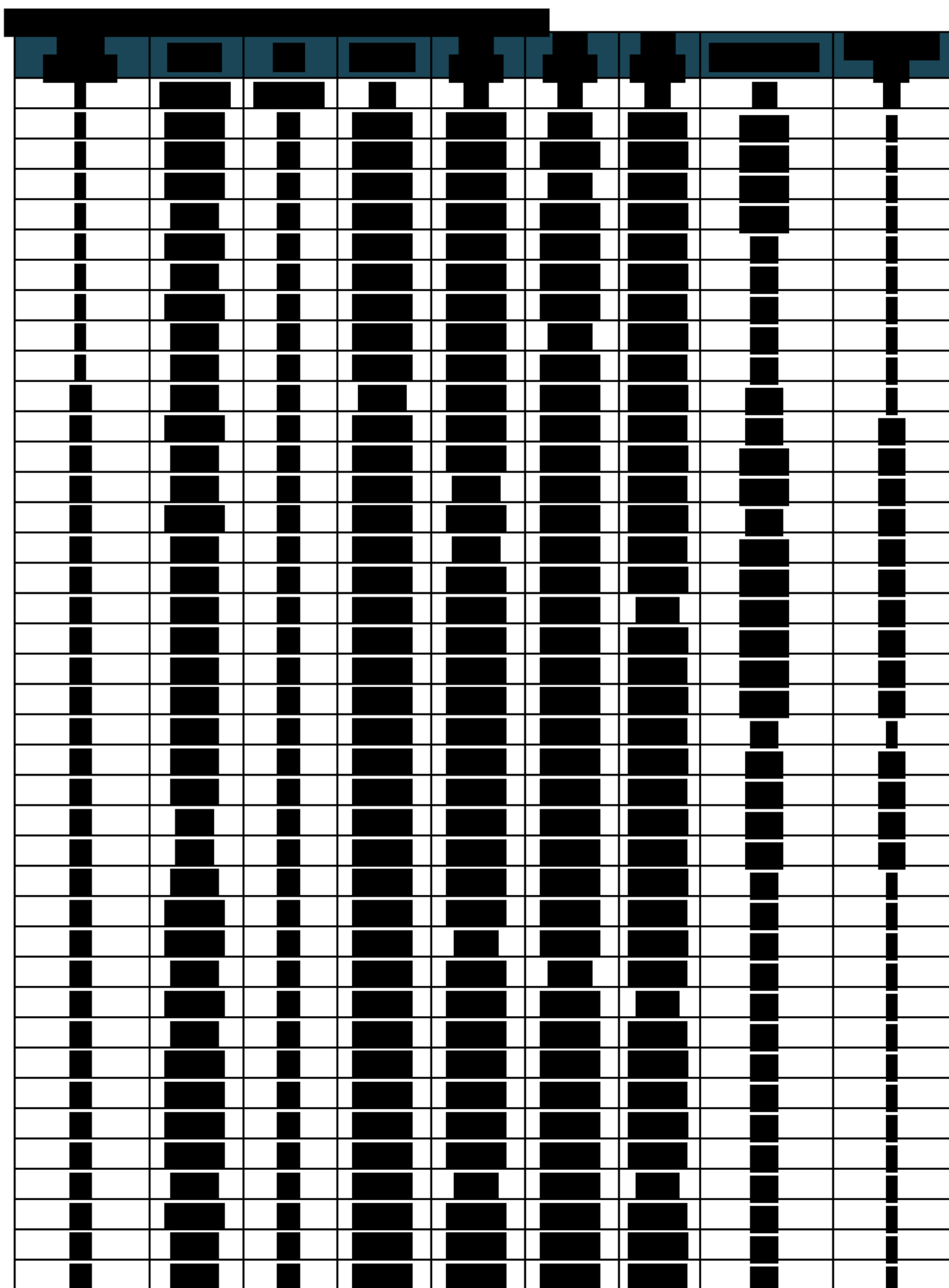
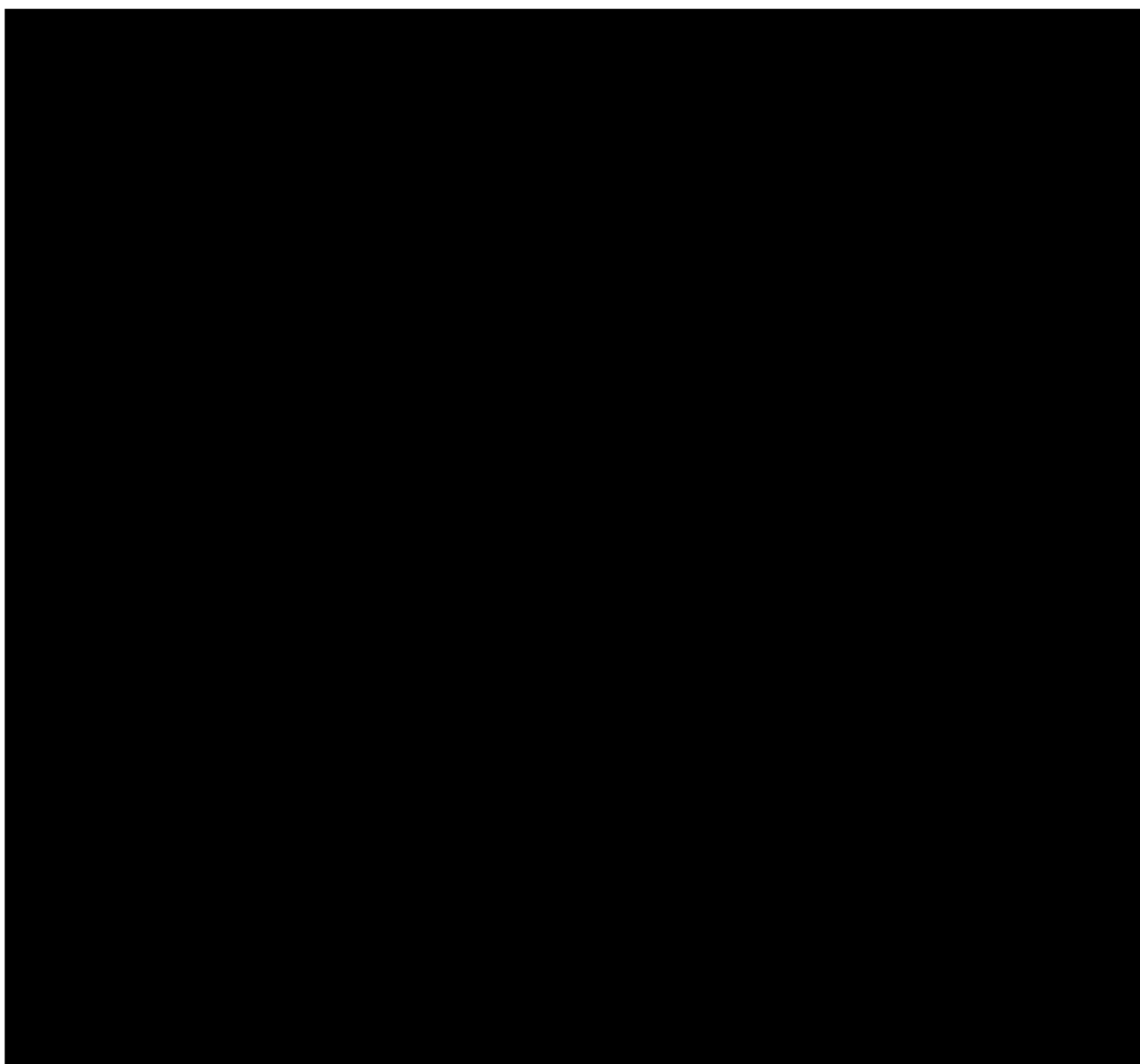
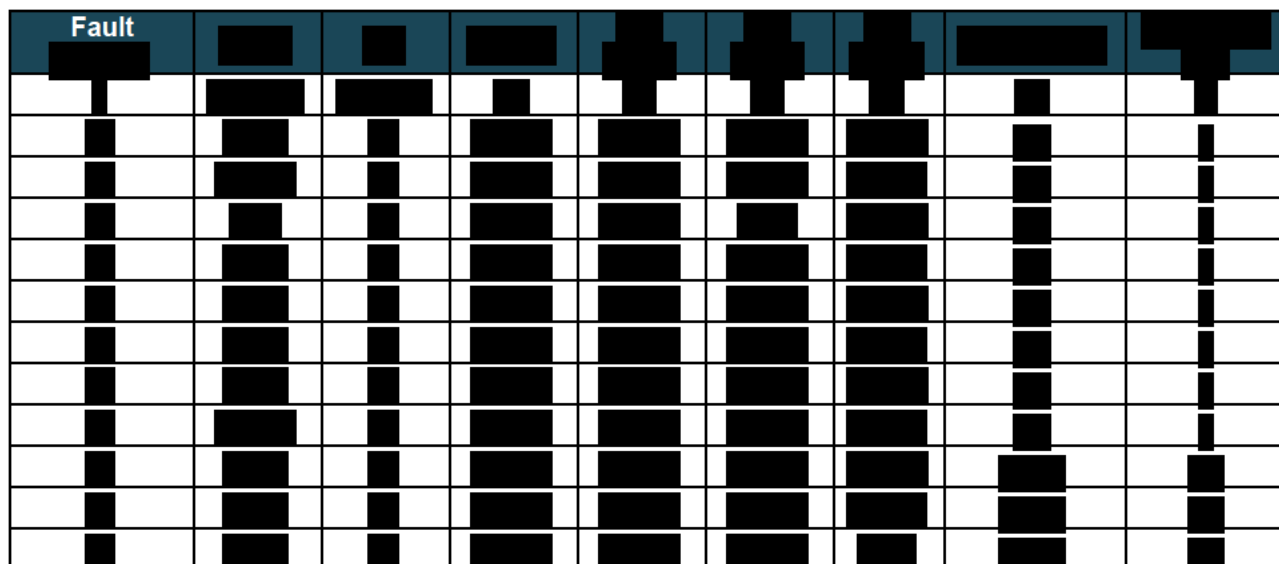


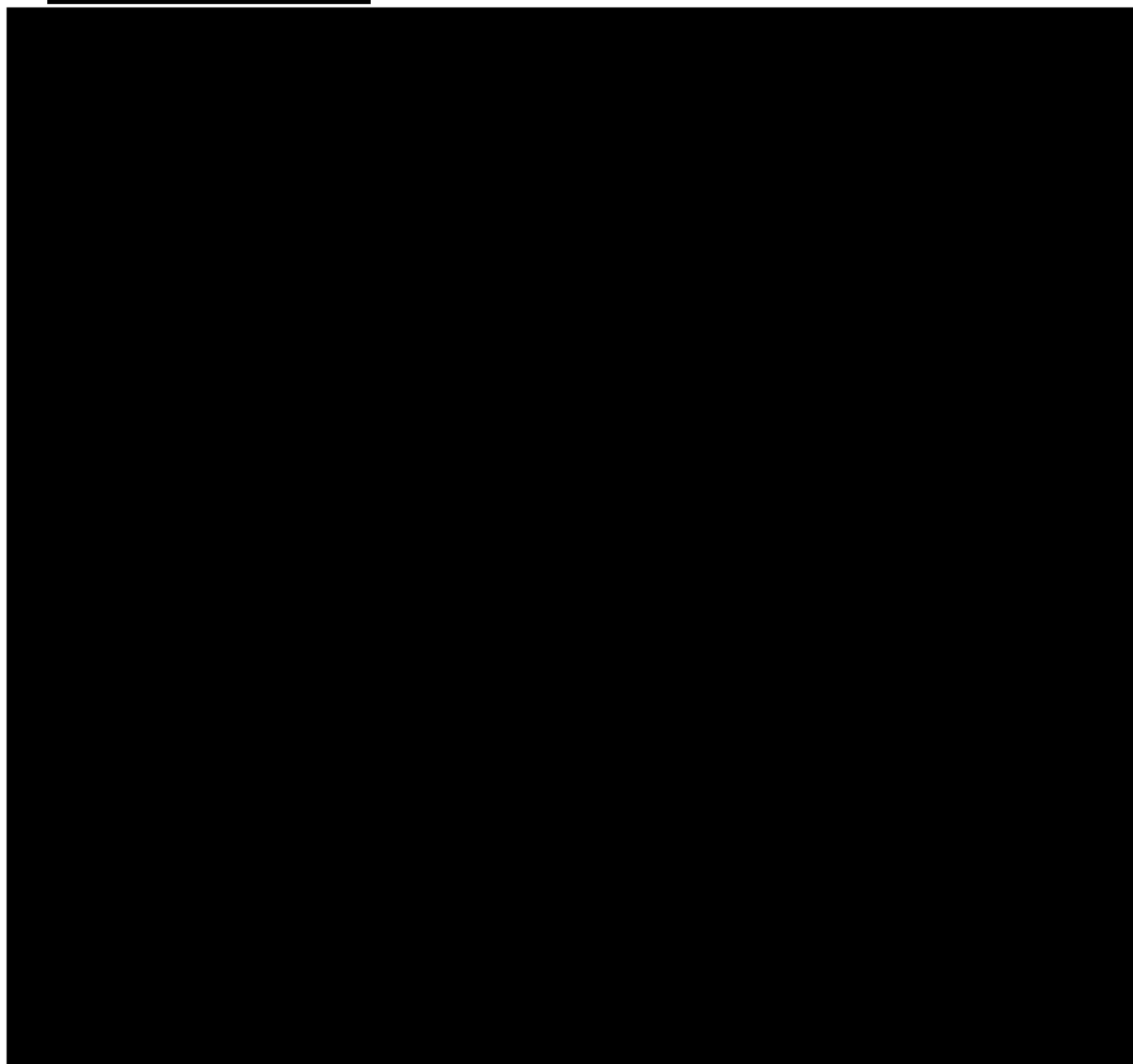
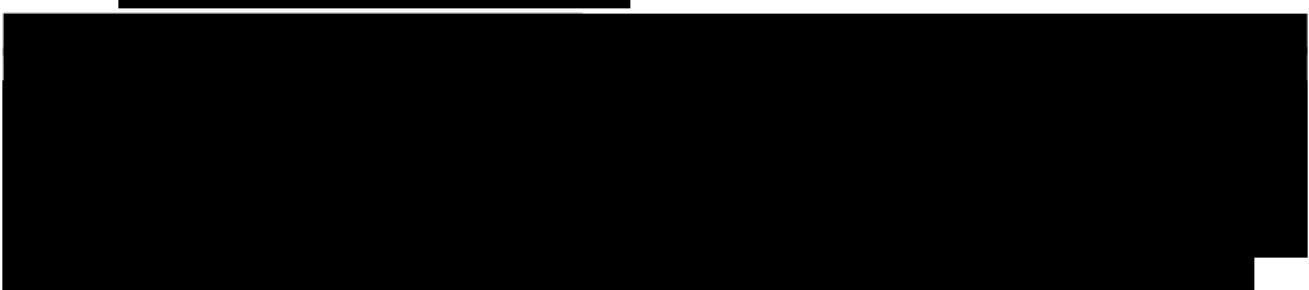
Table 1-11 illustrates the results of the Ellenburger probabilistic FSP analysis. The P10, P50, P90

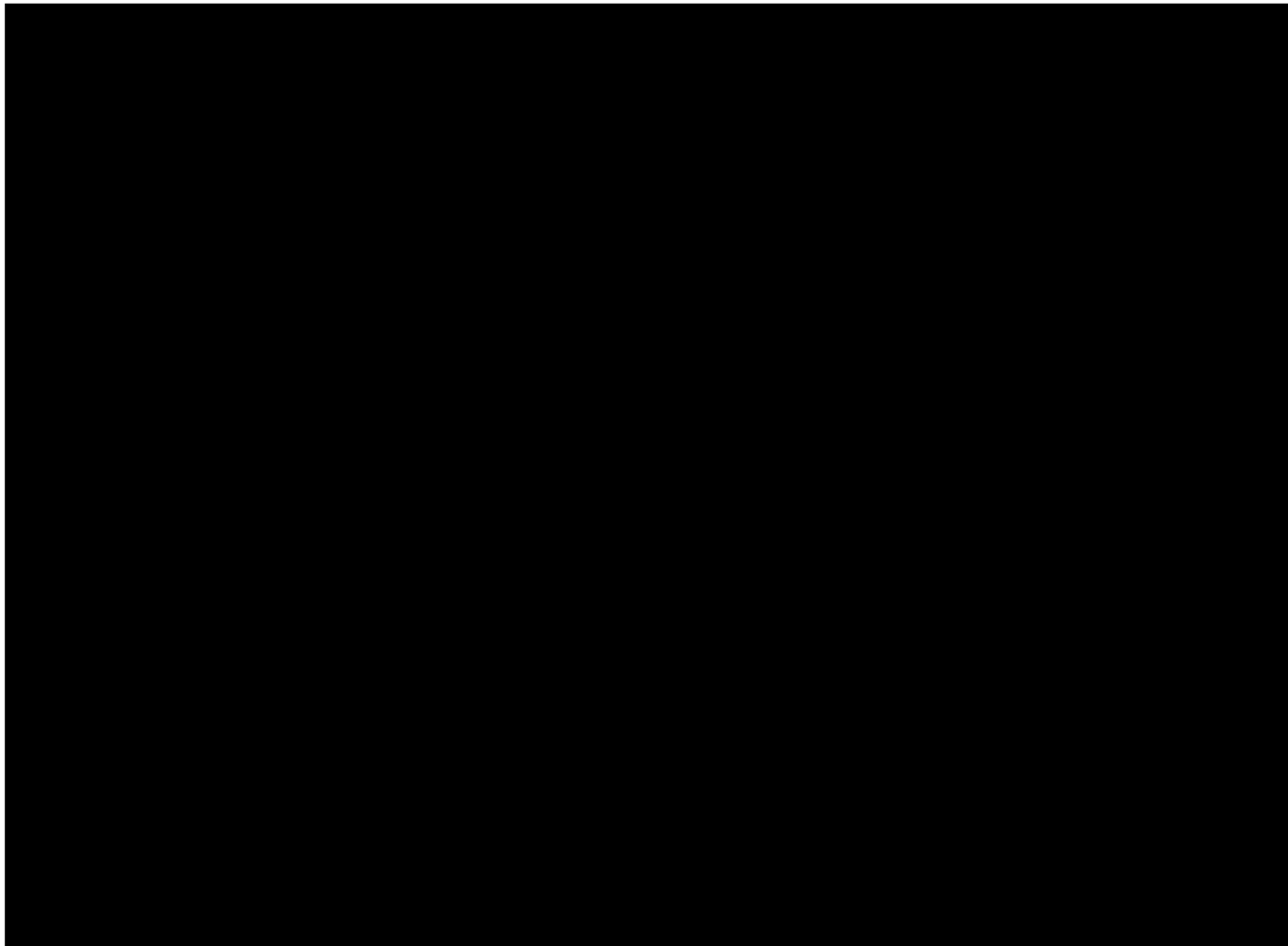
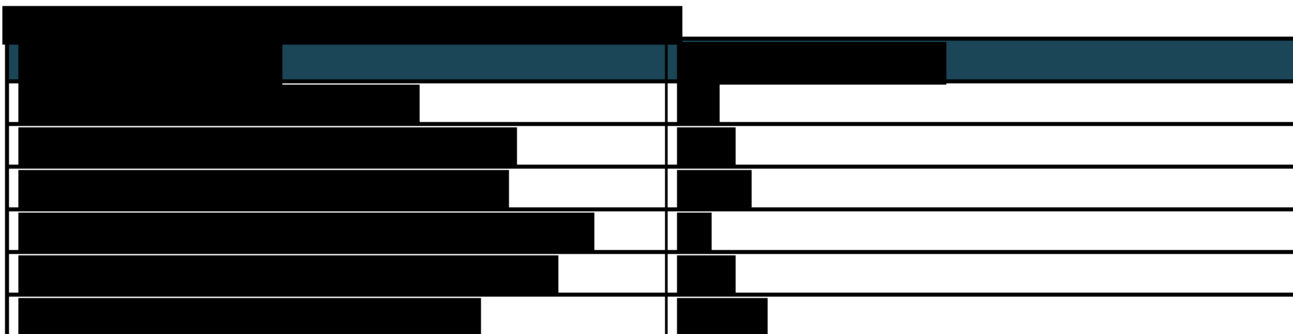


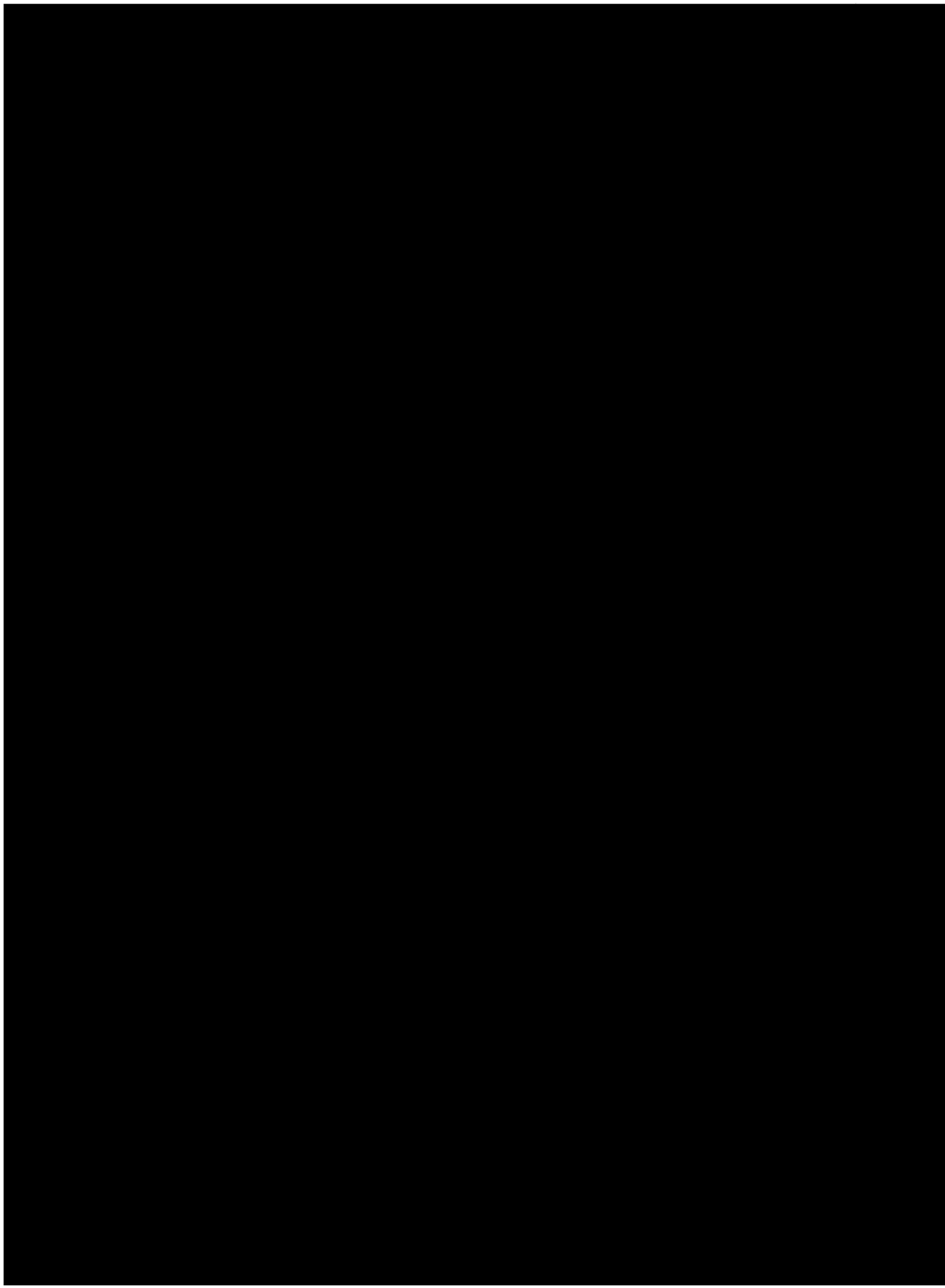


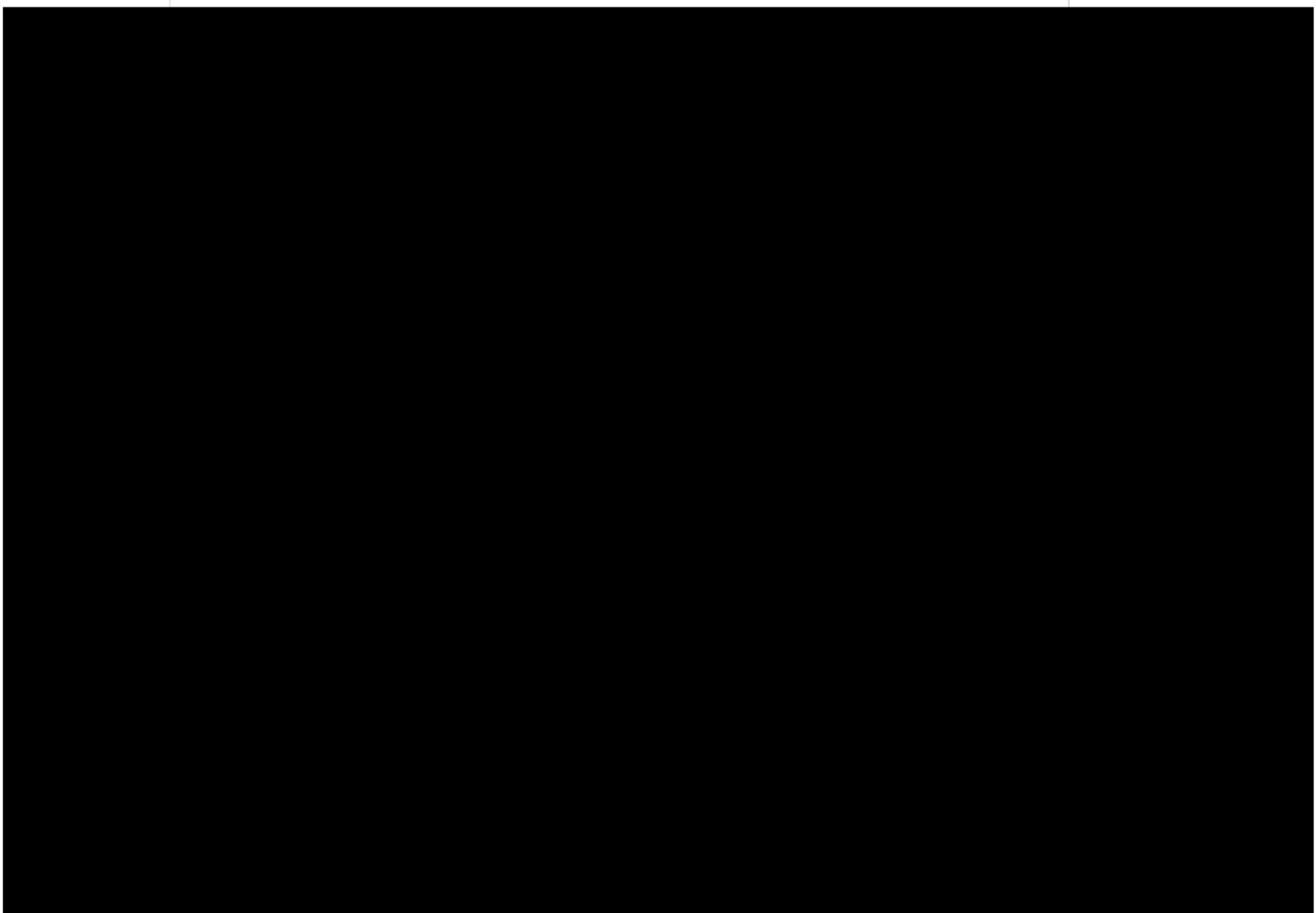


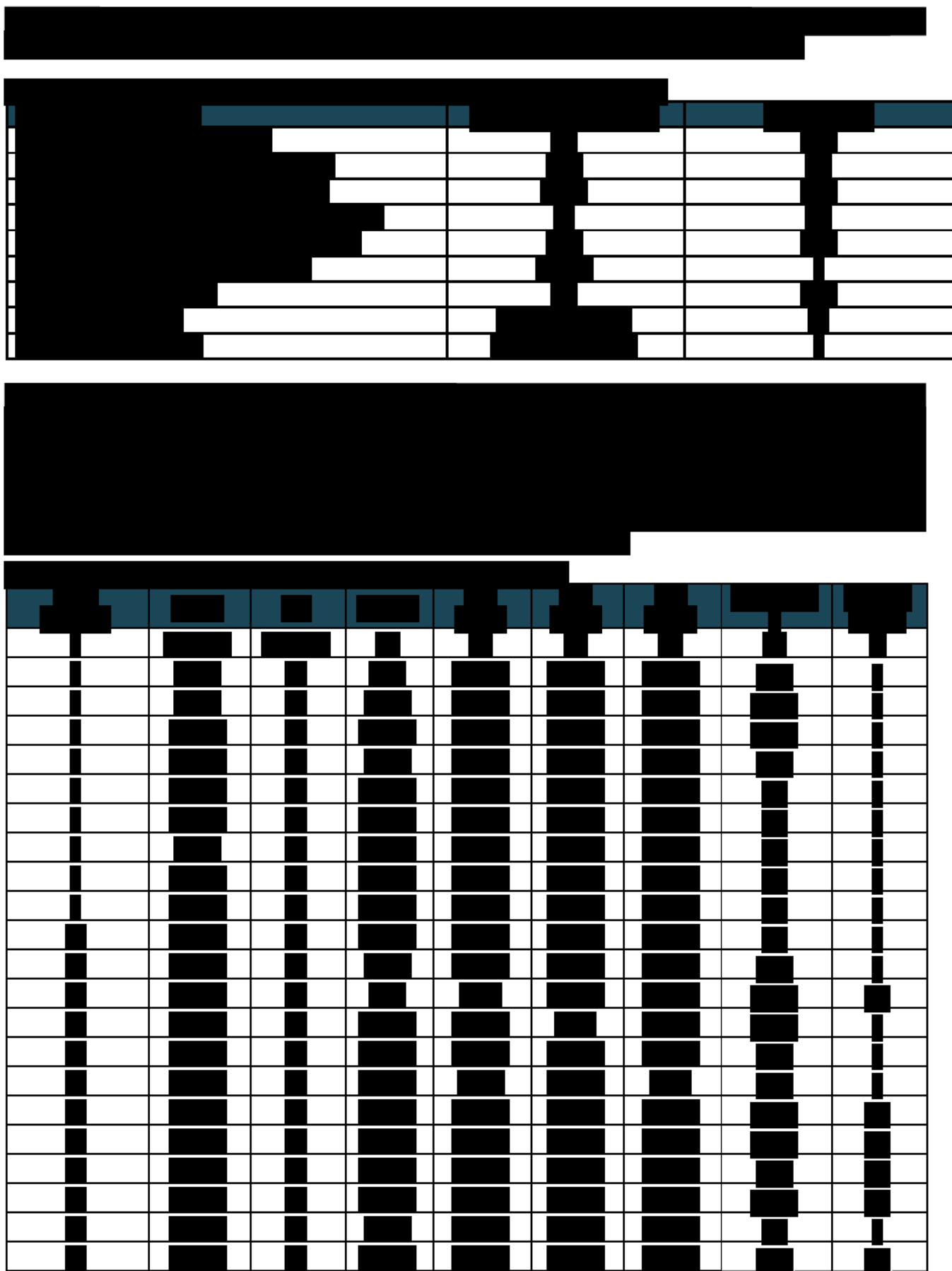
1.8.5.2

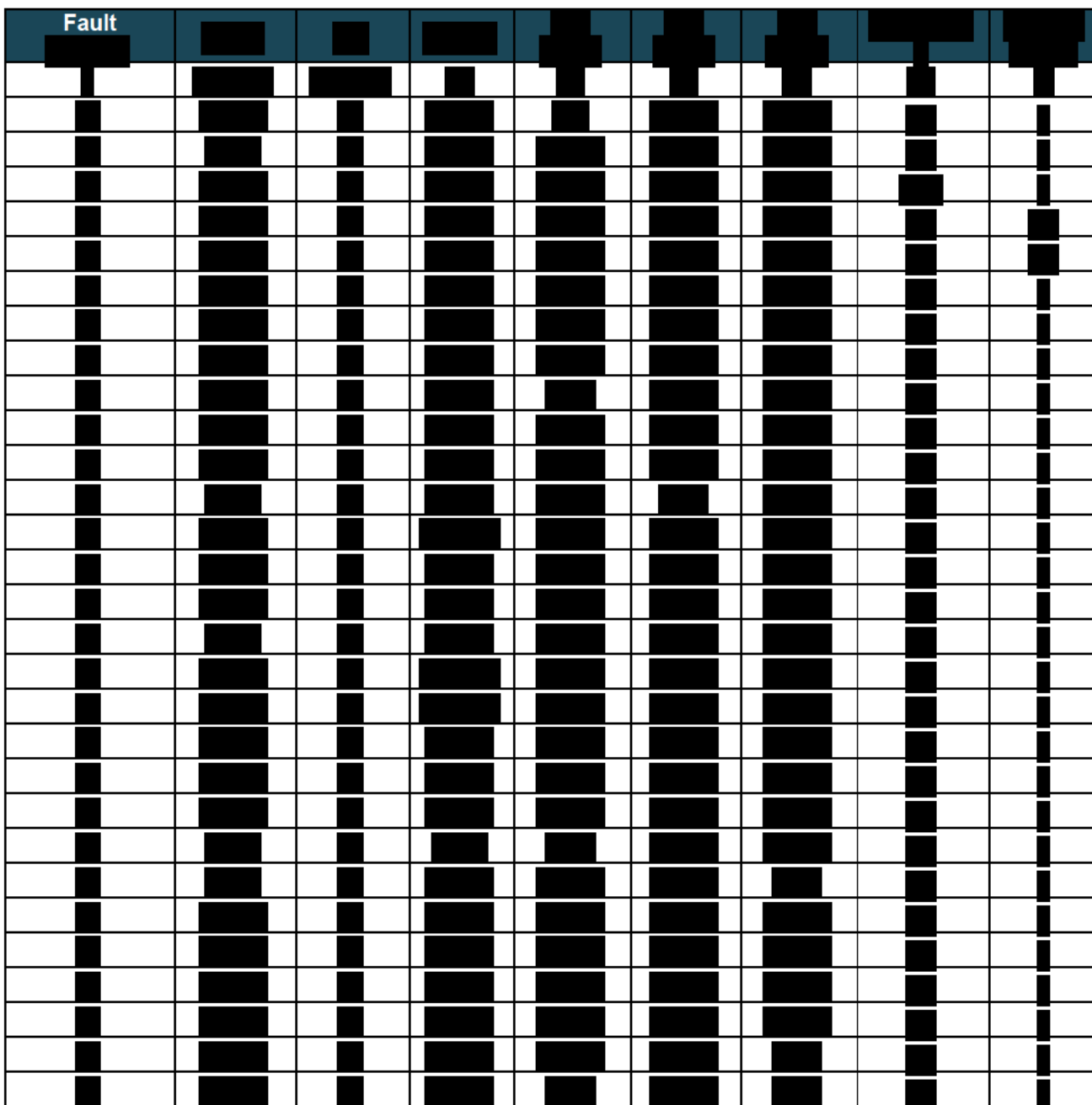










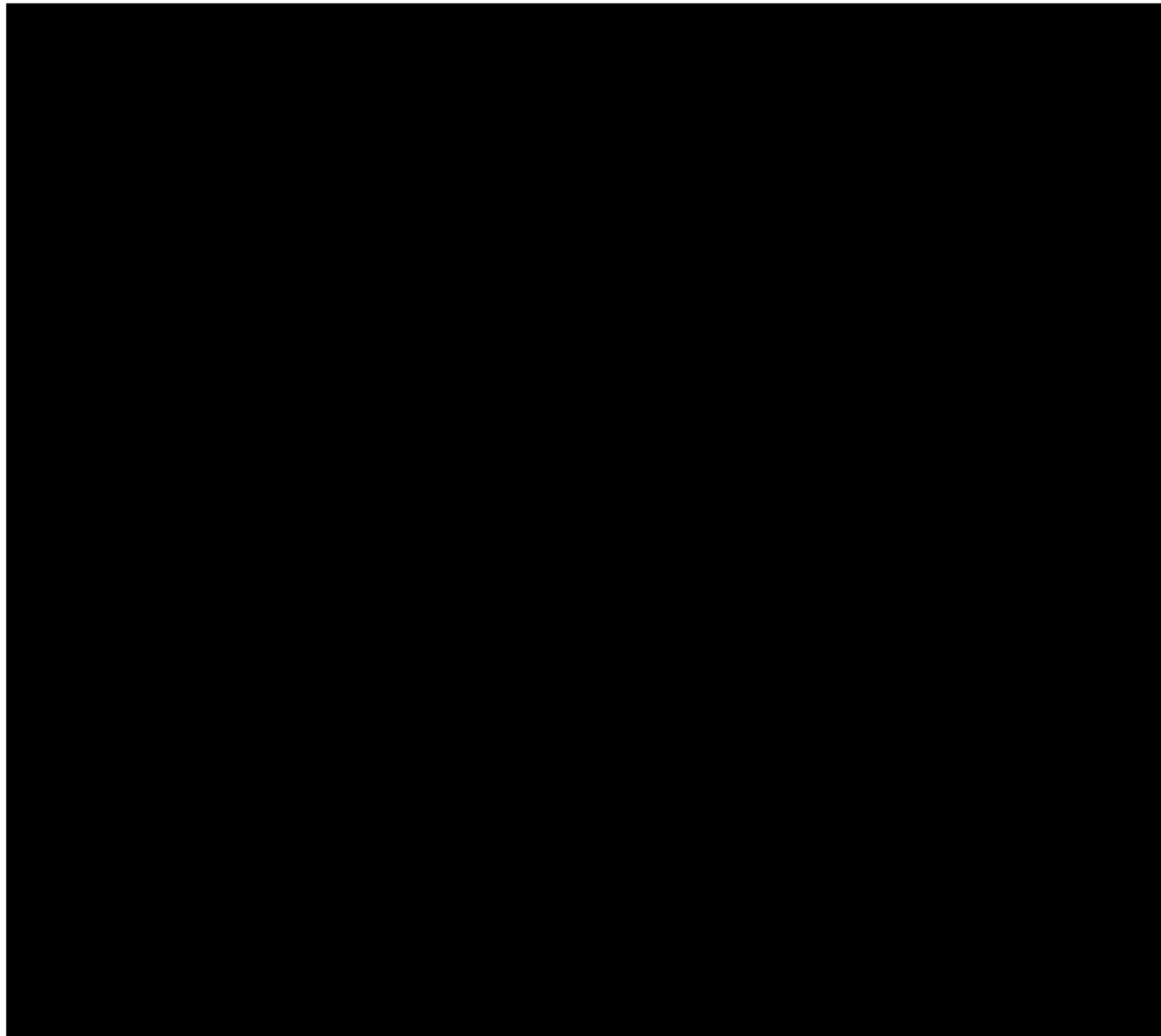


1.8.6 Summary

In summary,

[REDACTED]

[REDACTED]



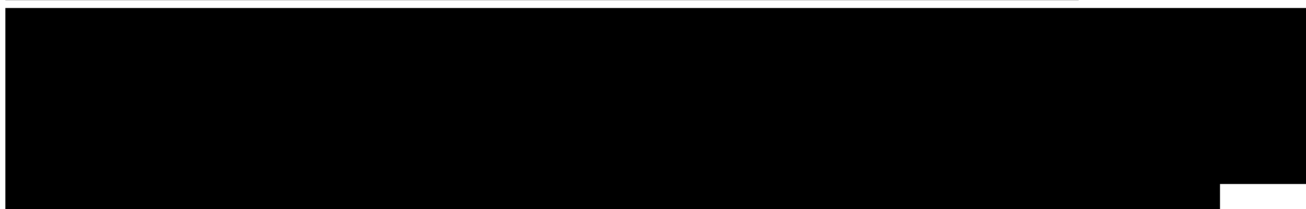
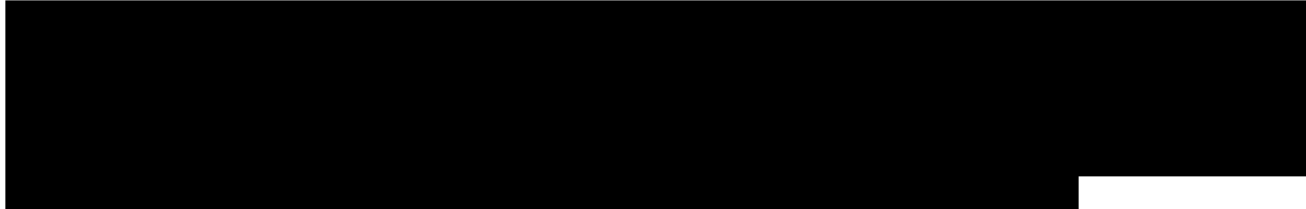
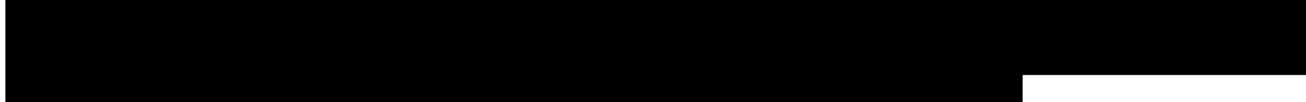
1.9 Petrophysical Characterization [40 CFR 146.82(a)(3)(iii)] [40 CFR 146.82(a)(3)(iv)]

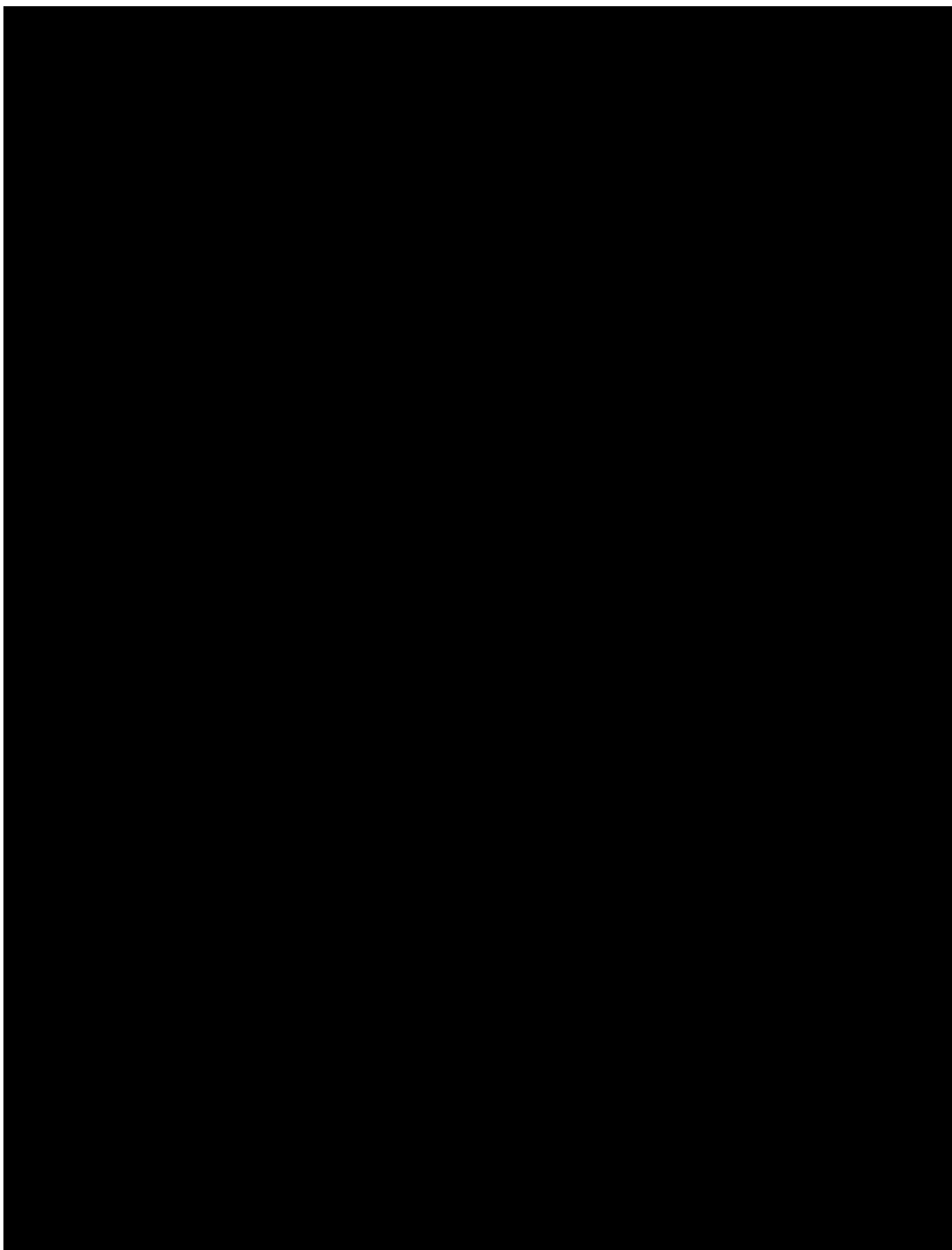
This section includes a petrophysical characterization of the injection and confining zones and includes discussion on porosity, permeability, salinity, capillary pressure and related properties. The petrophysical properties indicate the proposed Well location is suitable for the project due to it having sufficient storage (porosity), ability to inject (permeability) and the in-situ formation waters have a salinity that is significantly higher than the statutory lower limit of 10,000 parts per million (ppm) at an average salinity



1.9.1 Type Log

The type-log in Figure 1-82 is a penetration to the west of the Facility



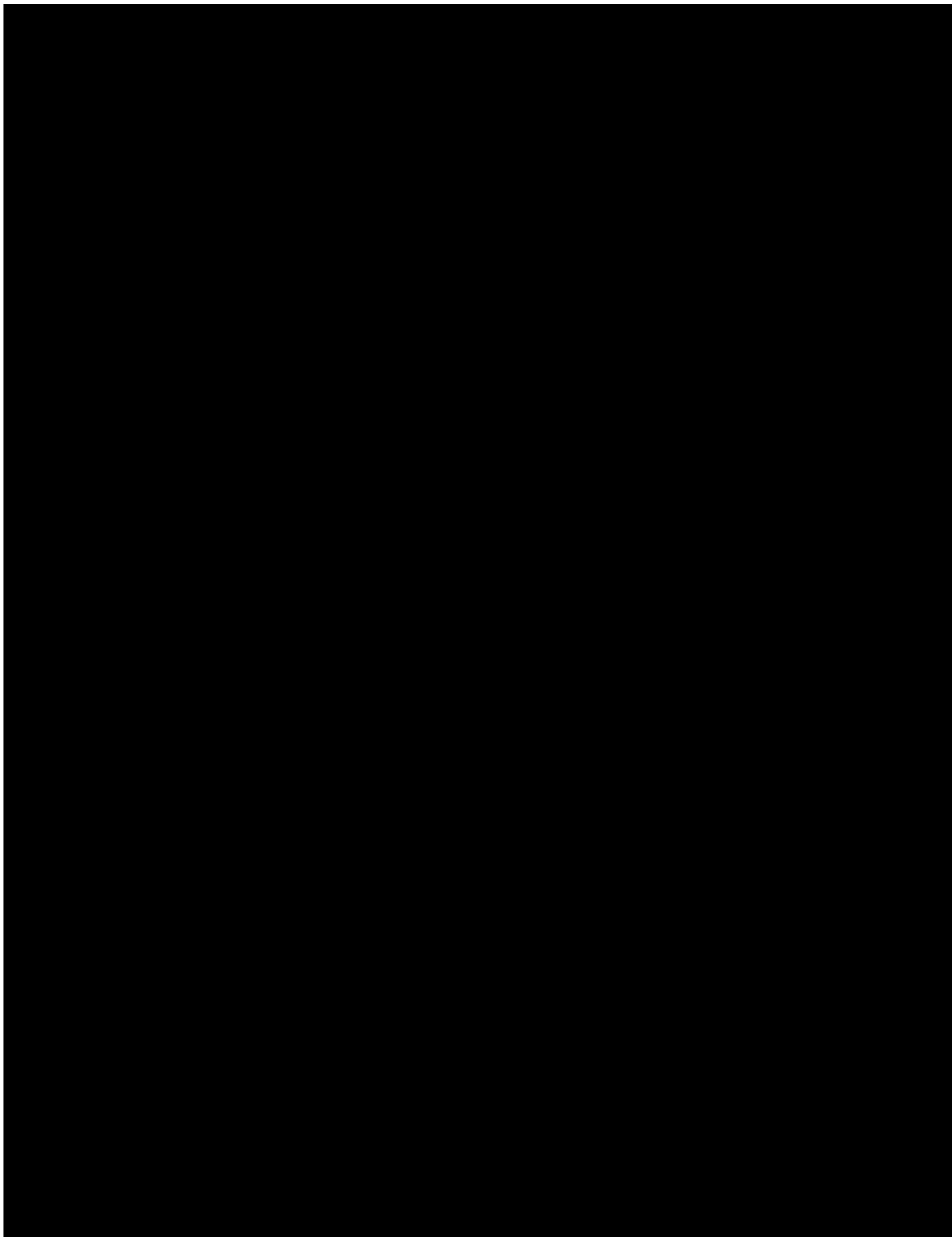


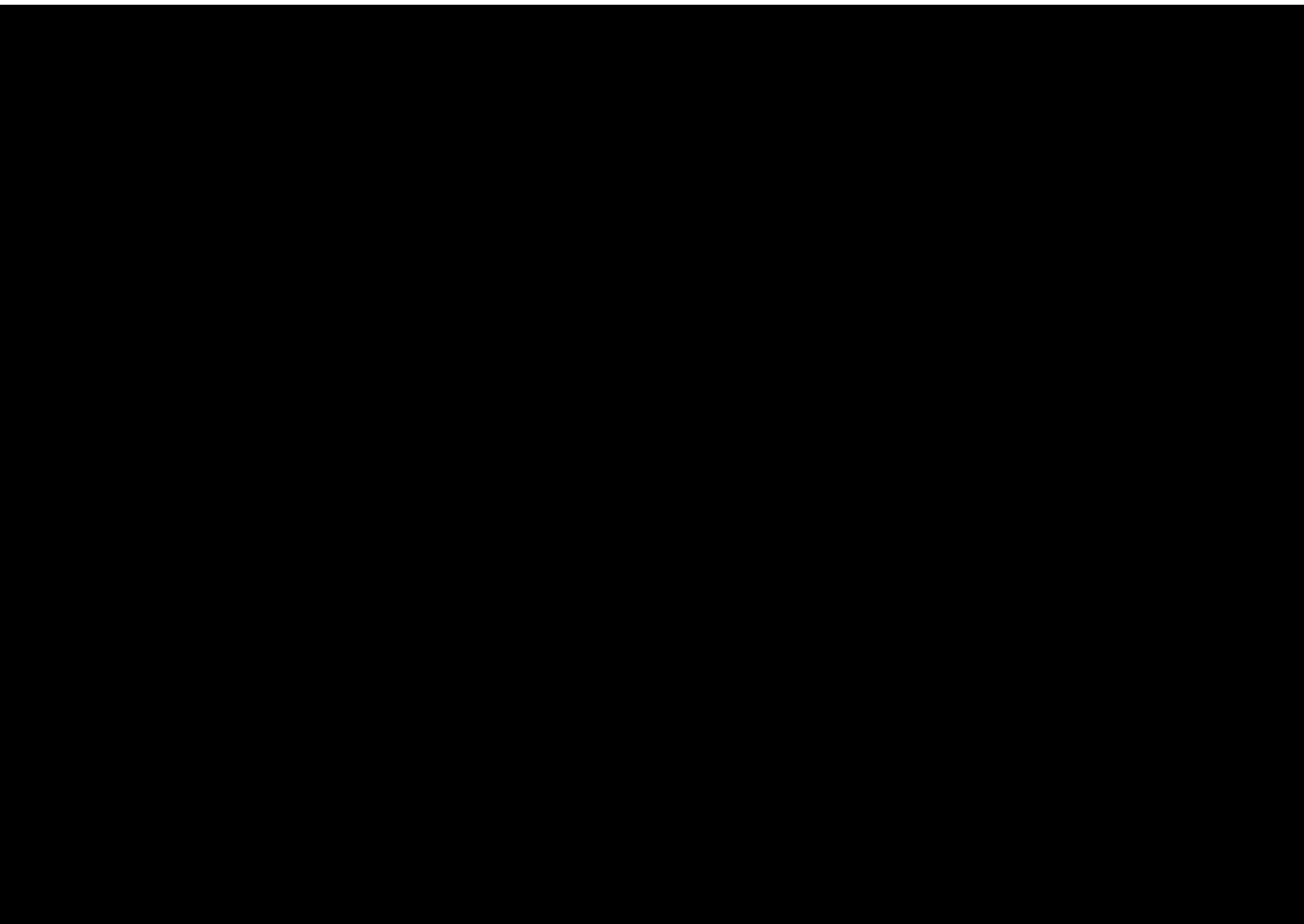
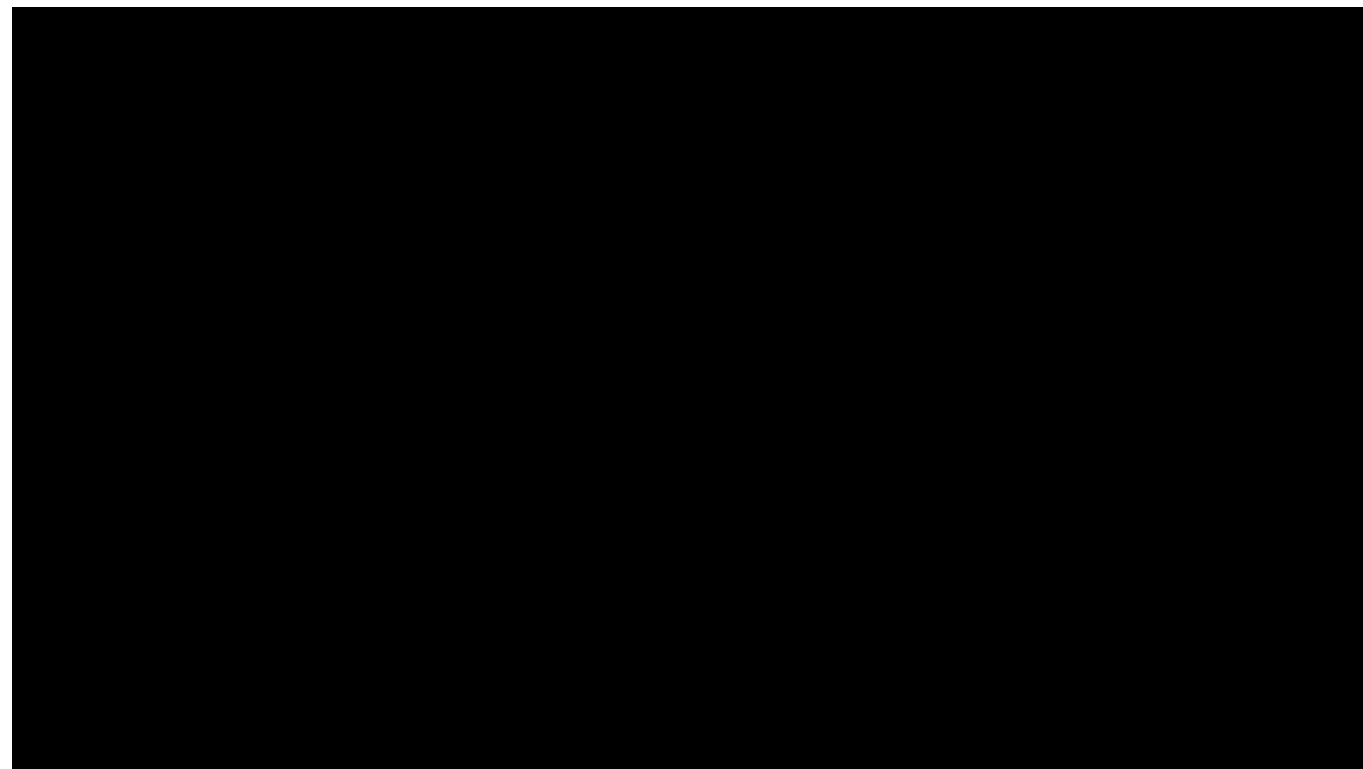
1.9.2 Porosity



1.9.3 Permeability

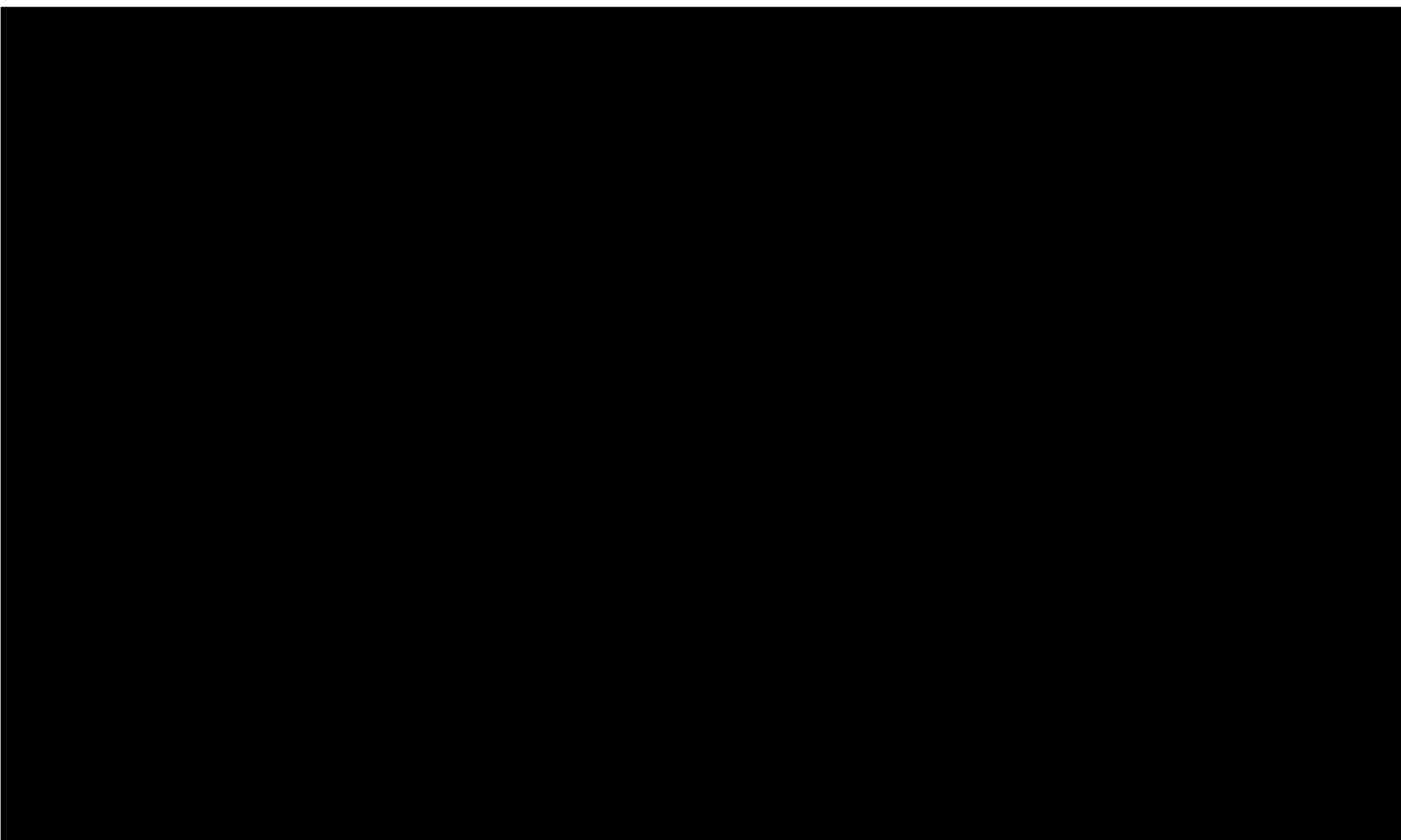






1.9.4 *Salinity*

The salinity of the injection unit is expected to be high and greater than 100,000 ppm. Offset data has

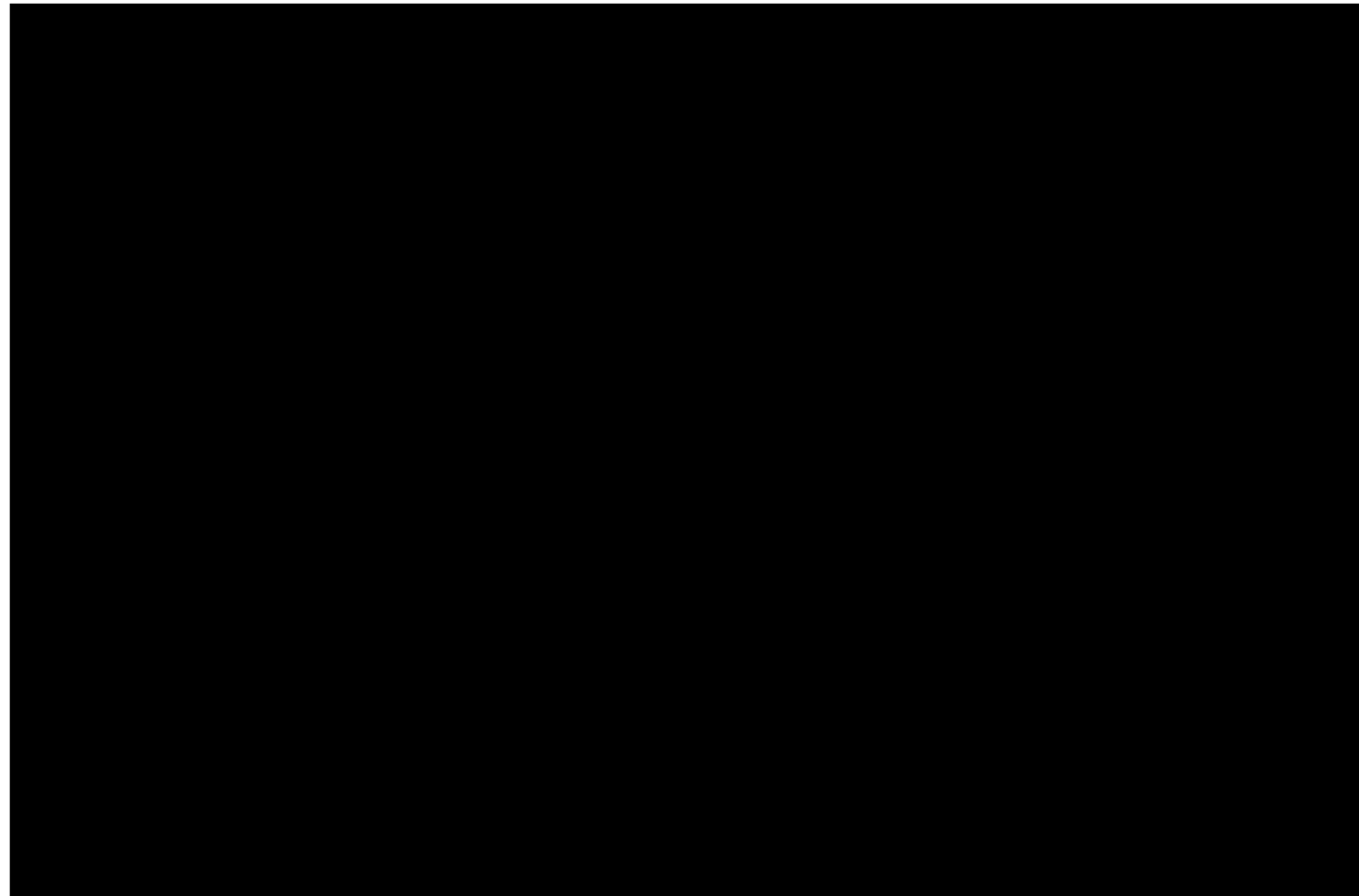


1.9.5 Capillary Pressure

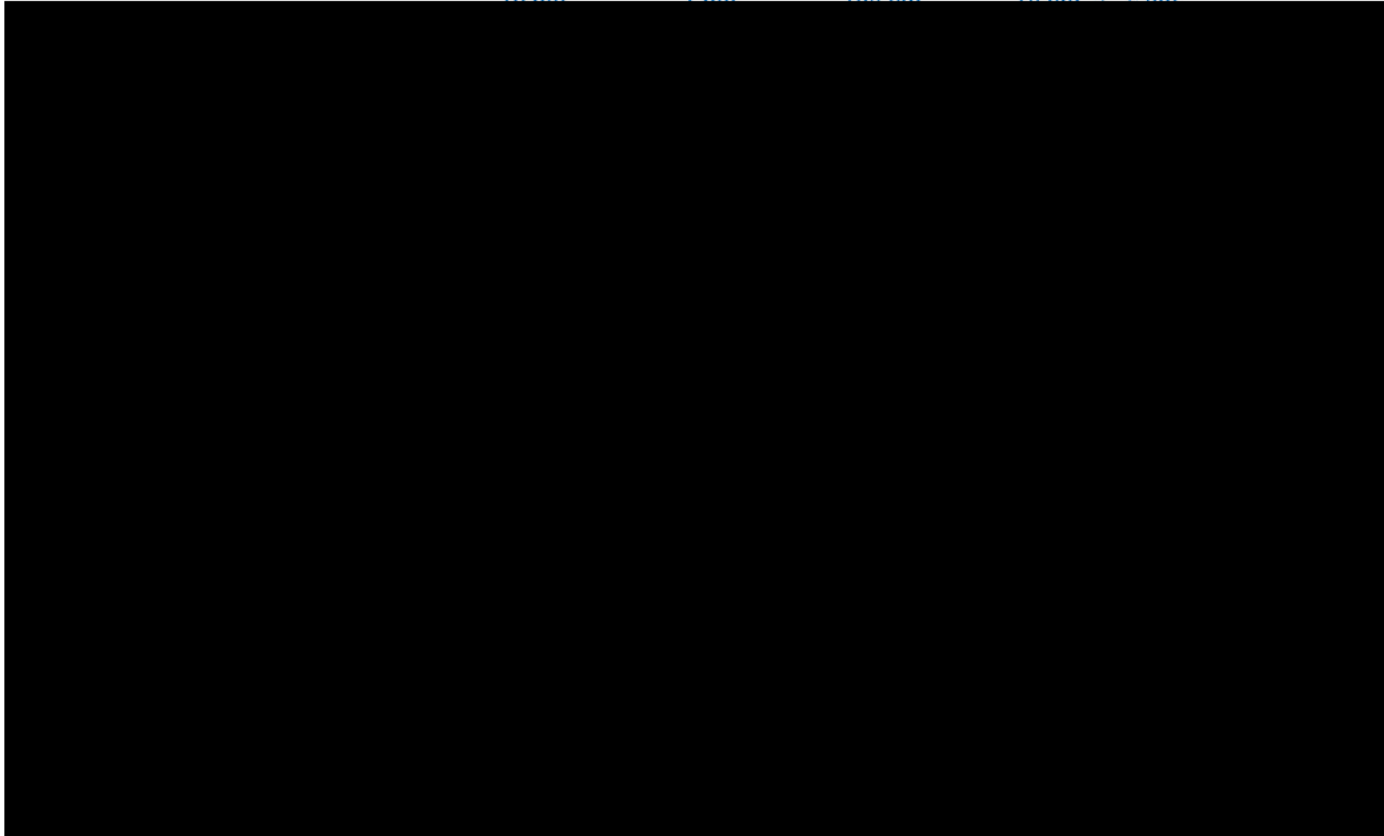
After the initial test well, associated with the Well is drilled, more data will be collected. Therefore, this application will focus on the capillary pressure

Existing literature supports the idea that the elevated pressure from injection activity

Capillary pressure tests in the



10 μ m 1 μ m 100 nm 10 nm - 5 - 2 nm



1.10 Geomechanics [40 CFR 146.82(a)(3)(iv)]

1.10.1 Methods

[REDACTED]

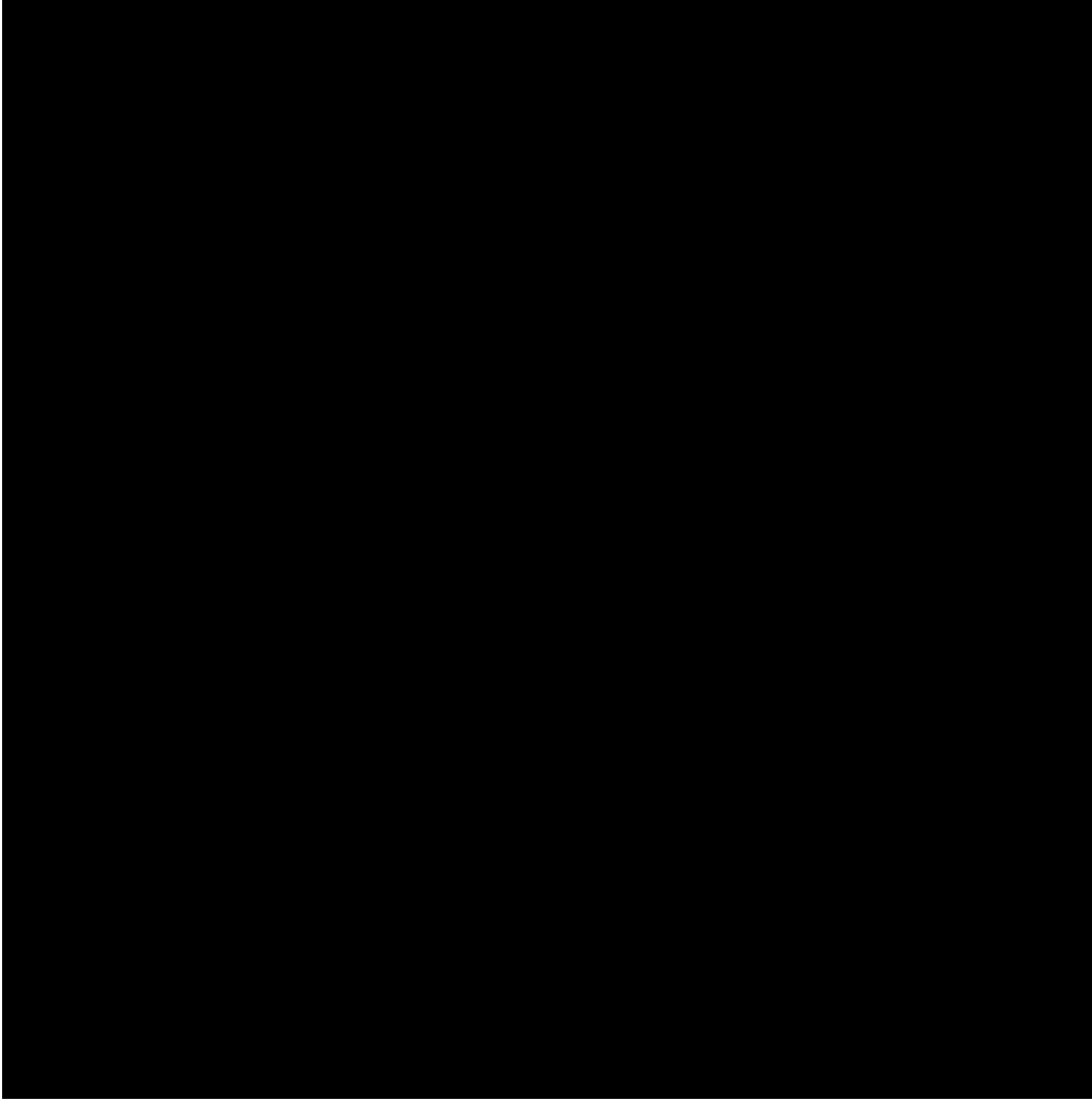
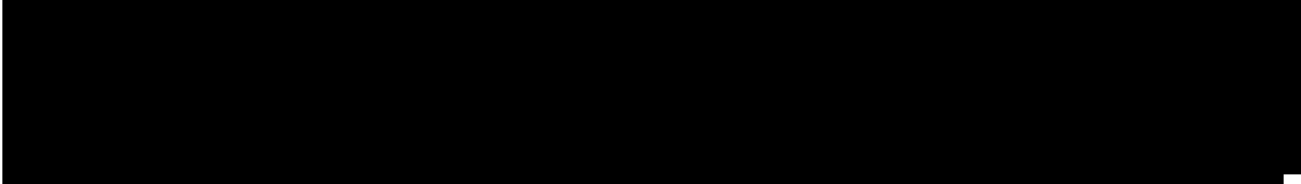
1.10.2 Pore Pressure

[REDACTED]

1.10.3 Stress Magnitude

[REDACTED]

and Simpson minimum horizontal stress was calculated using a VTI matrix. This typically yields higher



SPACE INTENTIONALLY LEFT BLANK TO LINE UP LOGS FROM PREVIOUS PAGE

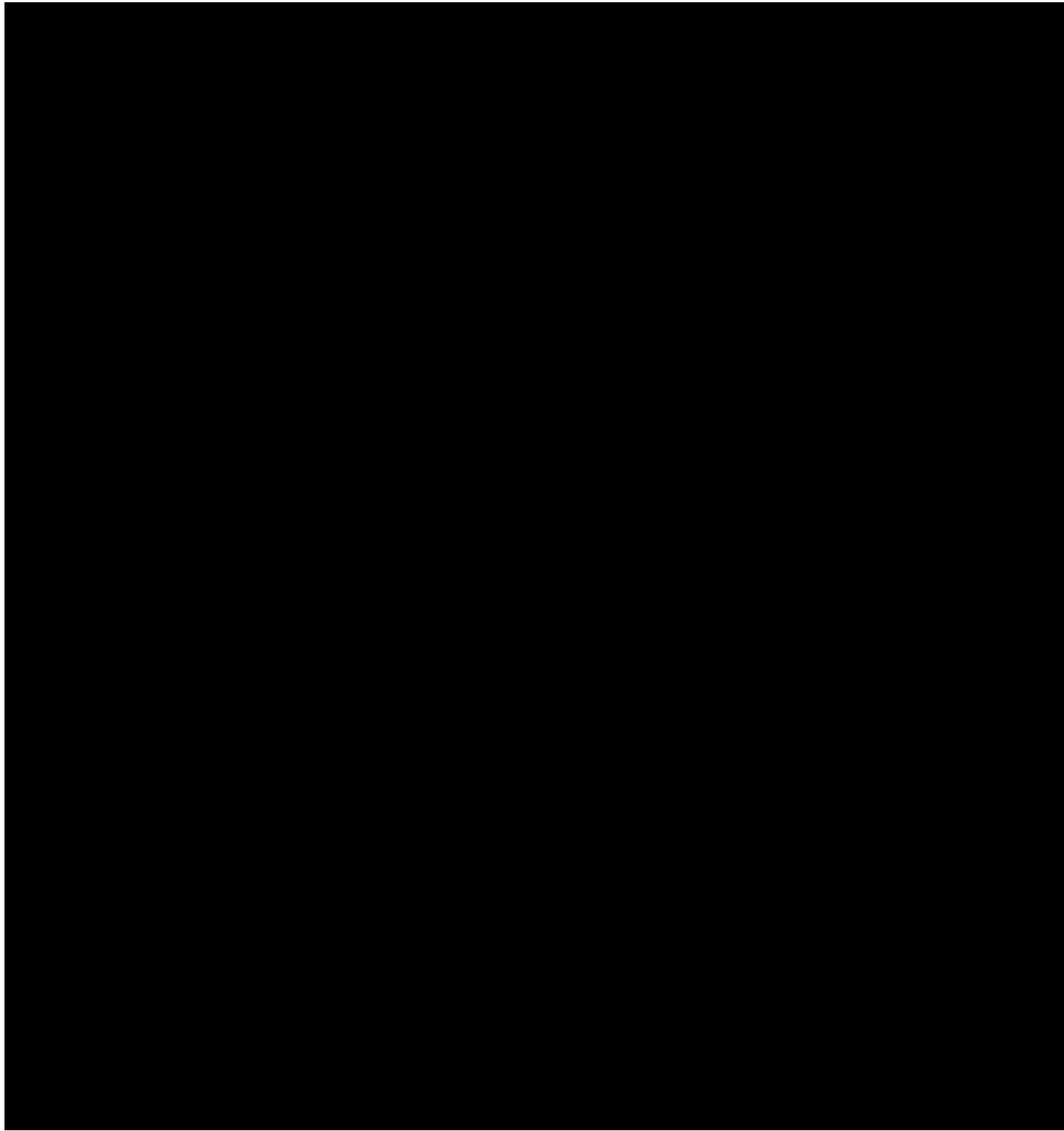
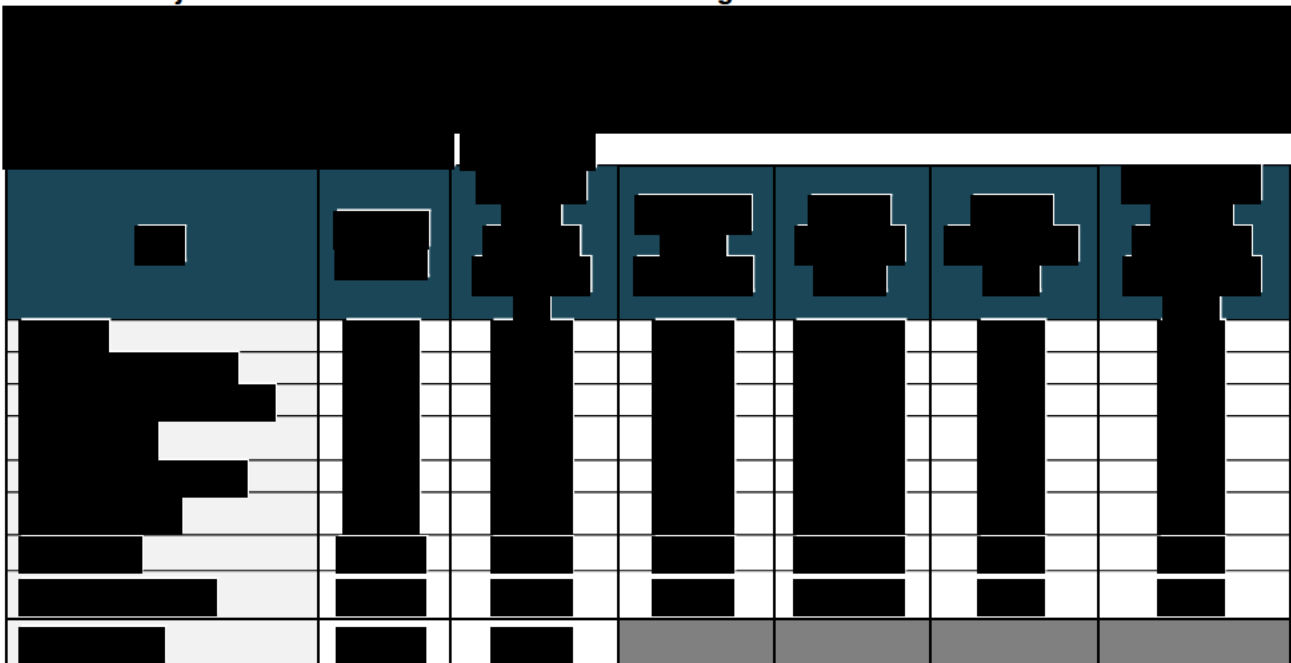




Table 1-17: Injection Zones / Seal Stress Gradients & Magnitudes

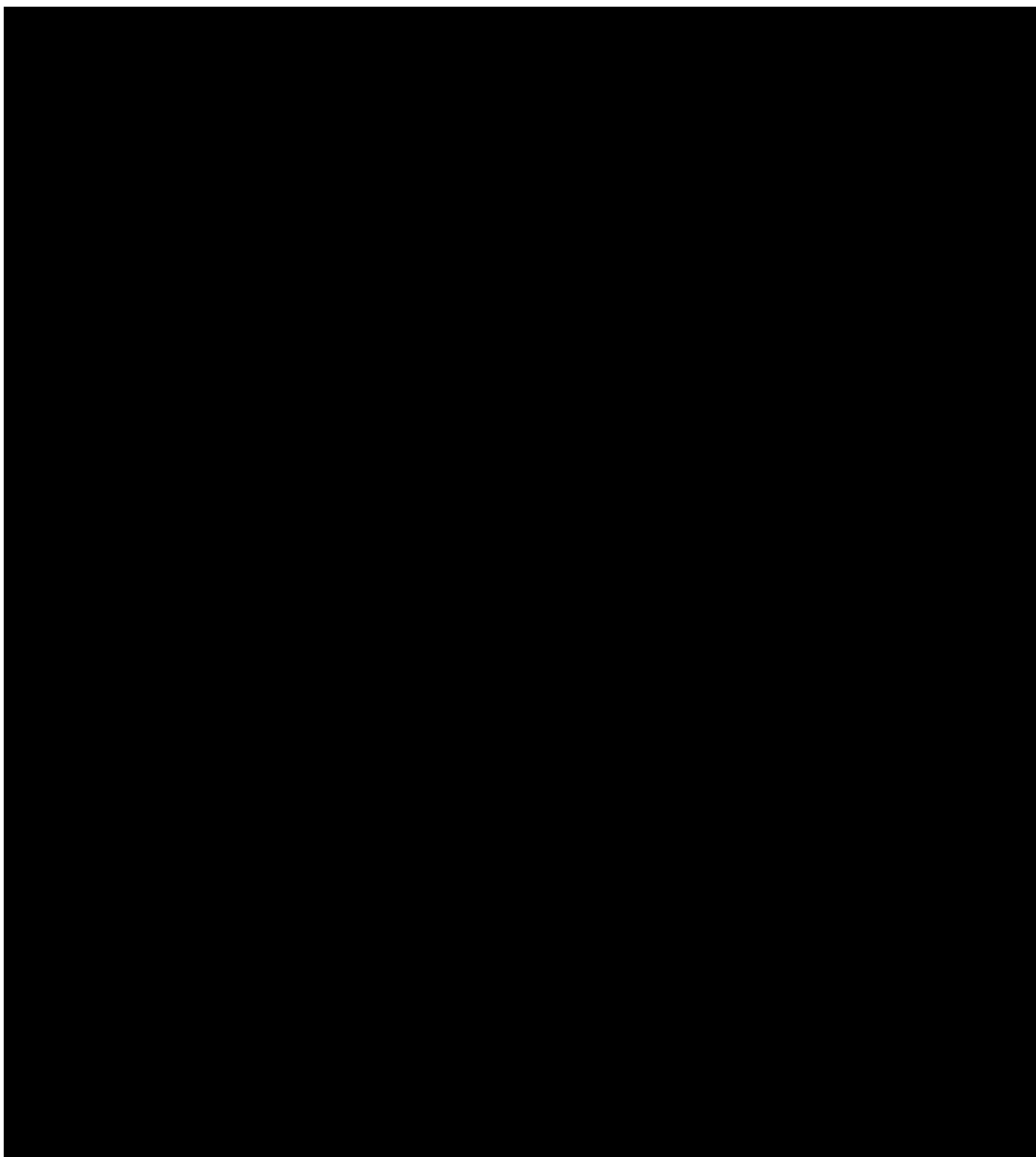


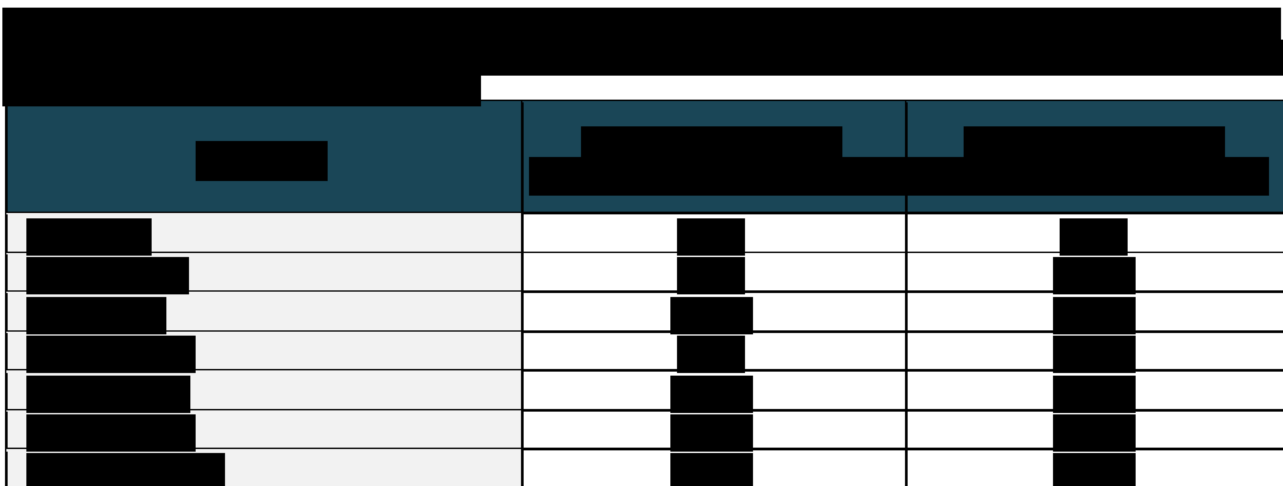
1.10.4 Stress Orientation



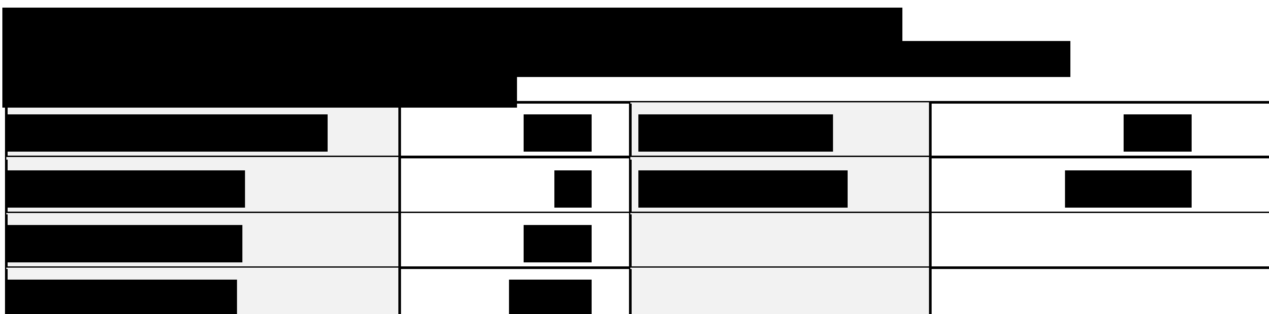
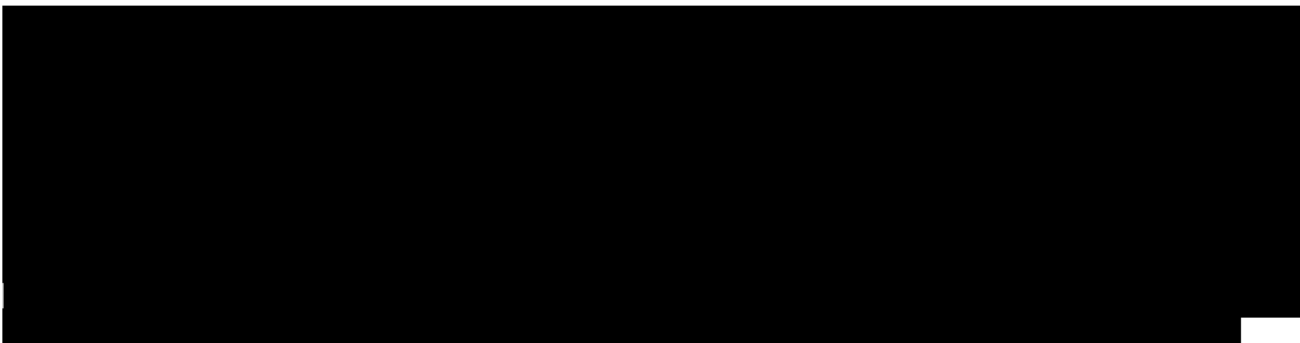
1.10.5 Rock Strength







1.10.6 Ductility



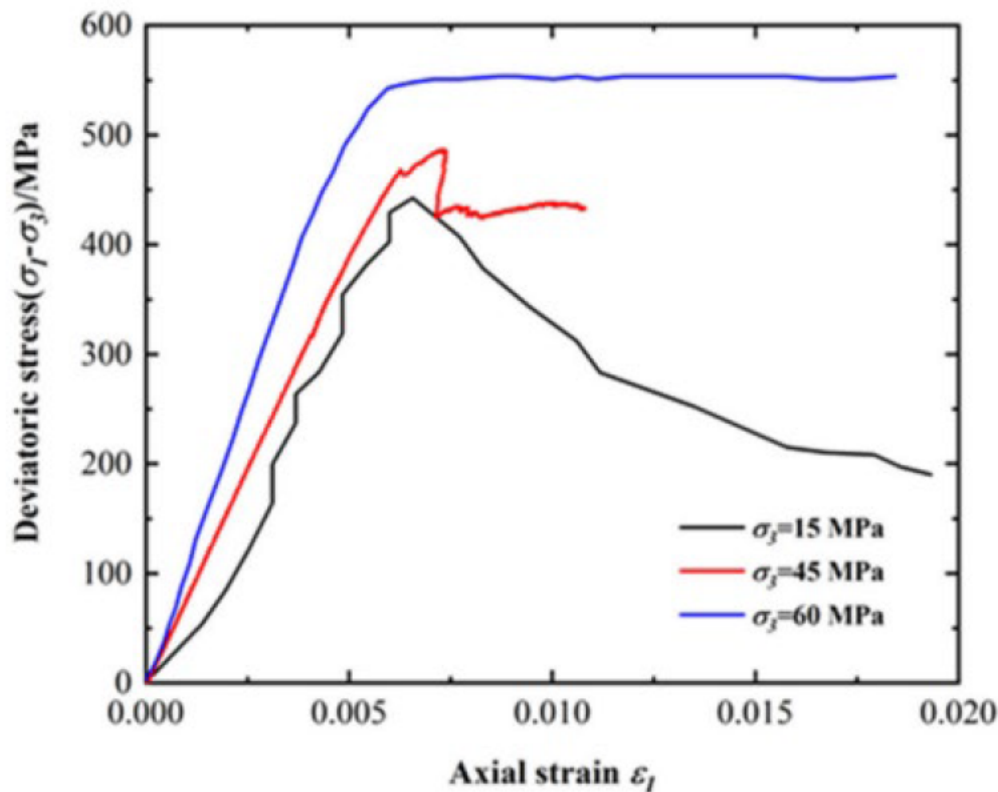


Figure 1-101: Dolomite Triaxial Test from Analogous Low Porosity Dolomite

Dolomite triaxial test from analogous low porosity dolomite found in China. Exhibits brittle behavior at low confining stress (σ_3). Red line or 45 MPa is very close to expected initial confining pressure for Ellenburger Formation at proposed Midland CCS #2 Well.

1.10.7 Additional Testing

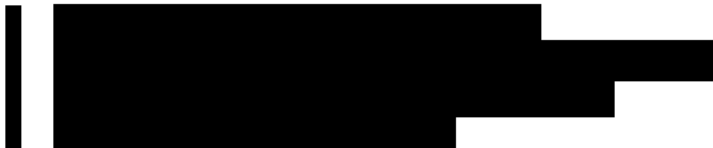
1.11 Geochemistry [40 CFR 146.82(a)(6)]

This section covers the fluid and solid-phase geochemistry of subsurface formations in the AoR and modeling of the mineral-brine-CO₂ system across the mineralogical facies associations present for the injection Well.

Milestone Carbon, LLC (Milestone) has requested that Daniel B. Stephens & Associates, Inc.



1.11.1



1

1

Black box

10. *Journal of the American Statistical Association*, 1980, 75, 338-342.

11. **What is the primary purpose of the *Journal of Clinical Endocrinology and Metabolism*?**

A 10x10 grid of black bars on a white background. The bars are arranged in a pattern where they are longer in the first and last columns and shorter in the middle columns. The bars in the first and last columns are dark blue, while the others are black. The grid is bounded by a thick black border.

10

PHREEQC Mineral	Chemical Formula	Molar Mass (g/mol)	Input for Ellenburger Injection Zone		Input for Simpson Seal Zone		Input for Devonian Injection Zone		Input for Woodford Seal Zone	
			%	mol/L	%	mol/L	%	mol/L	%	mol/L
Quartz	SiO ₂	60.08	10	150.1	20	332.9	80	993.0	20	162.4
K-Feldspar	KAlSi ₃ O ₈	278.33	0.5	1.6	2	7.2	1	2.7	2	3.5
Calcite	CaCO ₃	100.09	3	27.0	9	89.9	10	74.5	9	43.9
Dolomite	CaMg(CO ₃) ₂	184.40	80	391.2	20	108.5	2	8.1	20	52.9
Kaolinite	Al ₂ Si ₂ O ₅ (OH) ₄	258.16	0.5	1.2	3	7.7	1	1.9	3	3.8
Chlorite (14A)	Fe ₂ Al ₂ SiO ₅ (OH) ₄	664.18	0	0.0	1	2.6	0	0.0	1	1.3
Illite	K _{0.6} Mg _{0.25} Al _{1.8} Al _{0.5} Si _{3.5} O ₁₀ (OH) ₂	389.34	6	13.9	45	115.6	6	11.5	45	56.4

Gas	Mole Percent	Mass Percent	Volume Percent
Carbon dioxide	95.00	97.72	94.98
Carbon monoxide	0.43	0.28	0.43
Hydrogen sulfide	0.02	0.02	0.02
Nitrogen	1.00	0.65	1.01
Methane	3.56	1.33	3.57

1.11.2.1

[REDACTED]

[REDACTED]

[REDACTED]

[REDACTED]

[REDACTED]

[REDACTED]

[REDACTED]

[REDACTED]

1.11.4 Geochemical Modeling Results and Discussion

1.11.4.2

- K-feldspar and kaolinite tend to precipitate in the models, removing calcium, magnesium,

■

■

■

■

■

■

■

1

1

1

1

1

1

1

1

1

1

1

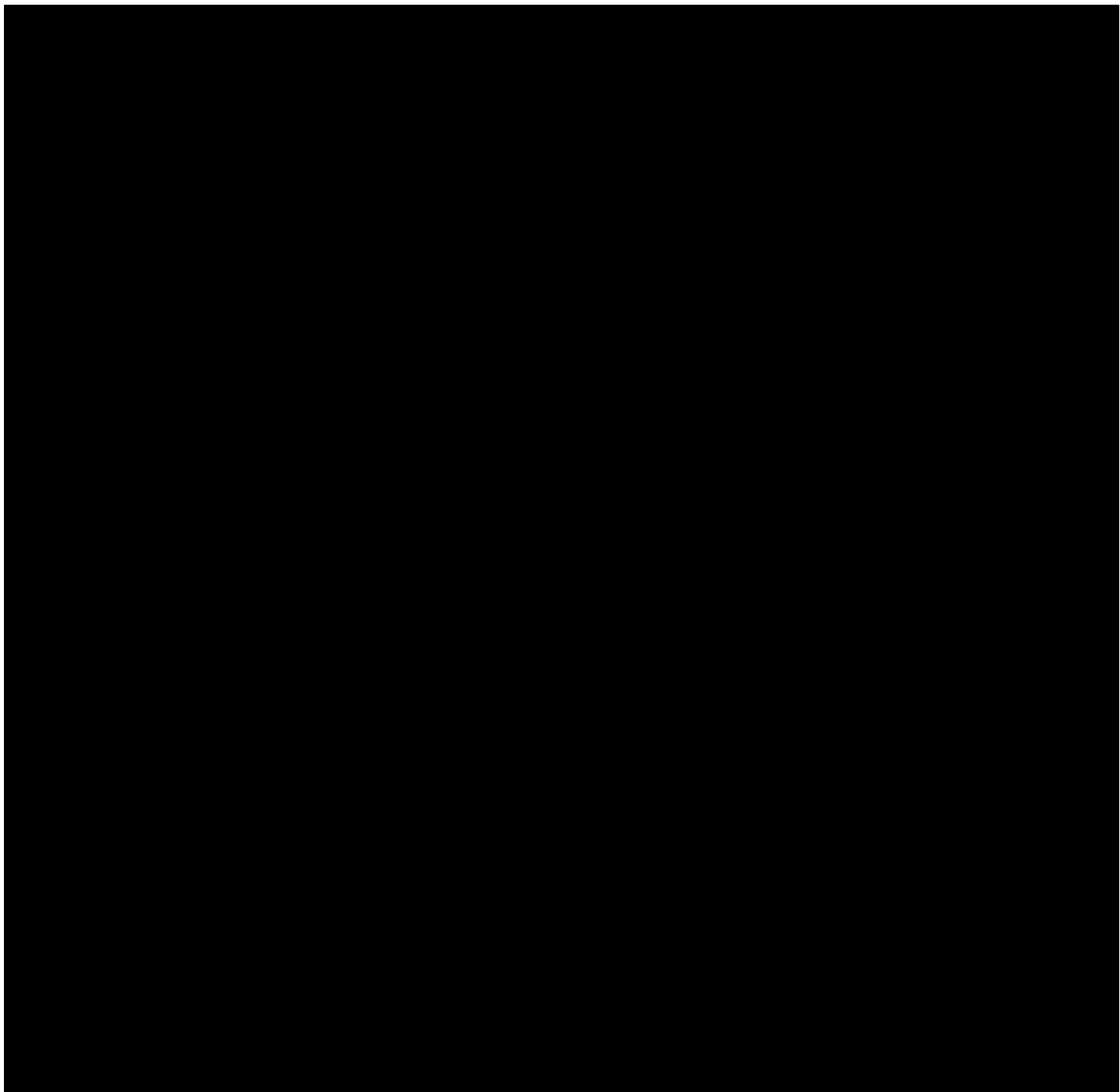
1

1

1

1.12 Mineral Resources

A series of black horizontal bars of varying lengths, each ending in a white rectangular marker. The bars are arranged vertically, with the first bar at the top and the last bar at the bottom. The lengths of the bars decrease from top to bottom. Each bar is followed by a white rectangular marker, which is positioned at the end of the bar's length. The markers are aligned vertically with the bars. The background is white.



1.13 Site Suitability [40 CFR 146.83]

A series of horizontal black bars of varying lengths and positions on a white background. The bars are arranged in a descending order of length from top to bottom. The first bar is the longest and spans most of the width of the image. Subsequent bars are shorter and are positioned lower down on the page. There are some irregularities in the lengths and positions of the bars, suggesting a manual or experimental nature of the data representation.

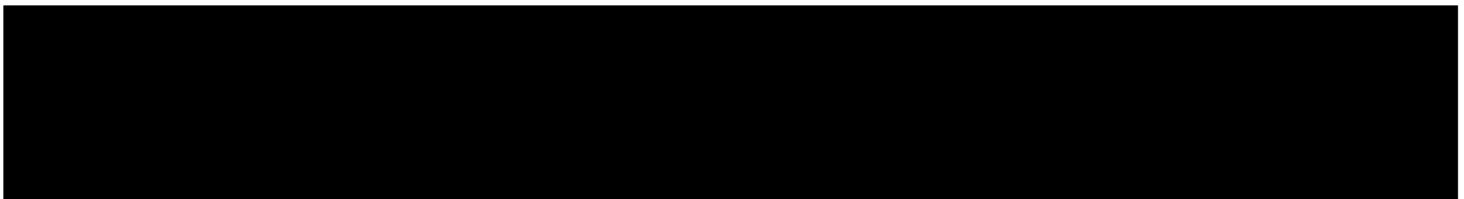
1.13.2 Injectability

1.13.4 Secondary Confinement Zones



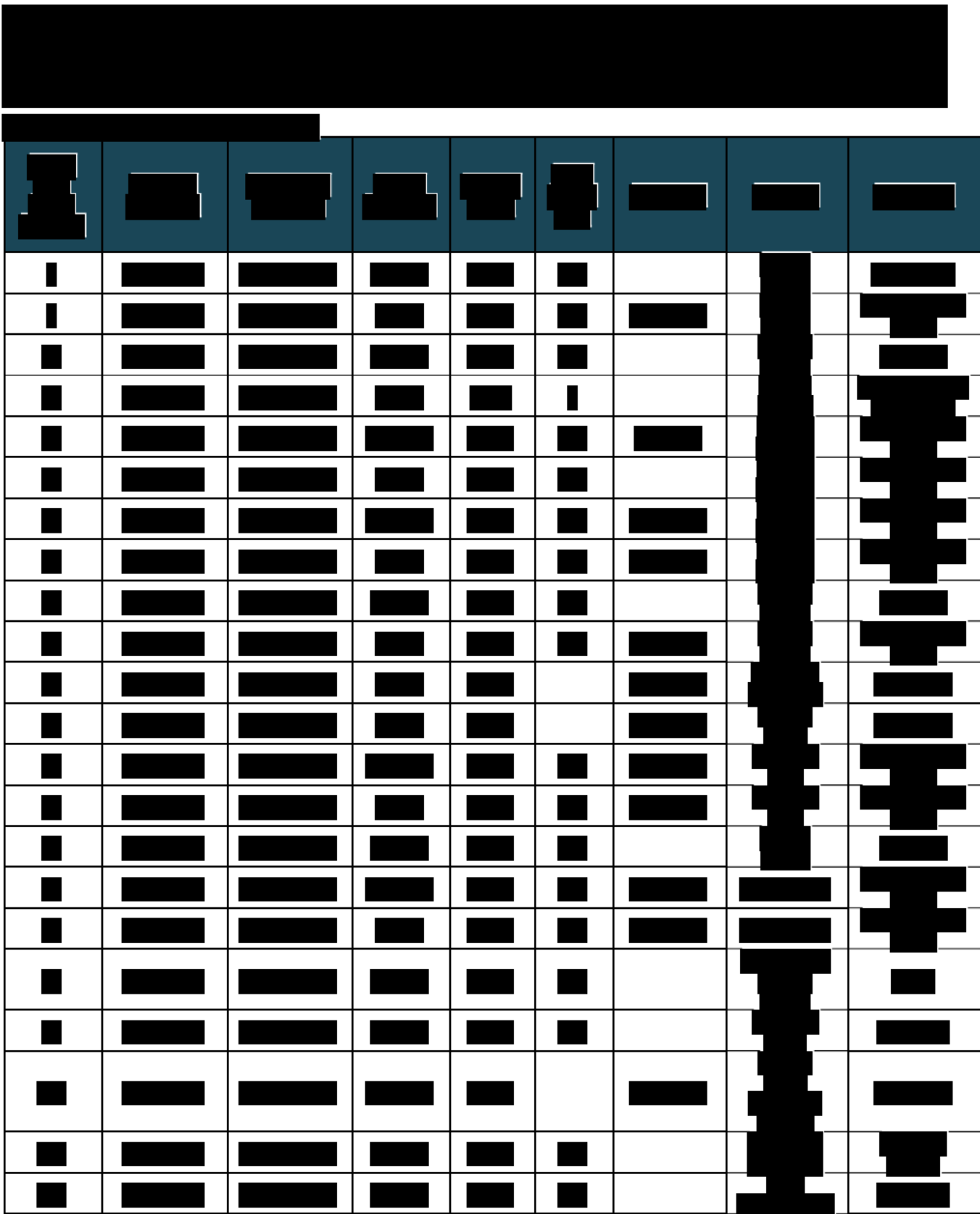
1.13.6 Total Storage Capacity

The Ellenburger and Devonian are regional, multi-state formations that span hundreds of miles in any

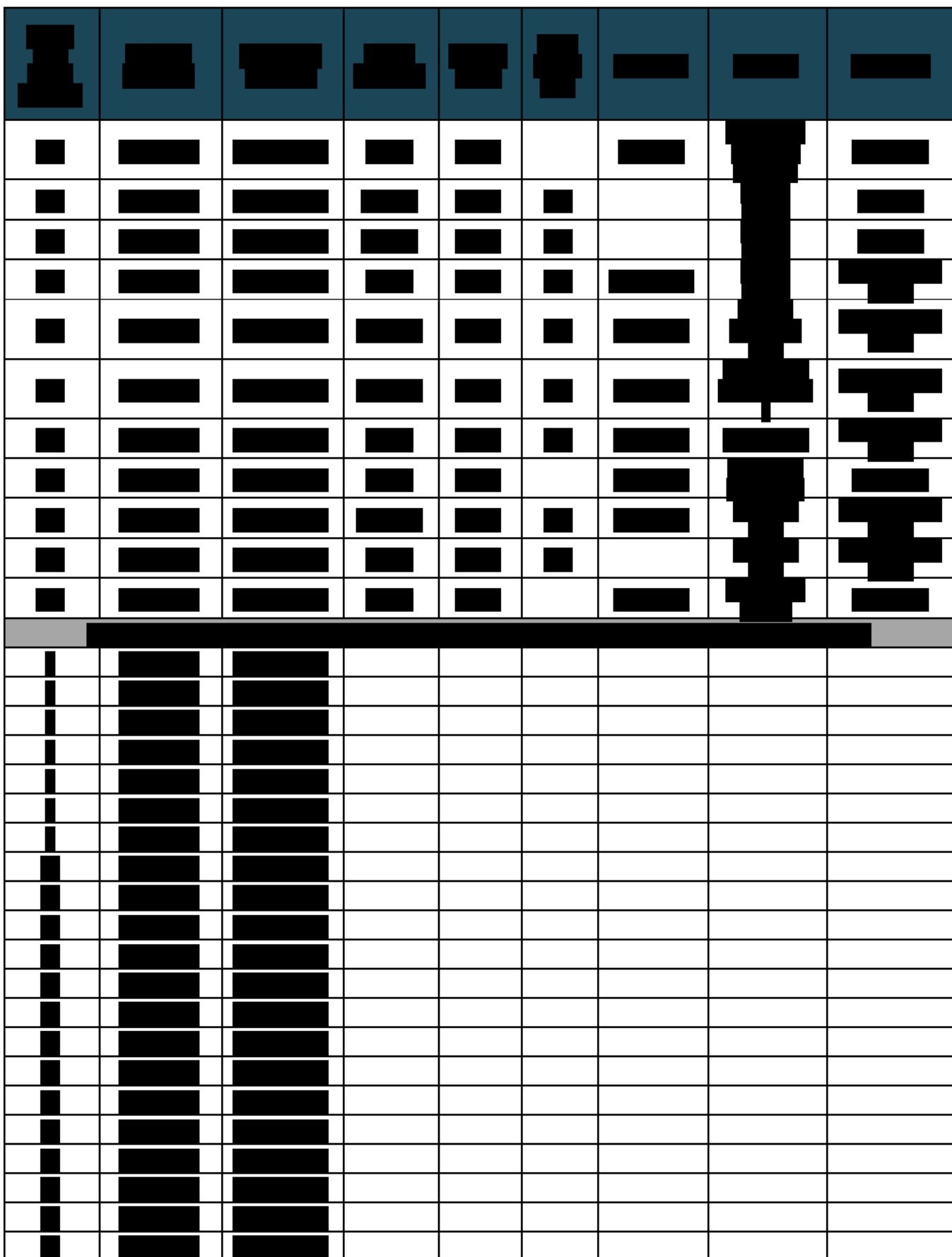


1.14 Well Index Tables

1.14.1 Water Well Index Table



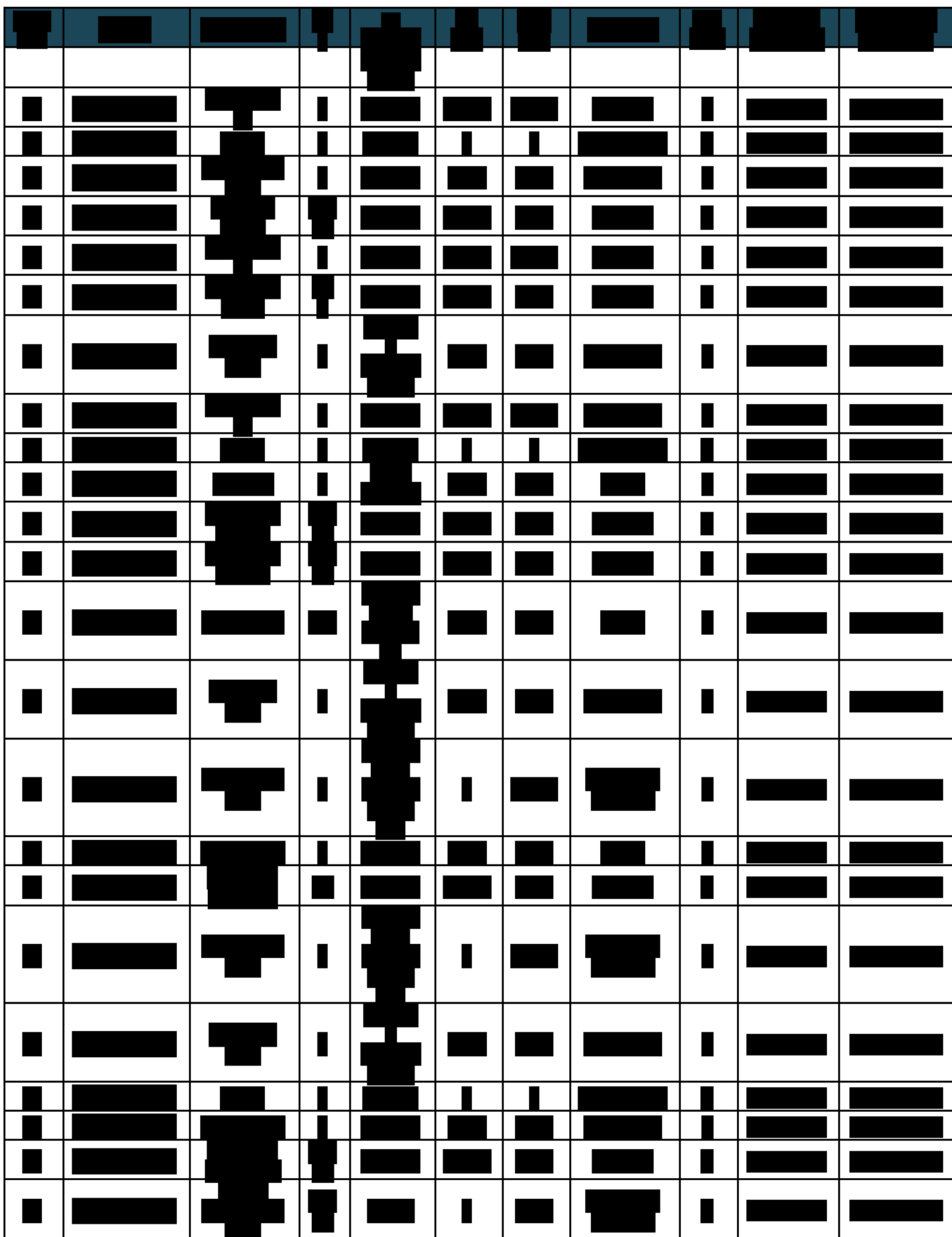
The table is a 20x9 grid of cells. The first column contains 20 black squares. The second column contains 19 black squares, with the last cell being white. The third column contains 19 black squares, with the last cell being white. The fourth column contains 19 black squares, with the last cell being white. The fifth column contains 19 black squares, with the last cell being white. The sixth column contains 19 black squares, with the last cell being white. The seventh column contains 19 black squares, with the last cell being white. The eighth column contains 19 black squares, with the last cell being white. The ninth column contains 19 black squares, with the last cell being white.



							
							
							
							
							
							
							
							
							
							
							
							
							
							
							
							
							
							
							
							
							
							
							
							
							
							
							
							
							
							
							
							
							
							
							
							
							
							
							
							
							
							
							
							
		<img alt					

1.14.2 Oil and Gas Index Table

This figure displays a 2D grid of data, likely a sparse matrix, with a high density of black pixels. A prominent, roughly triangular cluster of black pixels is centered in the grid, with its base along the bottom edge. This central cluster is surrounded by a dark border of black pixels. The rest of the grid is mostly white, with scattered black pixels representing the non-zero elements of the matrix. The overall pattern suggests a sparse matrix with a central, more concentrated region of data.



The figure displays a 20x20 grid of binary images. A central black cluster of pixels moves horizontally from left to right across the grid. The cluster starts at approximately (10, 10) and ends at approximately (10, 20). The background is white, and the cluster is black. The grid lines are thin and light gray.

